ABSTRACT

Title of Thesis: Modeling a Fuel Rich Premixed Laminar
Methane Flame. OH CN NH CH Profiles
Including Prompt NO.

Md. Hasan Ul Karim, Master of Science, 1990

Thesis directed by: Dr. Joseph Bozzelli
Prof. Dept. of Chemistry, Chemical
Eng. and Environmental Science.
New Jersey Institute of Technology.

A detailed reaction mechanism based upon fundamen-
tal thermochemical kinetic principles has been de-
veloped to describe the concentration profiles of OH,
CH, NH, CN, and NO including prompt NO radicals in
laminar flow, fuel rich methane flames as well as
flames doped with 700 ppm ammonia.   A one dimensional
laminar flat flame code which incorporated diffusion,
and the detailed reaction mechanism was used to predict
the radical concentration profiles from the model.
These calculated values are compared to experimental
data of Dean (1984).

The model consist of two reaction subsets, hydro-
carbon oxidation set and an ammonia oxidation set. The
reactions most important for coupling the two subset

are :

$$CH + N_2 \longleftrightarrow HCN + N \qquad (1)$$

$$CH_2 + N_2 \longleftrightarrow HCN + NH \qquad (2)$$

$$CH_3 + NO \longleftrightarrow HCN + H_2O \qquad (3)$$

The mechanism shows good agreement (within experimental error) with experimental concentration as function of distance above the burner, except for NO. The mechanism predicts that reaction (1) is mainly responsible for nitrogen fixation in the fuel rich flame studied. The contribution to the nitrogen fixation by reaction (2) and the Zeldovich (1948) mechanism are negligible.

A rate constant for reaction (1) (from QRRK) consistent with the shock tube data of Bowman (1990) results in under prediction of the NO concentration by a order of magnitude. A higher value corresponding to a barrier of 10 Kcal for reaction (1) increases the NO peak by a factor of 4.5. Inclusion of the following reaction :

$$CH_3 + N_2 \longleftrightarrow HCN + NH_2 \qquad (4)$$

improves the NO profile by a factor of six.

NO decomposition in the flames studied takes place mainly through reaction (3).
A higher value for rate constant for reaction 2 relative to the shock tube data of Bowman and Dean (1990) and an nitrogen fixation reaction in the form of (4) is needed to properly account for the observed nitrogen fixation.

MODELING A FUEL RICH PREMIXED LAMINAR METHANE FLAME
OH, CH, NH, CN, PROFILES, INCLUDING PROMPT NO

by

Md. Hasan Ul Karim

Thesis submitted to the Faculty of the Graduate School of
the New Jersey Institute of Technology in partial
fulfillment of the requirements for the degree of
Master of science in Chemical Engineering
1990

APPROVAL SHEET

Title of Thesis: Modeling a Fuel Rich Premixed Laminar
                Methane Flame. OH, CN, NH, CH Profiles
                Including Prompt NO

Name of Candidate: Md. Hasan Ul Karim
                   Master of Science in Chemical Engineering
                   September 1990

Thesis and abstract approved:

                                _____

                                Joseph Bozzelli
                                Professor
                                Department of Chemistry,
                                Chemical Engineering and
                                Environmental Science

                                _____

                                Dr. Dana Knox

                                _____

                                Dr. Robert Barat

VITA

Name: Md. Hasan Ul Karim

Permenant address:

Date of birth:

Place of birth:

Secondary education: Faujdarhat Cadet College
                         Chittagong, Bangladesh, June 1982

Collegiate institution attended	Dates	Degree	Date of degree
New Jersey Institute of Technology	Spring 88 to Summer 90	MSChE	October 1990
Indian Institute of Technology, India.	May 83 to May 87	B.Tech.	July 1987

Major: Chemical Engineering

ACKNOWLEDGEMENT

I am grateful to Professor Dr. J. W. Bozzelli for his guidance in this research. Completion of this thesis would not have been possible without his unflinching faith in my ability and financial support.

I would also like to thank the members of my thesis commitee for their patience in going over the thesis and recommendations.

I would also like to acknowledge the help of Mr. Karthik Krishnan (System Manager NJIT Computers) for introducing me to the world of supercomputers. His help was also essential in recovering deleted files.

I would like to thank the members of Pittsburgh Super Computer Center especially to Mis. Casey Porto for their generous extension of my account in the Center. CRAY YMP made it possible for me to take as many as 10 runs of my model.

Finally I would like to express my deepest gratitude towards my parents and wife whose sacrifice and love has made it possible on my part to come to U. S. A. and do this M.Sc.

TABLE OF CONTENTS

LIST OF FIGURES

Introduction

The advent of the Clean Air act of 1970 led to the recognization that ambient concentrations of nitric oxide (NO) and nitrogen dioxide (NO_2), collectively referred as nitrogen oxides (NO_x), constituted a significant air pollution problem in certain urban regions of the country. In the atmosphere of industrialized urban-metropolitan centers, NO_x concentrations can be on the order of 50 to 100 times that of the natural background, which is only 1 to 5 parts per billion (ppb). In contrast, estimates of total man made NO_x only amount to 5 to 10 percent of natural emissions on an annual, global basis (Bartok, et al, 1971, 1971a; NRC-NAE, 1972). This information lead to the conclusion by many environmental scientist that air quality problems involving NO_x are largely local, and can be solved by tailoring emission limitations of sources to the ambient air quality of geographical regions which those sources affect.

In the United States vehicular and stationary sources contribute approximately equal amounts to the total anthropogenic emission. Stationary sources result primarily from combustion processes. Non combustion sources such as nitric acid and nitrogen fertilizer plants can cause severe local problems, but contribute a relatively small amount (1.3 percent) to the composite stationary source emission rate. In 1972, total stationary source emission were estimated at 11.7 million tons per year as NO_2 with dominant contribution

from utility and industrial boilers, 48.6 and 18.1 percent, respectively (Sarofim and Flagan, 1976).

NO_x is produced in these large combustors by three mechanism :

1. Thermal fixation of N_2 from the combustion air according to the extended Zeldovich mechanism shown below (Zeldovich,1946 ; Sarofim and Pohl, 1973 ; Bowman, 1975).

$$O + N_2 \longleftrightarrow NO + N \qquad (-R-124)$$
$$N + O_2 \longleftrightarrow NO + O \qquad (R-125)$$
$$N + OH \longleftrightarrow NO + H \qquad (R-126)$$
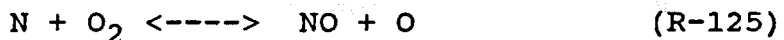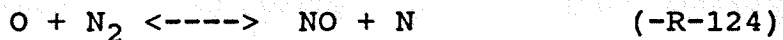
2. Fixation of N_2 from combustion air by reaction with hydrocarbon fuel fragments present in the flame, and subsequent oxidation of these fixed nitrogen species (primarily HCN) to NO . This NO is referred to as "prompt" NO because it is formed primarily in the reaction zones of flames (Fenimore, 1971; Bachmaier, et al, 1973; Hayhurst and Mclean, 1974; Haynes, et al,1975; Blauwens, et al, 1977;)

3. Conversion of organically bound nitrogen in the fuel to NO during the combustion process (Fenimore, 1972; Martin and Berkau, 1972; Turner et. al, 1972; Pershing and Wendt, 1977). It had been demonstrated in flame systems operated at fuel lean and fuel rich equivalence ratios (equivalence ratio is defined as ratio between oxidant stoichiometrically required for complete combustion of fuel

Figure 1.1 FLOW DIAGRAM FOR CONVERSION OF FUEL NITROGEN

FUEL NITROGEN

↓

HCN, CN

↓

HNCO, NCO

↓

NH3, NH2
NH, N

N2   NO
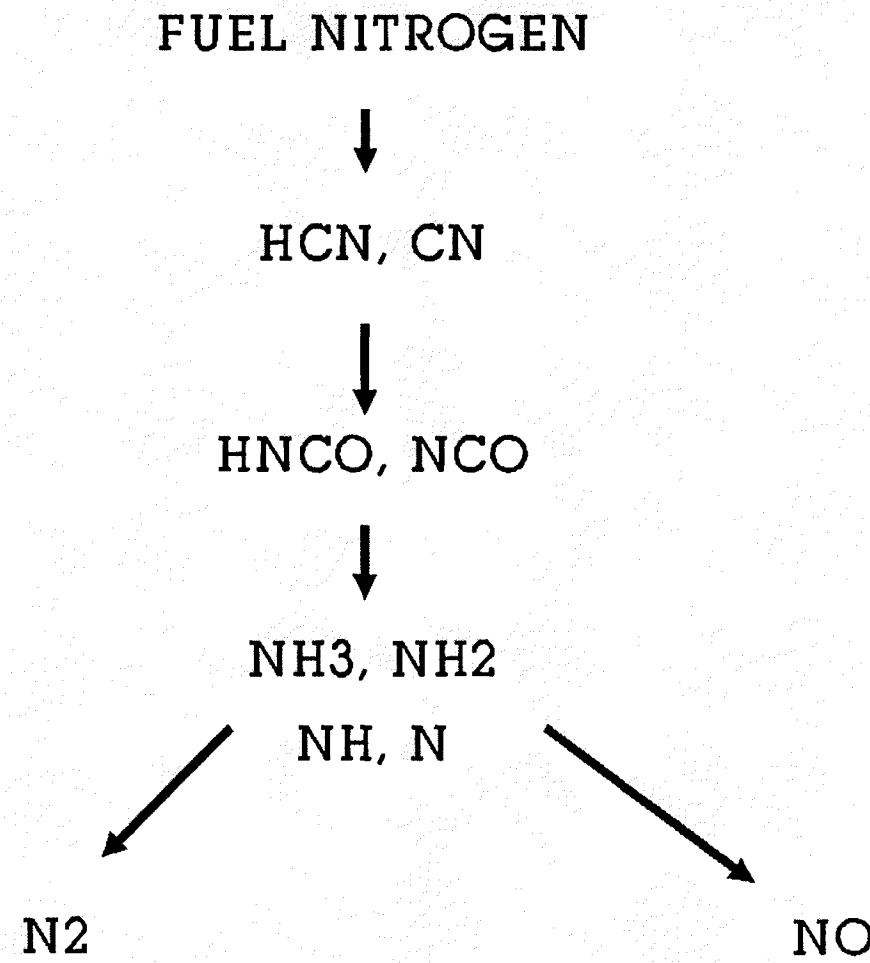
to that of oxidant actually provided in the fuel) that the yield of NO_x from fuel nitrogen is independent of the chemical composition of the parent nitrogen compound (Fenimore, 1973; de Soete, 1973; Sarofim et al. 1973; Morley 1976). NO is the only fixed nitrogen additive which is the exception to this generality. The observation that NO_x yield was independent of fuel nitrogen type led to the hypothesis of a common nitrogenous intermediate which was formed rapidly from parent nitrogen species in the flame, before the formation of NO and other nitrogenous intermediate or end product could occur to an appreciable extent. Fenimore (1972) was the first to propose this now widely accepted concept. In flames with a hydrocarbon fuel and/or with a fuel nitrogen component having a C-N bond, the common intermediate is generally believed to be HCN. Fenimore originally proposed that the common intermediate reacted directly with oxidizing species to form NO, and with NO to form N_2. However the destruction of HCN is now believed to be the first step in a sequence of reactions which ultimately results in the formation of NO and N_2 as shown from Haynes (1975) in Figure 1-1. Haynes et al, (1975) provided the first flame data which shed light on critical intermediates in the conversion process and identified the rate limiting steps. This reaction sequence is later supported by Miller and Bowman (1989) in their study with fixed nitrogen species. In addition, these intermediates provide the only known reaction pathways for conversion of HCN and CN to NH_i species which are ener-

getically favorable, and which can be used with reasonable rate constants to describe the observed rates of conversion.

Significant progress has been made in the past twenty five years in identifying the mechanisms of thermal nitric oxide formation in flames and in developing strategies for emission control (Bartok, et al, 1969; Lachapelle,et al,1974; Sarofim and Flagan, 1976; Chen, et al, 1982). Development of emission control technology for NO formed by the Zeldovich mechanism has been particularly successful. The rate of NO formation by this mechanism increases as oxidizing species become more abundant (more specifically in the burnt gases far down stream from the flame front, the rate is proportional to the square root of the O_2 concentrations (Sarofim and Flagan, 1976). Reaction R-124 which is rate limiting in this sequence, is endothermic by approximately 75 Kcal mole^{-1}. The rate of NO formation by this mechanism increases dramatically with temperature and becomes significant at temperatures greater than 1700 K for residence times associated with typical combustors. Techniques developed to control emissions of NO formed by this mechanism have incorporated low excess air firing technology to reduce concentrations of oxidizing species and various means of reducing peak flame temperature.

While the fixation of nitrogen by hydrocarbon has definitely been identified as a mechanism for NO formation in flames (Bachmaier,et al 1973; Haynes et al 1975; Blauwens 1977.), data on its importance as a source of fixed nitrogen in

various types of flame systems (especially under fuel rich condition) relative to emission standards is scarce. It has been found (Miller and Bowman, 1989) that thermal NO produced by the Zeldovich mechanism and super equilibrim O atom concentration is insufficient to account for the experimentally observed NO in fuel rich flames. This appears to be a general observation. Typical level of prompt NO range from a few parts of per million by volume to more than 100 ppmv (Miller and Bowman, 1989).

Thesis Objective & Approach

The present research is motivated by the need to refine the existing mechanism for prompt NO formation by updating the rate constants of existing reactions and by evaluating other reactions which may be important under fuel rich flame conditions. This work is also directed towards determination of the important, hydrocarbon radicals, and reaction pathways for coupling hydrocarbon oxidation and ammonia oxidation. This relates directly to the formation of HCN in the flame front. The uncertainities in rate constants for important prompt NO formation reactions were also evaluated. In developing a fundamental mechanism for prompt NO formation a model for conversion of fuel nitrogen to nitric oxide is also developed because both involve the same intermediate HCN.

The approach was to develop a mechanism and calculate the radical concentrations (for which experimental data were available Dean and Chou, 1984) using the one dimensional Sandia Flame (Kee, Miller, Smooke, and Grcar, 1987) code which accounts for diffusion.

The mechanism incorporates bimolecular Quantum Rice -Ramsperger Kassel (QRRK) (Kassel, 1948) theory to account for reactions of chemically activated species, formed from addition and combination reactions. In addition unimolecular QRRK theory is used to account for collisional fall off in simple dissociation, beta Scission & isomerization reactions of stabilized radicals. Where data are not available generic

parameters are used. Required thermodynamic properties for radical intermediate is calculated using THERM computer code (Ritter, 1989) or estimated from literature values.

Sensitivity and rate-of-production analysis play a central role in identifying the important reactions for species formation and destruction. In the flame the sensitivity coefficients is displayed as :

$$\beta_{ik}(x) = \frac{A_i}{X_k} \frac{\delta X_k}{\delta A_i}(x)$$

where $\beta_{ik}(x)$ is the sensitivity coefficient for change in the mole fraction of the kth species, X_k, due to a small change in the temperature independent factor of the ith reaction rate coefficient, A_i. The position above the burner surface is denoted by x.

Sensitivity coefficients are more useful when they are calculated at the maximum value of each dependent variable.

$$\beta_{ik}(x) = \frac{A_i}{(X_k)^{max}} \frac{\delta X_k}{\delta A_i}(x) \qquad (2.1)$$

$(X_k)^{max}$ indicates the maximum value of X_k occured in the calculation. This normalization avoids artificially high sensitivity coefficients in regions where the mass fractions are approaching zero, and thus subject to numerical error. This "maximum" normalization was done by developing a post-

processor for the flame code. (Kee, Smooke, Miller, and Grcar, 1987)

Contribution factors obtained from the rate-of-production (or reaction path) analysis are calculated from:

$$R_{ik}(x) = r_{ik(forward)}(x) - r_{ik(reverse)}(x)$$

where r_{ik} is the rate of the forward or reverse reaction i involving the kth species. This reaction path analysis was also done by developing a post processor for the flame code (Kee, Smooke, Miller and Grcar, 1987).

Flat Flame Structure & General Chemistry

Ideally a flat flame has no gradient perpendicular to the axis of gas flow: i.e, horizontal temperature and species profiles are flat. In such a flame where unidirectional changes occur only along the axis of gas flow it is relatively easy to determine species reaction rates from measured temperature and composition profiles along the axial dimension. This characterstic of the flat flame makes it attractive to study flame chemistry, including reaction rate determination, hydrocarbon oxidation, prompt NO formation and fixed nitrogen conversion.

In this study interest is focussed on the kinetics of prompt NO formation and its destruction in the flame front of fuel rich methane flames. It was found (Blauwens, 1977; Fenimore, 1971, Haynes, 1975) that due to abundance of hydrocarbon fragments, a high amount of prompt NO is formed in the primary reaction zone (flame front), which can not be explained by the Zeldovich mechanism (Zeldovich 1946) alone. This NO is later carried on to the secondary zone where some of it may be converted to molecular nitrogen by reaction R-124 :

$$N + NO \longleftrightarrow N_2 + O \qquad\qquad (R\text{-}124)$$
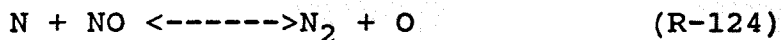
The pathway for formation of prompt NO from hydrocarbon radicals involves the same key intermediate HCN found during the fuel bound Nitrogen conversion as illustrated in Fig.1.1

This study focusses on the major radical species

profiles in the flame front of a rich methane flames, and a methane flame doped with ammomia.

Flat Flame Structure

A schematic diagram of a flat flame is shown in Fig-2.1. The charcteristic times and distances shown correspond to a flame operated at atmospheric pressure. The boundaries between the zones are not distinct. Therefore the spatial and characteristic time assignments in the figure are arbitrary, but they provide an idea of scale for each of the regions in the flame.

Transport processes dominate in the preheat zone. Gases in the preheat zone are heated by conduction of energy released in the primary reaction zone back along the very steep temperature gradient which separates the two regions. Simultaneously, free radicals generated in the primary reaction are transported back into the unburnt gases, the preheat zone, by molecular diffusion. The unburnt gases enter the primary reaction zone by a combination of convective and diffusive transport processes.

Several phenomena are characteristic of the primary reaction zone. Gases become hot enough for the branching reactions R-1 and R-2:

$$H + O2 \longleftrightarrow OH + O \qquad (R1)$$

$$O + H2 \longleftrightarrow OH + H \qquad (R2)$$

to proceed at appreciable rates. These reactions are respon-

$$H + H + M \rightleftharpoons H_2 + M$$

$$H + OH + M \rightleftharpoons H_2O + M$$

$$H + O_2 + M \rightleftharpoons HO_2 + M$$

$$H + O + M \rightleftharpoons OH + M$$

1.-100 MSEC

SECONDARY REACTION
(RECOMBINATION)
ZONE

$$OH + H_2 \rightleftharpoons H + H_2O$$

$$H + O_2 \rightleftharpoons OH + O$$

$$O + H_2O \rightleftharpoons OH + OH$$

$$O + H_2 \rightleftharpoons OH + H$$

$$CO + OH \rightleftharpoons CO_2 + H$$

AND

HYDROCARBON OXIDATION
REACTIONS

0.01-0.1 MSEC — PRIMARY REACTION ZONE

0.3 MSEC — PREHEAT ZONE

FLAME HOLDER

PREMIXED GAS
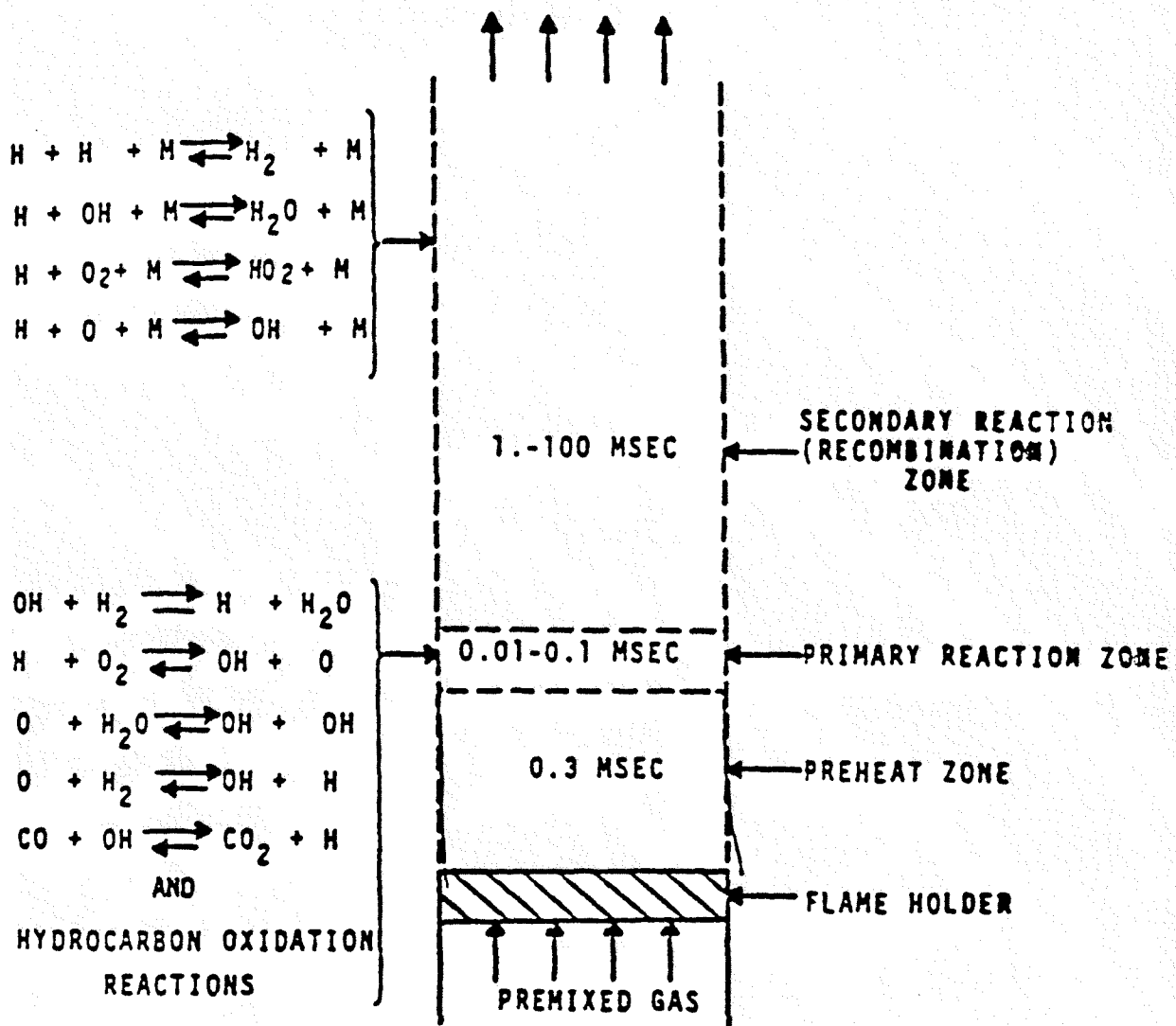
FIGURE 2-1

SCHEMATIC OF UNIDIMESIONAL FLAT FLAME

sible for generating the radical concentrations in excess of equilibrim values observed experimentally in the primary reaction zone or early in secondary reaction zone.

Consumption of hydrocarbon fuel by oxidation reactions to form CO and other combustion products is another important process characteristic of the primary reaction zone. The exothermicity of these reactions provide the major pathway for the release of chemical potential energy in the form of sensible heat during the combustion. In flames with lean or near stoichiometric fuel equivalence ratios hydrocarbon are completely converted to CO, CO_2, and H_2. The end of the primary reaction zone in fuel lean flames can be characterized by the disappearance of hydrocarbons (CH_4, C_2H_6) and the maximization of radical (CH_2, CH) concentrations, all of which occur at roughly the same position. In such lean flames the concentration of CH and CH_2 is infintesimal. As a result the rates for the reaction R-98 and R-193:

$$CH + N_2 \; \texttt{<----->} \; HCN + N \qquad\qquad (R-98)$$

$$CH_2 + N_2 \; \texttt{<------>} \; HCN + NH \qquad\qquad (R-193)$$
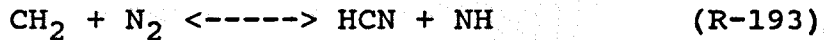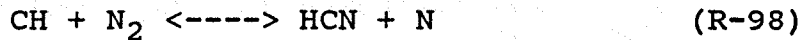
is not high enough to form prompt NO. In such flame the source of NO is the superequilibrim concentration of O atom (reaction -R-124) and the Zeldovich mechanism (Zeldovich 1946):

$$N + O_2 \quad \longleftrightarrow \quad NO + O \qquad (R-125)$$

$$N + OH \quad \longleftrightarrow \quad NO + H \qquad (R-126)$$

$$O + N_2 \quad \longleftrightarrow \quad NO + N \qquad (-R-124)$$
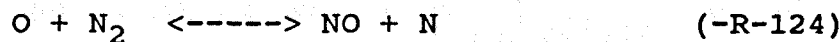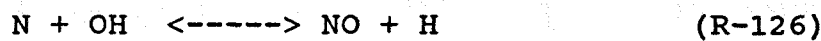
In rich flame hydrocarbon survive the primary reaction zone. Concentration of CH and CH_2 are high enough to make the prompt NO formation reactions important. In such cases the end of the primary zone are appropriately characterized by the maximization of radical concentrations such as CH_3, CH_2, CH.

The secondary zone is characterized by the reduction in radical concentrations and in total moles of the system. These reductions are governed by relatively slow termolecular recombination reactions such as R-5 through R-7 :

$$H + H + M \longleftrightarrow H2 + M \qquad (R-5)$$

$$H + OH + M \longleftrightarrow H2O + M \qquad (R-6)$$

$$H + O2 + M \longleftrightarrow HO2 + M \qquad (R-7)$$
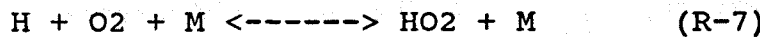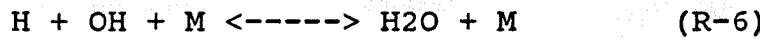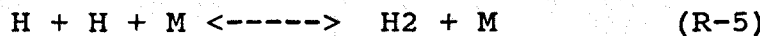
It is the slow rates of these combination reactions, relative to the fast bimolecular branching reactions, at the high flame temperatures which enable radicals to reach super equilibrim concentrations in the primary reaction zone. When concentrations of O_2 and H_2 become low near the end of the primary reaction zone, the branching reactions, as well as other bimolecular reactions becomes equilibrated. The net rate of radical generation by the branching reactions decreases to the point where termolecular, recombination reactions dominate changes in radical concentrations. In

fuel rich flames, where hydrocarbons and hydrocarbon radicals persist beyond the primary reaction, the chemistry of the early secondary zone is affected and sometime dominated by hydrocarbon oxidation chemistry.

Reviews of the literature for the rate constant of the above mentioned chain branching and recombination reactions have been conducted by seveal authors (Baluch, et al 1972, 1973; Dixon Lewis, 1979; Warnatz, 1979). The Baluch reviews are widely used critiques and summaries of rate constant information derived from flame as well as other experimental systems more suitable for study of the kinetic mechanisms.

The work of Dixon-Lewis (1979) is more recent. The recommended rate constants by Dixon-Lewis (1979) are the product of optimizing the fit of model predictions based upon reactions of hydrogen and oxygen bearing species data from flame and explosion limit systems involving $H_2/O_2/N_2$ mixtures. To the extent that transport properties influence the parmeters investigated, the rate constant recommended by Dixon Lewis et al, may reflect bias and errors introduced by the particular transport model and properties selected for inclusion in their numerical models.

The recommended rate constants of Warnatz (1979) are attractive in principle because they are based upon input from independent sources, without attempting to fit flat flame model prediction to data. The Warnatz (1979) recommendations thereby eliminate potential bias in rate constants due to approximations and uncertainty in modelling of the

flat flame transport phenomena. Warnatz (1979) recommenda-
tions for the chain branching and recombination reactions
are therefore used in the mechanism developed here.

Premixed Flame Equation

The equations governing steady, isobaric, quasi-one dimensional flame propagation is written as (Kee, Miller, Smooke and Grcar, 1987):

$$\dot{M} = \rho u A \tag{3.1}$$

$$\dot{M}\frac{dT}{dx} - \frac{1}{c_p}\frac{d}{dx}\left[\lambda A \frac{dT}{dx}\right] + \frac{A}{c_p}\sum_{k=1}^{K}\rho Y_k V_k c_{p_k}\frac{dT}{dx} + \frac{A}{c_p}\sum_{k=1}^{K}\dot{w}_k h_k W_k = 0 \tag{3.2}$$

$$\dot{M}\frac{dY_k}{dx} + \frac{d}{dx}\left[\rho A Y_k V_k\right] - A\dot{w}W_k = 0 \qquad (k=1,\ldots,.K) \tag{3.3}$$

$$\rho = \frac{p\overline{W}}{RT} \tag{3.4}$$

Where x = Spatial coordinate;

M = Mass flow rate (which is independent of x);

T = temperature ;

Y_k = mass fraction of kth species;

p = pressure;

u = velocity of the mixture;

$\int$ = Mass Density;

W_k = the molecular weight of kth species;

= Mean molecular weight of the mixture;

R = universal gas constant;

= the thermal conductivity of the mixture;

c_p = constant pressure heat capacity of mixture;

c_{pk} = constant pressure heat capacity of kth

species;

= the molar rate of production by chemical

reaction of the kth species per unit

volume;

h_k = the specific enthalpy of kth species;

V_k = the difusion velocity of kth species;

A = cross sectional area of the stream tube

encompassing the flame (normally increas-

ing).

Equation 3.1 is for the continuity of mass flow or preservation of total mass. Equation 3.2 results due to the conservation of energy in flame (an important assumption in this derivaion is, negligible heat loss). The first term in equation 3.1 denotes the temperature gradient in x direction (vertical) arising due to the conduction (2nd term), convection (3rd term) and generation (4th term) of heat. Equation 3.3 represents the individual species preservation. The first term in equation 3.3 denotes the species concentration gradient along the x direction (vertical) due to species diffusion (2nd term) and destruction or creation (3rd term). Equation 3.4 is the equation of state for ideal gas.

The net production rate w_k of each species k results from a competition between all chemical reactions involving that species. It is assumed that each reactions in the mechanism are elementary and follow the law of mass action. The forward rate coeficients are in the modified Arrhenius

form:

$$k_f = A*T^{\beta} \exp(-E_a/RT) \qquad\qquad (3.5)$$

Transport properties of the species, thermal conductivities and diffusion coefficients are calculated by the Transport code of Sandia National laboratory (J.F. Kee, J.F. Grcar, M.D. Smooke, 1987). The code uses the Stockmayer (Hirschfelder, Curtiss,and Bird, 1954) potential in calculating the transport properties. An extended Eucken-Hirschfelder (Hirschfelder, Curtiss, and Campbell, 1976) correction for polyatomic species is used in computing the single component conductivities. The gas mixture thermal conductivity is determined from the individual component conductivities using an empirical combination average formula (Mathur, 1967).

The formulation of species diffusion is documented in the report by Kee (1983). Briefly the diffusion velocity V_k is assumed to be composed of three parts.

$$V_k = \sqrt{}_k + W_k + V_c$$

$\sqrt{}_k$ is the ordinary diffusion velocity and is given by the Curtiss-Hirschfelder (1949) approximation:

$$\sqrt{}_k = -D_k(1/X_k)(dX_k/dx)$$

where X_k is the mole fraction, and where the mixture averaged diffusion coefficent D_k is given explicitly in terms of

the binary diffusion coefficents D_{jk} by:

$$D_k = (1 - Y_k)/(\Sigma_{j=k} X_j/D_{kj})$$

A non-zero thermal diffusion velocity W_k is included only for the low molecular species H, H_2, and He . The trace light component limit is employed in determining W_k i.e.

$$W_k = (D_k k_{tx}/X_k)(1/T)(dT/dx)$$

where k_{tx} is the thermal diffusion ratio (Chapman and Cowling, 1970). The positive sign of k_{tx} makes the lower molecular weight species diffuse from low to high temperature regions.

The correction velocity V_c (independent of species but a function of x) is included to ensure that mass fractions sum to unity (or equivalently $\Sigma_{k=1} Y_k V_k = 0$). This formulation of the correction velocity is the one recommended by Coffee and Heimerl (1981,1983) in their extensive investigation of approximate transport models in hydrogen and methane flames.

Boundary Conditions.

The appropriate boundary condition for burner stabilized laminar flame is deduced from the early work of Hirschfelder and Curtiss (1949). For burner stablized laminar flame M the mass flow reate is a known constant, the temperature and mass flux fractions:

($\epsilon_k = Y_k + \lceil Y_k V_k A/m$) are specified at the cold

boundary (flame holder), and vanishing gradient are imposed at the hot boundary.

Numerical Solution Method

The equations (3.1,3.2,3.3,3.4) for the burner stabilized flames are solved by using the FLAME code developed at Sandia National Laborataries (J.F. Kee, J.R. Grcar, M.D. Smooke, M.D. Miller, 1987). The numerical solution procedure begins by making finite difference approximations to reduce the boundary value problem to a system of algebraic equations. The initial approximation are usually on a very coarse mesh that may have as few as five or six points. After obtaining a solution on the coarse mesh, new mesh points are added in regions where the solution or its gradient changes rapidly. An initial guess for the solution on the finer mesh is obtained by interpolating the coarse mesh solution. This procedure continues until no new mesh point are needed to resolve the solution to the degree specified.

The system of algebraic equation are solved normally by by damped Newton method. If the Newton algorithym fails to converge, the solution estimate is conditioned by a time integration. This provides a new starting point for the Newton algorithm that is closer to the solution and thus more likely to be in the domain of convergence for Newton
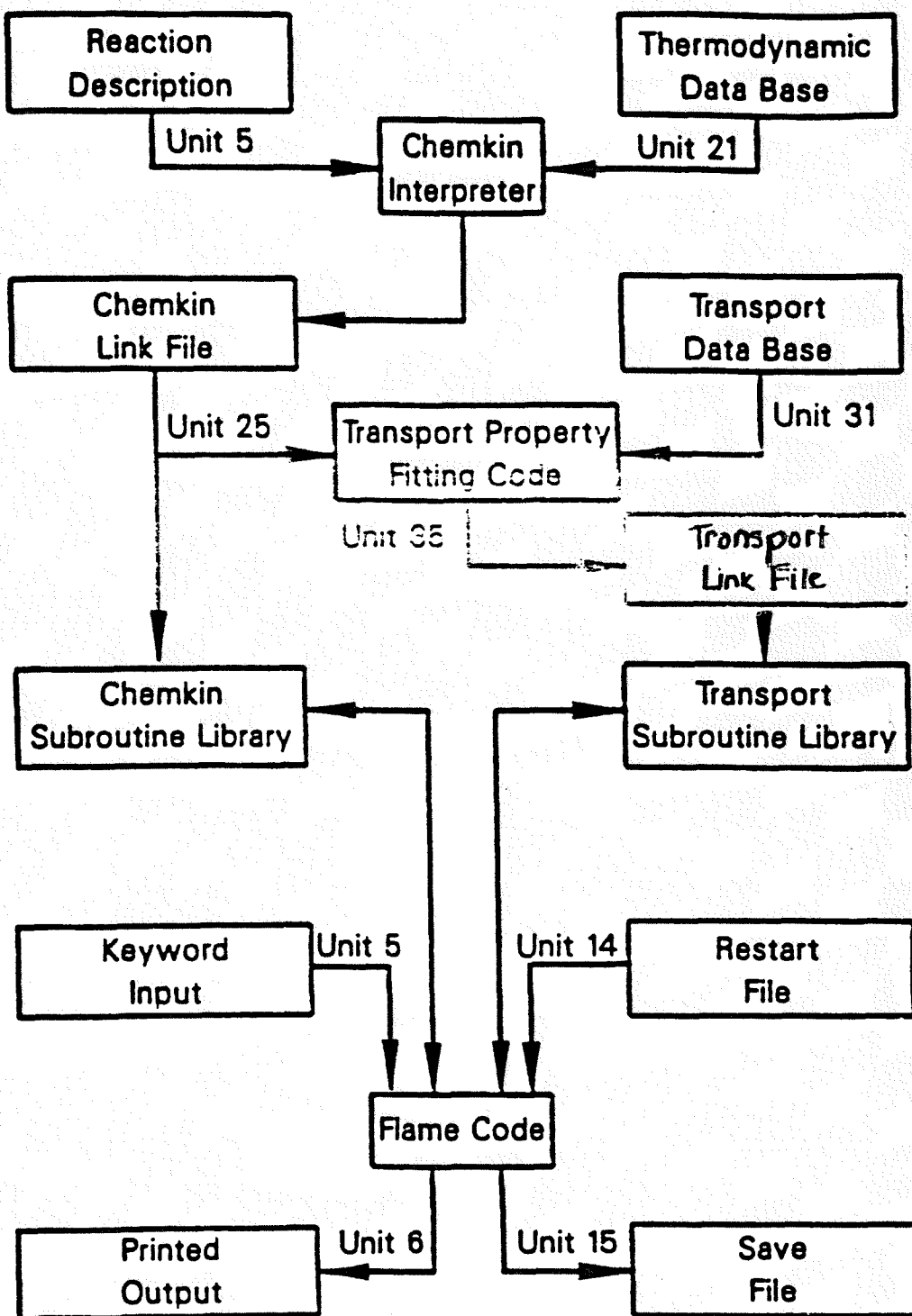
Figure 2.2 : Relationship of the flame program to CHEMKIN & TRANSPORT preprocessors and input and output file. (Kee. Miller, 1986)

method. As the mesh becomes finer it is normally found that the estimate interpolated from the previous mesh is within the domain of convergence of Newton's method. This is the key point to the solution strategy.

Finally the structure of the Flame code in relation to the CHEMKIN (Kee, Miller, Jefferson, 1980) code is given in the Figure 2.2. In figure 2.2 unit 5 is the elementary reaction mechanism developed in this study and unit 21 is the thermodynamic data base for the species in the mechanism. These are the two inputs for the Chemkin interpreter (Kee, Miller, Jefferson, 1988) which generates a binary link file (Unit 25). The transport property fitting code (Kee, Warnatz, Miller, 1988) generates the binary transport link file (Unit 35) for the species in the mechanism. These two binary file along with the Keyword input (Unit 5 which species the flame condition) are the input for the flame code (Kee, Miller, Smooke, Grcar, 1988). The flame code then solves the equation 3.1, 3.2, 3.3, 3.4 following the procedure stated earlier. It generates a output file (Unit 6) which contains the solution (species concentrations, temperature and Mass flow rate in all the mesh), along with a binary version of the output.

Discussion of Bimolecular QRRK

In the mechanism developed in this work bimolecular QRRK is extensively used to predict rate constants for reactions which proceed through energized adducts, including radical recombination, insertion, and addition to unsaturates. The fate of the chemically activated adduct as shown in Figure 3-1 is determined among the following pathway:

a. It can decompose back to reactants.

b. It can be collisionally stabilized.

c. It can isomerize.

d. It can decompose to new products.

Bimolecular QRRK formulated by Dean (1985) is used to determine the temperature and pressure dependencies of the above mentioned pathways.

Dean bimolecular QRRK is based on quantum version of Kassels (1928) unimolecular theory. Kassel in his now famous article showed that for unimolecular reactions the rate constant at high pressure k_{∞} is truely independent of pressure.

Similarly Dean (1985) showed that for bimolecular reactions the stabilization and the chemically activated pathways have different pressure dependencies. The stablization channel rate constant is independent of pressure at its high pressure limit. The rate constants for the activated reactions are pressure independent in its low pressure limit.
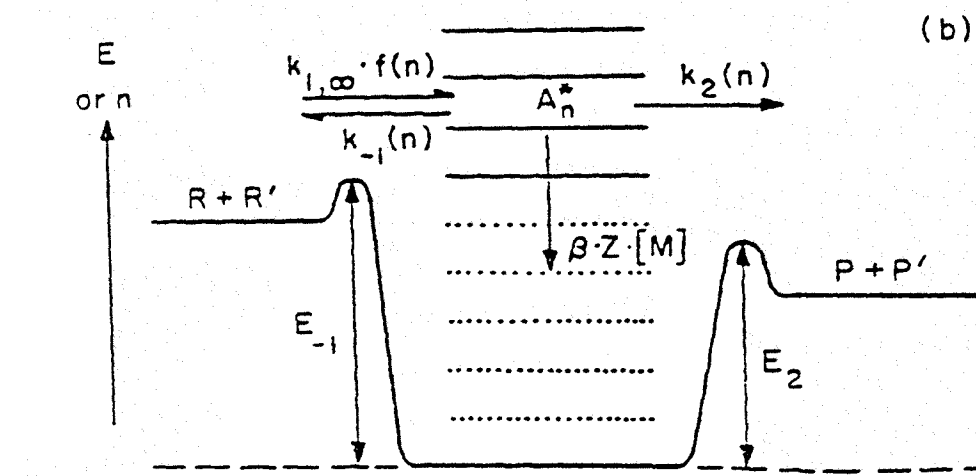
FIGURE 3.1 ENERGY DIAGRAM FOR BIMOLECULAR REACTIONS

Bimolecular QRRK with isomerization

Chemically activated isomerization is a plausible extension for Bimolecular QRRK pheonomena. Any unimolecular reaction that is open to the ground state adduct is also available to the excited adduct, and isomerization clearly fits this requirement. Dean (1985) QRRK approach has been extended to allow the chemically activated complex to isomerize twice, such that the system has three potential wells. The following scheme represents this where A, B, C are the stable isomers, P_2 to P_7 are the possible reaction products from the chemically activated complexes and R + R^* are the combining reactant species.

```
      P2          P3     P5           P6             P8
       \          /       \           |  /            |
        \K2    /K3          \K5       |  /K6          | K8
         \    /                \     / /              |
 *   K1   \  /      K4          \   / /     K7        |
R↑R ====== A* ====== B* =============C*------P9
    K-1    |      K-4          |       K-7           |
           |                    |                     |
           A                    B                     C
```
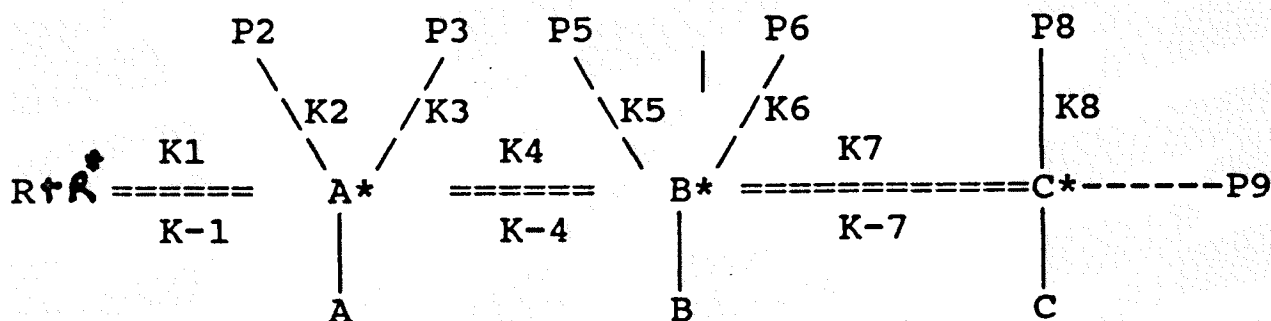
Applying the steady state assumption to the activated activated species A^*, B^*, C^* one can define the follow ing apparent rate constants :

$$k_{stab\ A} = d[A]/dt/[R][R^*] = k_1 \Sigma[\{ZY - k_{-7}(E)\}\beta k_S[M]]/DENOM\ f(E,T)$$

$k_{p2} = d[p_2]/dt/[R][R^*] = k_1 \Sigma k_2(E)\{ZY + k_7(E)k_{-7}(E)\}/DENOM\ f(E,T)$

$k_{stab\ B} = d[B]/dt/[R][R^*] = k_1 \Sigma \{k_4(E)\beta k_s[M]\}/DENOM\ f(E,T)$

$k_{p6} = d[p_6]/dt/[R][R^*] = k_1 \Sigma \{Zk_4(E)\beta k_s[M]/DENOM\ f(E,T)$

$k_{stab\ C} = d[C]/dt/[R][R^*] = k_1 \Sigma \{k_7(E)k_4(E)\beta k_s[M]/DENOM\ f(E,T)$

$k_{p9} = d[p_9]/dt[R][R^*] = k_1 \Sigma \{k_7(E)k_4(E)k_9(E)\}/DENOM\ f(E,T)$

Note that all summation runs from $n=m_i$ to $n=\infty$, where n and m_i are defined below.

Where DENOM = $X*Z*Y - X*k_{-7}(E)*k_7(E) - Z*k_{-4}(E)*k_4(E)$

$X = \{k_{-1}(E) + k_2(E) + k_4(E) + k_3(E) + \beta k_s[M]\}$

$Y = \{k_5(E) + k_6(E) + k_7(E) + k_{-4}(E) + \beta k_s[M]\}$

$Z = \{k_8(E) + k_9(E) + k_{-7}(E) + \beta k_s[M]\}$

Where f(E,T) is the fraction of A^* at a specific energy level with energy content of E. The hv and E_{crit} is the threshold energy to dissociate back to reactant. The chemical activation distribution function f(E) can be expressed as :

$$f(E) = k_{-1}(E)K(E)/\{\Sigma_0^\infty k_{-1}(E)K(E)\}$$

With $K(E) = \alpha^n (1-\alpha)^n (n+s-1)/\{n(s-1)\}$

Where $\alpha = \exp(-hv/KT)$; s = Number of vibrational degrees of freedom. v is the geometric mean of the vibrational frequencies.

The energy dependent rate constant $k_i(E)$ is written

from Kassel (1928):

$$k_i(E) = A_{i,\infty} \frac{n!(n - m_i + s - 1)!}{(n - m_i)!(n + s - 1)!}$$

where $A_{i,\infty}$ is the high pressure preexponential factor

for reaction i. $n = E/hv$, i.e. the total number of quanta

of energy available, $m_i = E_i/hv$, i.e. the number of quanta

corresponding to the energy threshold for reaction i.

The value of collisional rate constant k_s is comput-

ed by using Lennard Jones collision rate:

$$k_s = 2.708 \ k_{hs}(e/KT)$$

where k_{hs} is the hard sphere collision rate constant.

Collision efficiency is calculated from Troe

(1977) expression :

$$\beta/(1-\beta^{1/2}) = -<\Delta E_{coll}>/F(E) \ KT$$

The term $<\Delta E_{coll}>$ denotes the average amount of

energy transfered per collision and $F(E)$ is a factor weakly

dependent on energy, that is related to the number of excit-

ed states. $F(E)$ was found to have a median value of 1.15

(Troe, 1977) over the temperature interval of 300-2500 for a

series of reactions. Note that β is dependent on tempera-

ture.

A computer program following the above scheme has

been developed, by modifying the existing QRRK/CHEMACT code

(Ritter, 1989) which predicts the temperature and pressure

dependency of the different chemical activated pathways for a three well system.

All the QRRK or CHEMACT (Ritter,1989) calculation reported in the subsequent section had been carried out by using this code. Another improvement in this code over earlier code is in the manner it writes the output. It writes out apparrent generated rate only for the activated products, for any specified temperature and pressure in a format which is easily amenable for LOTUS or HARVARD GRAPHICS plotting.

Necessary Input data for bi-molecular QRRK and limitations:

Reasonably accurate predictions can be made quickly using QRRK, in part because the input data are few and relatively easy to obtain. These data are:

a. Pre-exponential factors and activation energies in the high pressure limit, A_∞ and $E_{act,\infty}$;

b. The number of vibrational degrees of freedoms for the adduct, ($3*n_{atoms}-5$ for linear, $3*n_{atoms}-6$ for nonlinear);

c. The geometric mean vibrational frequencies, of the adduct $< v >$;

d. Molecular weight and the Lennard -Jones transport properties σ and ϵ/k, for the adduct and for the third body gas; and

e. The average energy transferred per collision with the third body gas, $<\Delta E_{coll}>$, which has been experimentally evaluated for a variety of gases.

Obtaining A_∞ and $E_{act,\infty}$ may be the most difficult. These parameters are obtained from literature data, thermochemical kinetic methods (Benson, 1976;Benson, 1983), generic rate constants (e.g. Dean, 1985), or the reverse rate constant (high pressure limit) and the equilibrim constant.

Lennard - Jones collisional properties (Reid, Prausnitz and Sherwood, 1977; Kee et al. , 1983)for the stabilized species A and the third-body gas M are used to calculate a collision number Z_{LJ}. Establishing the $<\text{\textae} E_{coll}>$ needed to calculate collisional efficiency β is an active area of research. The geometric mean frequency for the adduct is obtained from literature. In the absence of literature data CPFIT from THERM computer code (Ritter,1989) is used to obtain the necessary data.

Ambiguities in these parameters cause uncertainty in the rate constant predictions. For example the QRRK $k_{rxn}(E)$ equation contains the assumption that A_∞ and $E_{act,\infty}$ are independent of temperature, but they may not be. Second the vibrational degrees of freedom include internal rotations, which are not well approximated as harmonic oscillators. The equivalent frequency for an internal rotation can be rather low, so uncertainity in this can affect a geometric mean frequency $<v>$ dramatically. Third the assignment of all the excess energy to vibrational energy can be inexact when there are significant energy changes in angular momentum. Finally, the rationale for using a single $<v>$ to represent all the v's in a molecule may not always be correct.

CH RADICAL ADDITION AND COMBINATION REACTIONS

CH is one of the most important radicals in the present mechanism for the formation of prompt NO. It is also proposed as the key radical in a wide variety of reaction systems. Examples include chemionization in hydrocarbon flames [Kistiakowsky et al. 1964] and chemiluminescence [Lichtin, 1984]. It is also implicated as a major species in the chemistry of planetary atmospheres [Strobel, 1982]. Chemiluminescence originating from the $A^2\Delta \longrightarrow X^2\pi$ transition of CH at 430 nm has been observed in a number of hydrocarbon and hydrocarbon doped systems. It also has been found to accompany the low temperature reactions of O atoms with hydrocarbons, especially in discharge flow studies involving unsaturated compounds.

In this section result from the QRRK analysis for CH radical reactions with H_2, N_2, NO, O_2, CH_4 are discussed. Note that in this section Chemact (for chemical activation) and QRRK may be used interchangeably.

Temperature and pressure dependencies of these reactions as predicted by chemical activation analysis provides plausible pathways for these reactions under high temperature oxidation condition. Comparisons of the temperature and pressure dependent predictions are made with experimental data wherever it is available. Prior to the more recent kinetic investigation using tunable dye lasers (Berman and

Lin, 1983, Zabarnick, and Fleming, 1984) experimental data for CH kinetics were scarce. In fact there were only two such studies, both only at room temperature. Braun et al (1967) measured the rate of reactions of CH with H_2, N_2, and CH_4 by the vacuum UV flash photolysis/UV absorption technique, monitoring the disappearance of CH via the $C^2\Sigma^+$ <----- $X^2\pi$ transition at 314 nm. Bosnali and Perner (1971) used a combination of electron beam initiation and UV absorption (at 314 nm) to determine the rates of CH reactions with a number of reaction partners. No studies of temperature and pressure effects were included in these earlier works.

The development of new experimental techniques with the advent of tunable dye lasers facilitated some of the recent experiments on CH reactions. These will be referenced in later sections, on temperature and pressure dependence of the CH radical reactions

Reaction of CH with Hydrogen molecule

The reaction :

$$CH + H2 \longleftrightarrow CH_3 \qquad (5.1)$$

$$\longleftrightarrow CH_2 + H \qquad (5.2)$$
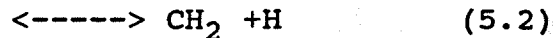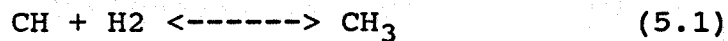
is a very important in the flame chemistry. Because the reverse of reaction 5.2 establishes the CH profile in the flame, which in turns largely governs the prompt NO formation via the reaction:

$$CH + N_2 \longleftrightarrow HCN + N. \qquad\qquad (5.4)$$
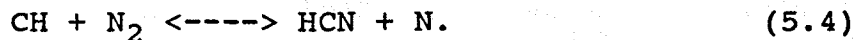
In addition to its importance in combustion and in planetary atmospheres, the reaction $CH + H_2$ is of considerable fundamental interest as a prototype for carbyne chemistry. It involves the methylidyne radical the simplest carbyne and H_2 the simplest diatomic molecule. As a result, this reaction has attracted both experimental and theoritical atention. Ab initio molecular orbital calculation by Brooks and Schaefer (1977) showed that the least motion insertion path occur when the CH radical is perpendicular to the H_2 molecule, with an energy barrier of about 75 Kcal/mole. For the non least motion or parallel approach they found there was little or no energy barrier.

Experimental studies (Berman and Lin, 1984, Bosnali and Perner, 1971, Butler and Fleming 1981, Zabarnick and Fleming, 1984) for this reaction were carried out under quite different conditions. As a result these experimentally determined rate constants varied by a factor of 20. In this study we attempt to explain some of these results and describe the reaction mechanism.

The energy level diagram and the input parameters for the chemical activation calculation on the reaction of CH + H_2 are illustrated in Figure 5.1 and Table A-2 in the Appendix respectively. The parameters in table A-2 are referenced to the ground state (stablized) level of the complex.

The recently measured value of k_1 by Berman et al. (1984) was used for the insertion/addition forward direction

Figure 5.1 P.E. diagram for CH + H2
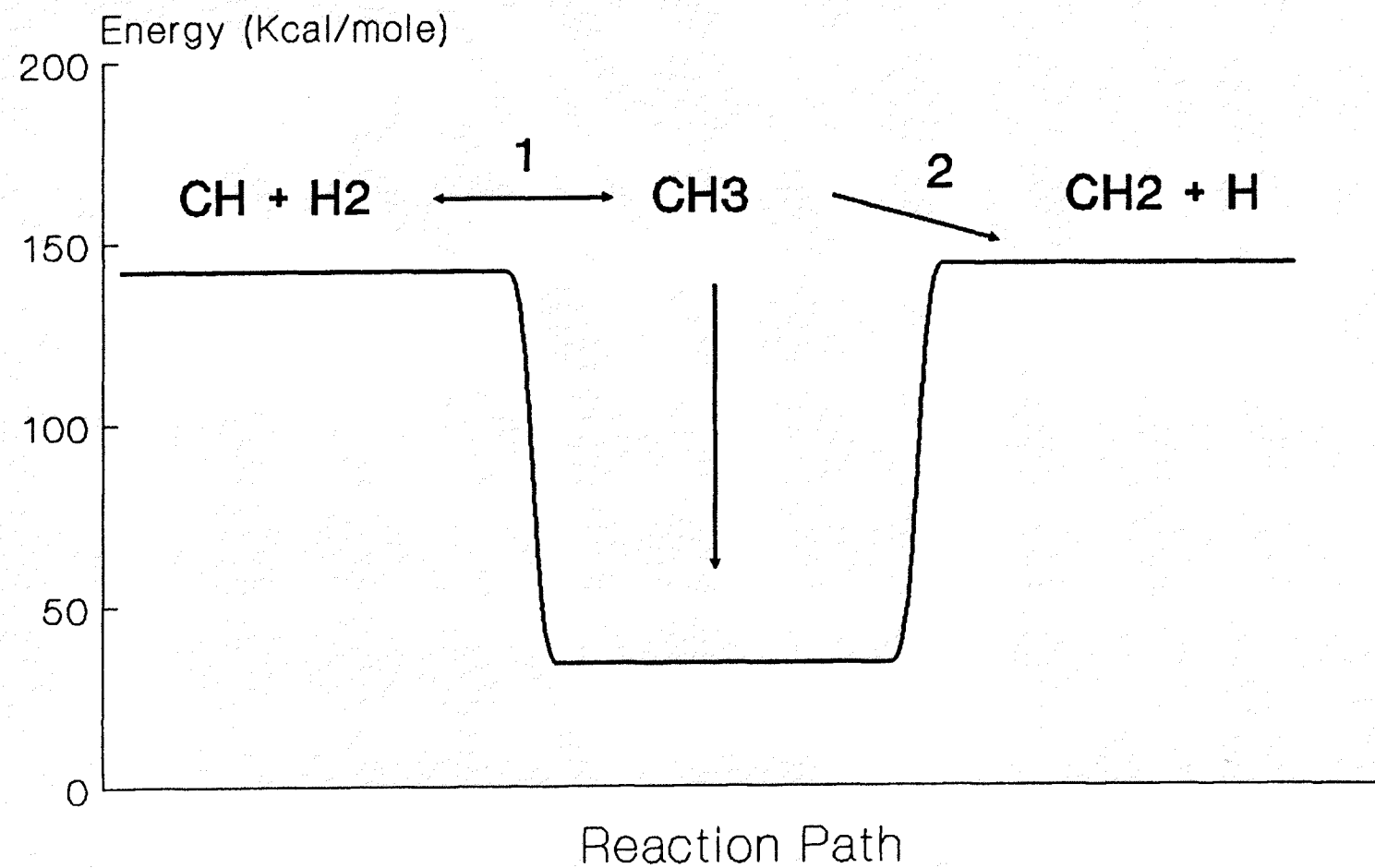
channel. A zero activation energy for the forward direction and initial structures are as per Brooks and Schaeffer (1977). The barrier and A factor for dissociation of the complex back to reactants were obtained via ΔH_{300} and ΔS_{300} (using an S_f of Transition state of CH_3 which is 1 cal/mole higher than stable CH_3). The kinetic parameters for the dissociation to $CH_2 + H$ were obtained using a value of 1.2E+14 suggested by Berman and Lin (1984) for the high pressure recombination rate constant for the reverse reaction. The geometric mean frequency was calculated by method of Benson (1976) for the transition state complex. The Lennard Jones collision diameter and well depth were taken from Kee, Warnatz and Miller (1988).

As shown in the Figure 5.1 the $CH + H_2$ system has two available reaction channels, a stabilization to CH_3 Equation (5.1) and an dissociation (abstraction) to $CH_2 + H$ equation (5.2). The abstraction pathway is slightly endothermic with $\Delta H_{298} = 2.5$ kcal/mole. The competition between reaction channels including dissociation back to reactant manifest itself in the observed over all rate constants. Figure 5.2 presents the available experimental data and the QRRK results. The data shows a decrease in overall reaction rate constants with increase in tempeature below 400 K. The QRRK/Chemact results are consistent with the data of Berman and Lin (1984).

In Figure 5.3 QRRK result demonstrates that stabilization will dominate in lower temperature. Dissociation to CH_2

CH + H2 -----) CH2 + H
Comparison of QRRK and Experiment

Rate Constant * 1.0E-12   ● 100 torr

CH + H2 -----) CH2 + H
Comparison of QRRK and Experiment

Rate Constant * 1.0E-12   ● 297 K

—— QRRK   + Experiment (Fleming)

—— QRRK   + Experiment (Berman & Lin)

CH + H2 -----) Products
Comparison of QRRK and Experiment:
@ 100 torr

Rate Constant * 1.0E-12

Temperature K

—— QRRK   + Experiment (Berman & Lin)
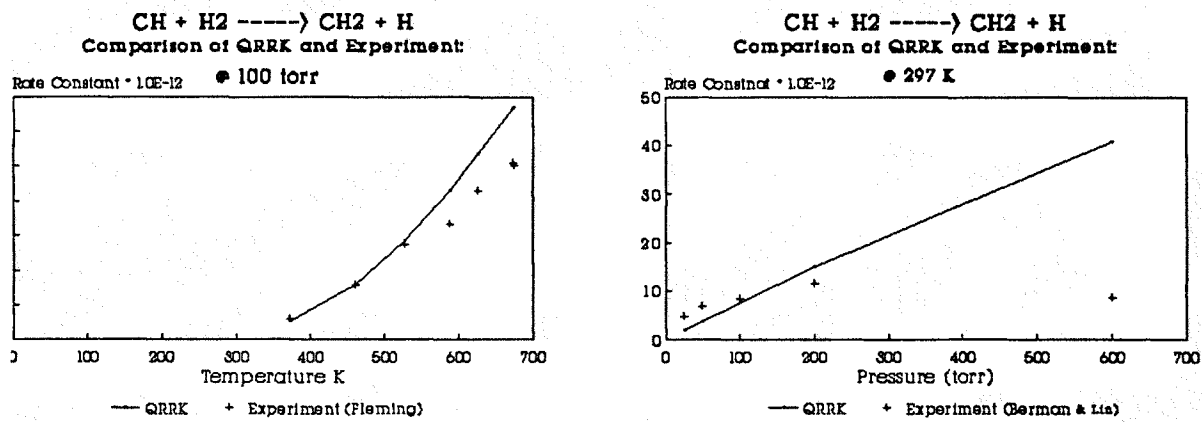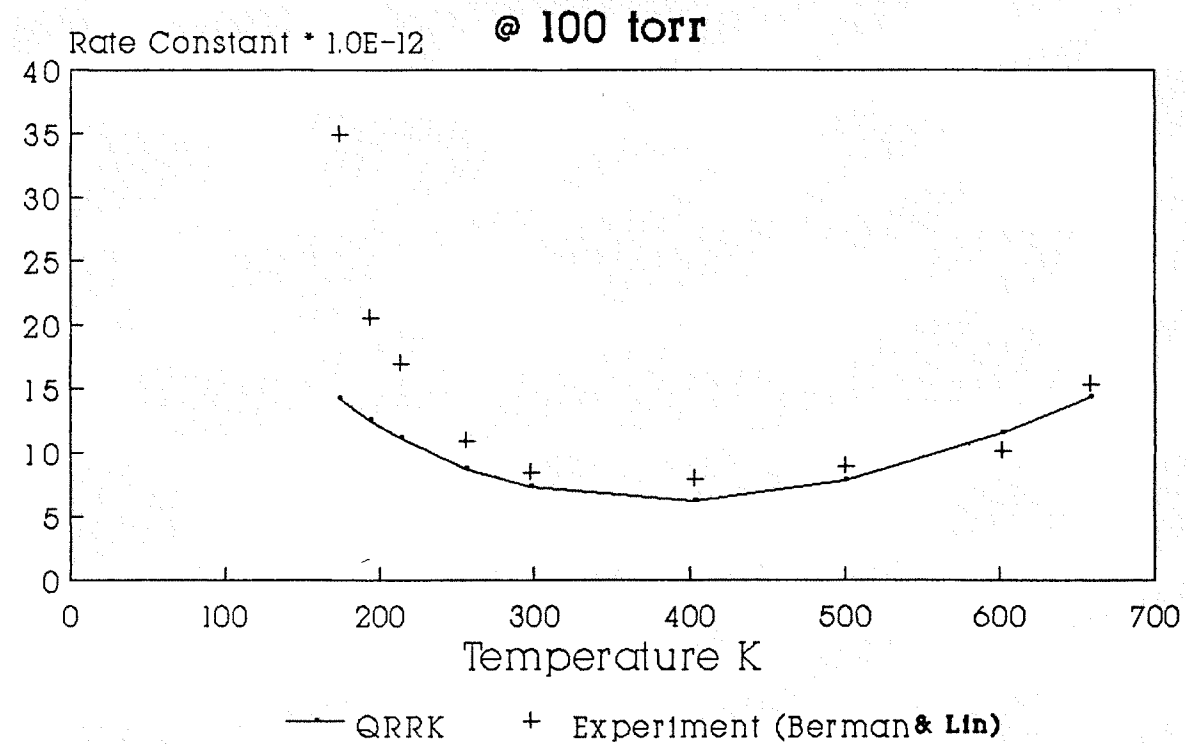
Figure 5.2: Comparison of Temperature & Pressure dependence
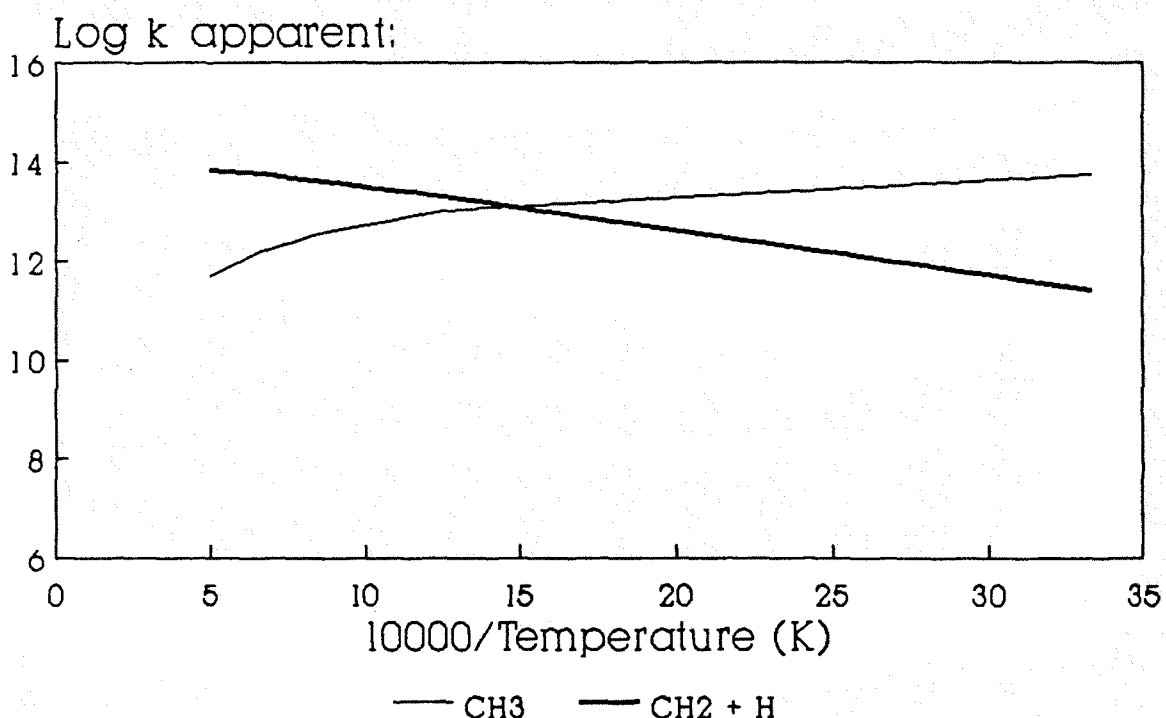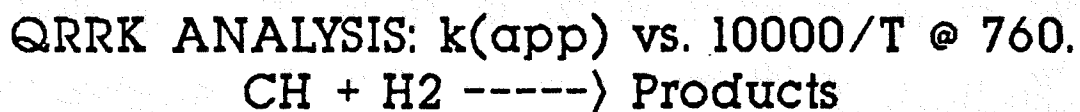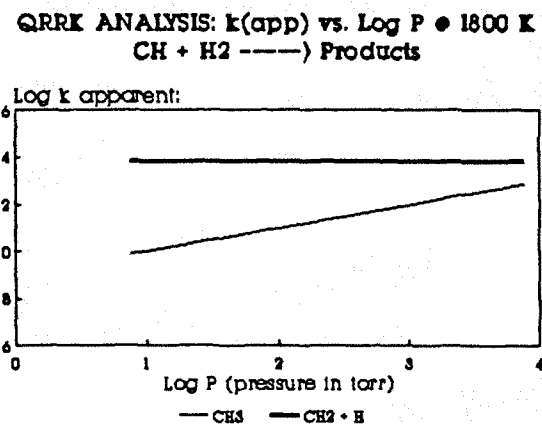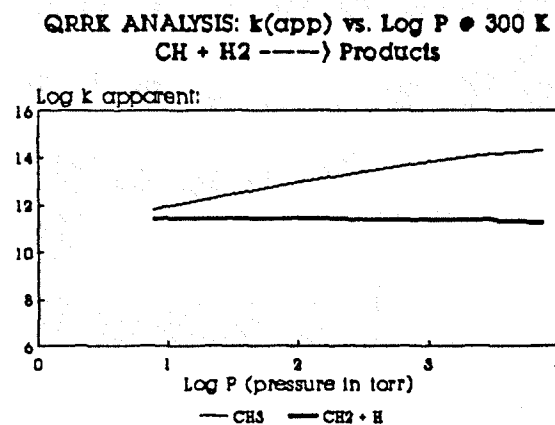
Figure 5.3 : Temperature & Pressure dependence

+ H will dominate at higher temperature, which is consisent with the Berman and Lin (1984) data. In the temperature region above 400 K the rate increases and as a result the overall total results show an inversion in the temperature dependence at 400 K. At lower temperatures the QRRK method underestimates the overall rate constant by factor of two and half. This is also the case in RRKM calculations by Berman and Lin (1984). This can perhaps be attributed to the temperature dependence of β_c (collisional efficiency) as defined by Troe (1977). We note that a shallower well (Higher Energy) would amplify this underestimation.

Comparison of the apparent rate constant for the abstraction channel with the data of Zabarnick and Fleming (1984) in Figure 5.2 also shows good agreement.

Even though at high pressure the QRRK over estimates the overall rate constant it is quite reasonable to use the predicted apparent rate constant for the abstraction channel at 760 torr in the mechanism developed for flame modeling. This is because of the pressure independence of the abstraction channel in the temperature regime of flame, where the stabilization channel is insignificant in comparison to the abstraction channel.

Reaction of CH with N2 molecule

The reaction of CH + N_2 is of considerable importance due to its role in the chemistry of planetary atmospheres and hydrocarbon flames. This reaction is included in modeling

the chemistry of the nitrogen and hydrogen rich atmosphere of Titan (Strobel, 1982) This reaction is also of considerable importance for the present mechanism because it establishes the NO profiles in the flames studied. The CH + N2 system is interesting to the modelers of such system in that it represents the least endothermic pathway for a hydrocarbon fragment to break the N#N triple bond. This provides for incorporation of N atom and other nitrogen containing compounds in the subsequent reaction mechanism.

Recent interest in the CH + N2 reaction has been part of an effort to unravel the mechanism of NO formation in hydrocarbon air flames similar to the flames studied in this research. Production of NO in such flame cannot be described by the Zeldovich (1946) mechanism which successfully accounts for NO production in the postcombustion region. Fenimore (1972) proposed the reaction of carbon or hydrocarbon radical with N2 such as:

$$CH + N2 \quad \longleftrightarrow \quad HCNN \qquad\qquad (5.3)$$

$$\longleftrightarrow \quad HCN + N \qquad\qquad (5.4)$$

followed by the oxidation of the intermediaite product HCN to account for the production of NO in the primary reaction zone. Blauwens et al (1977) measured absolute radical and molecule concentrations, by using molecular beam sampling with mass spectrometric detection. He found the activation energy for reaction (5.4) to be 11.1 kcal/mole. Matsui and

Nomaguchi (1978) found the amount of NO produced to be proportional to the CH concentration and estimated an activation energy for the reaction (5.4) to be 13.6 Kcal/mole. Miyauchi et al (1977), found that HCN formation takes place prior to NO formation supporting the above mechanistic suggestion for prompt NO formation. However they rejected reaction 3.4 for prompt NO formation on the ground of spin nonpreservation and proposed the reaction :

$$CH_2 + N_2 \text{ <----> } HCN + NH \hspace{2cm} (5.5)$$
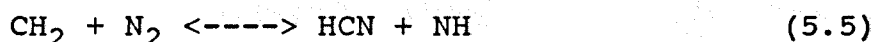
for prompt NO formation.

Braun et al (1967) and Bosnali and Perner (1971) each measured the rate constant of reaction 5.4 by monitoring CH $(X^2\pi)$ loss by absorption at 314 nm, and found rate constants at room temperature which differ by a factor of 14. Butler et al. (1981) using laser induced fluoroscence (LIF) detection determined a rate constants compatible to that of Bosnali and Perner, and found that the rate of CH + N_2 is pressure dependent, indicating that the reaction proceeds through a long lived intermediate. More recently Wagal et al (1982) using LIF confirmed the pressure dependence of this reaction and found a rate constant factor of two smaller than rate constant determined by Butler et al.

Berman et al (1983) has recently carried out a detail study of this reaction using photolysis of CH_3Br at 266 nm to generate CH radical which were detected by their LIF.

They measured rate constants for this reaction in the temperature range of 297 - 675 K at 100 torr and pressure range of 25 to 787 at 297 K. They found the second order rate to be pressure dependent, exhibiting a pronounced increase through the pressure range studied at 298 K.

Berman and Lin estimated a negative activation energy for the temperature range 297 - 675 K for the $CH + N_2$. At flame temperature Blauwens derived positive activation energy of more than 11 kcal/mole. These two set of contrasting data were reconciled by QRRK analysis on the formation of the activated complex $(CHN_2)^{\#}$:
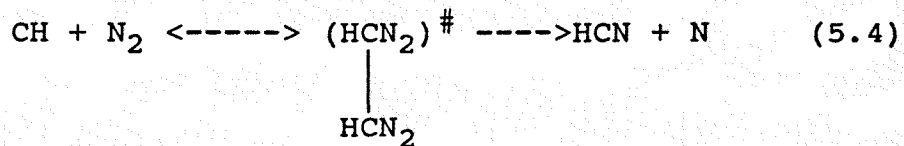
$$CH + N_2 \longleftrightarrow (HCN_2)^{\#} \longrightarrow HCN + N \qquad (5.4)$$
$$\downarrow$$
$$HCN_2$$

The energy level diagram and the input parameters for the chemical activation calculation on this reaction are shown in Figure-5.4 and Table A-4 of Appendix respectively. The parameters in Table A-4 are referenced to the ground level of the complex. The recently measured value of k_1 by Berman et. al (1984) was used for the high pressure addition channel. The A factor for dissociation of the complex back to reactants was obtained via ΔS_{300}. The well depth was calibrated to the stablization data of Berman (1984). The parameters for the dissociation to HCN + N were obtained by using 8.80E+12 for the reverse recombination and ΔS_{300}. The barrier height was adjusted to the recent experimental data

$$CH + N2 \longleftrightarrow_{1} (CHNN)^{\#} \xrightarrow{2} HCN + N$$
$$\xrightarrow{k_s} CHNN$$
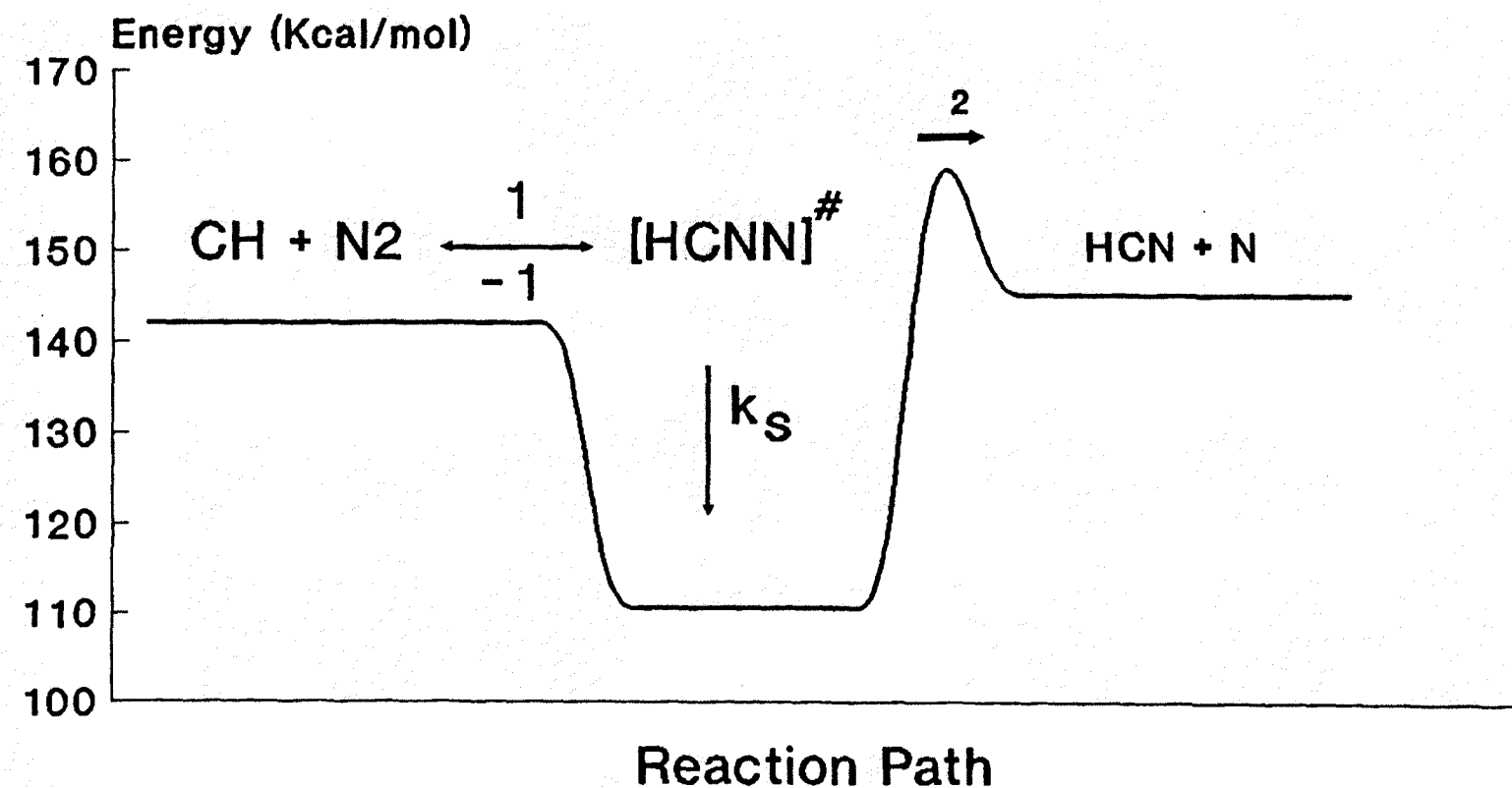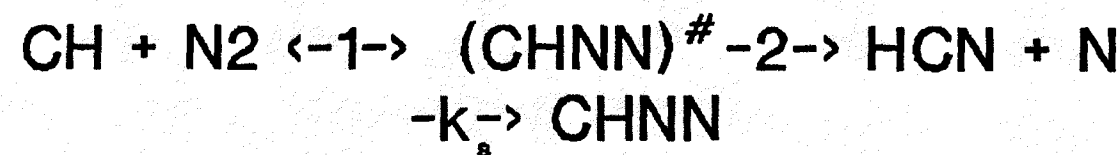
Figure 5.4 P.E diagram for CH + N2

Bond Energy 31.5 (+/− 2)
Consistent with Low T Data Berman / Lin

of Bowman and Hanson (1990). The geometric mean of the vibrational frequencies for the complex is from Berman (1984). The Lennard Jones collisional diameter and the well depth were estimated from Kee (1988).

The V shaped non Arrhenius temperature dependence curve shown in Figure 5.5 computed from QRRK analysis accounts for the grossly contrasting data of Berman and Blauwens in their respective low and high Temperature regimes. As seen in Figure 5.6 the pressure dependent stabilization channel dominates at low temperature. The abstraction starts dominating after 1500. The result are illustrated in Figure 5.5. At low temperature the overall rate for:

$$CH + N_2 <--- > (HCNN)^{\#} ----> HCN + N \qquad (5.4)$$

$$\downarrow$$

$$HCN_2 \qquad (5.5)$$
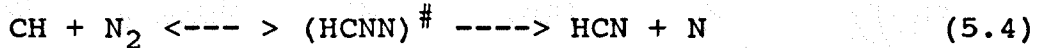
falls with increasing temperature resulting in an observed negative activation energy. Above 1500 K it increases with increasing temperature, yielding a positive observed activation energy.

It is interesting to note that the high pressure limit rate constant 4.0E+12 (A factor because of E_a= 0.0 from Table A-4) is more than two order of magnitude higher than the QRRK calculated apparent rate constant of 1.8E+10 to HCN + N, consistent with Bowman (1990). This result and from the fact that dissocition of the complex (HCNN)$^{\#}$ back to reactants has both high A factor and lower E than dissocia-

CH + N2 -----> Products
Comparison of QRRK and Experiment:
@ 100 torr

Rate Constant * 1.0E-10

— QRRK   + Experiment (Berman)   * Blauwens
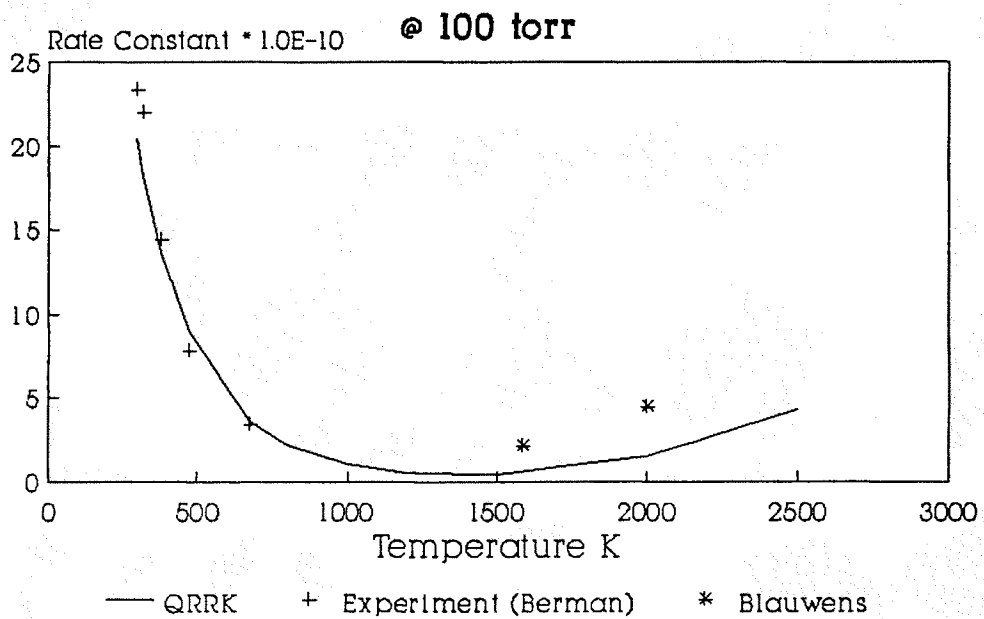
CH + N2 -----> HCN + N
Comparison of QRRK and Experiment:
@ 297 K
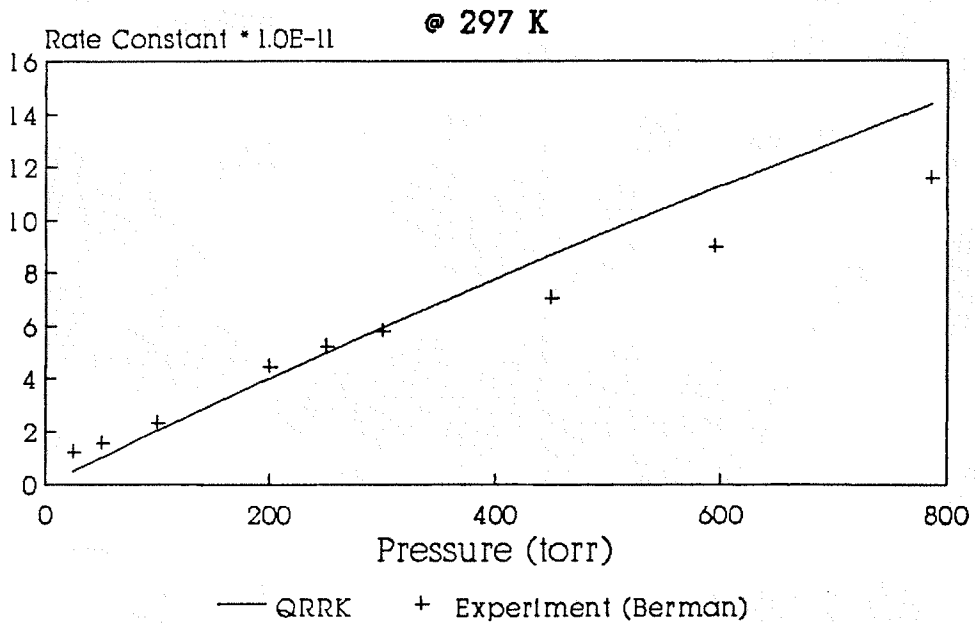
Rate Constant * 1.0E-11

— QRRK   + Experiment (Berman)

Figure 5.5: Temperatue & Pressure dependence comparison

25
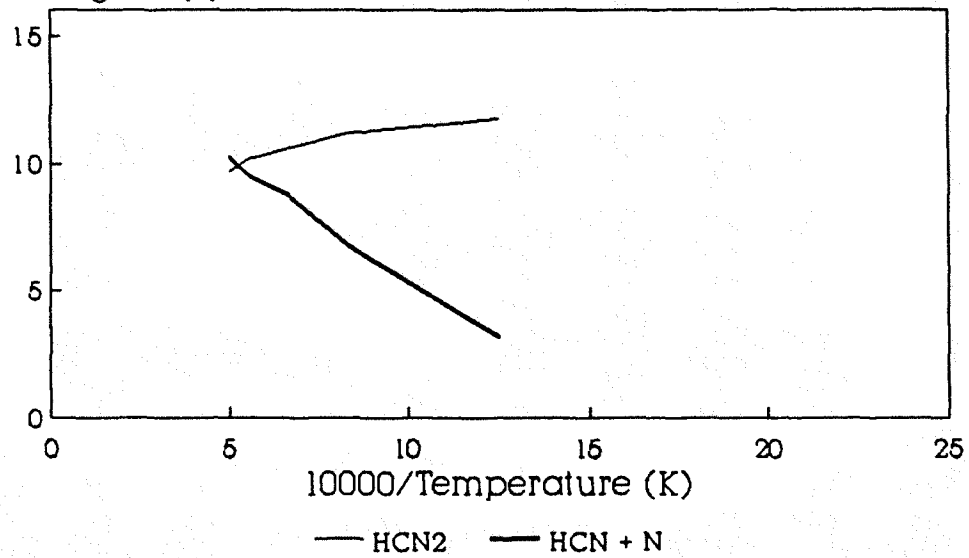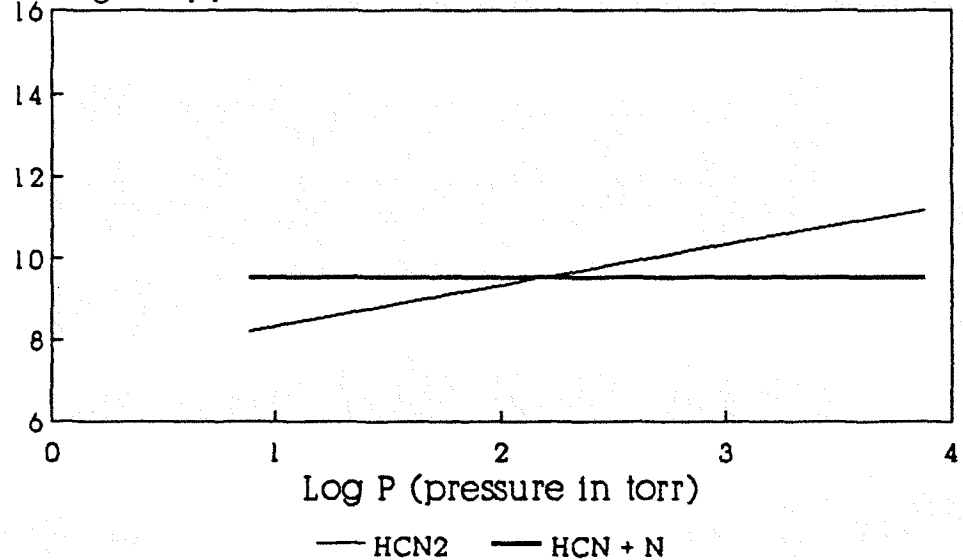
Figure 5.6: Temperature & Pressure dependence

tion to HCN + N (from Table A-4 of Appendix) indicates that the complex is indeed formed at the high pressure limit rate. But most of it dissociates (bleeds out) to the reverse channel than the HCN + N product. The observed low A factor to HCN + N is then the result of dominant energy and entropy path being reverse reaction to CH + N_2 for the adduct.

The QRRK results for temperature and pressure dependence as observed in Figure 5.5 is consistent with Berman data but QRRK underestimate at high temperature in comparison to the Blauwens data. This high temperature data is consistent with the high temperature data shock tube data of Dean and Bowman (1990).

Reaction of CH with NO

The reaction of CH with NO is important to flame chemistry because, along with other CH_x radicals it provides a pathway for destruction of NO in flames. Its contribution towards the destruction of NO in comparison to other CH_x radical is an important question which needs to be resolved. Experimental data on the temperature and pressure dependence of this reaction are scarce. Wagal et al (1982) determined rate constant for this reaction at 300 K to be $k_{NO} =$ 1.2 * 10^{14} cm^3/mole sec. Berman (1982) studied this reaction and found the rate constant to be independent of temperature in the range of 297 to 676 K at 100 torr.

The energy level diagram and important input parameters for QRRK analysis of this system are given in Figure 5.7 and

Figure 5.7: P.E. diagram for CH + NO

Energy (Kcal/mole)

250

200

CH + NO   1   HCNO

150

2

100

HCN + O

50

0

Reaction Path
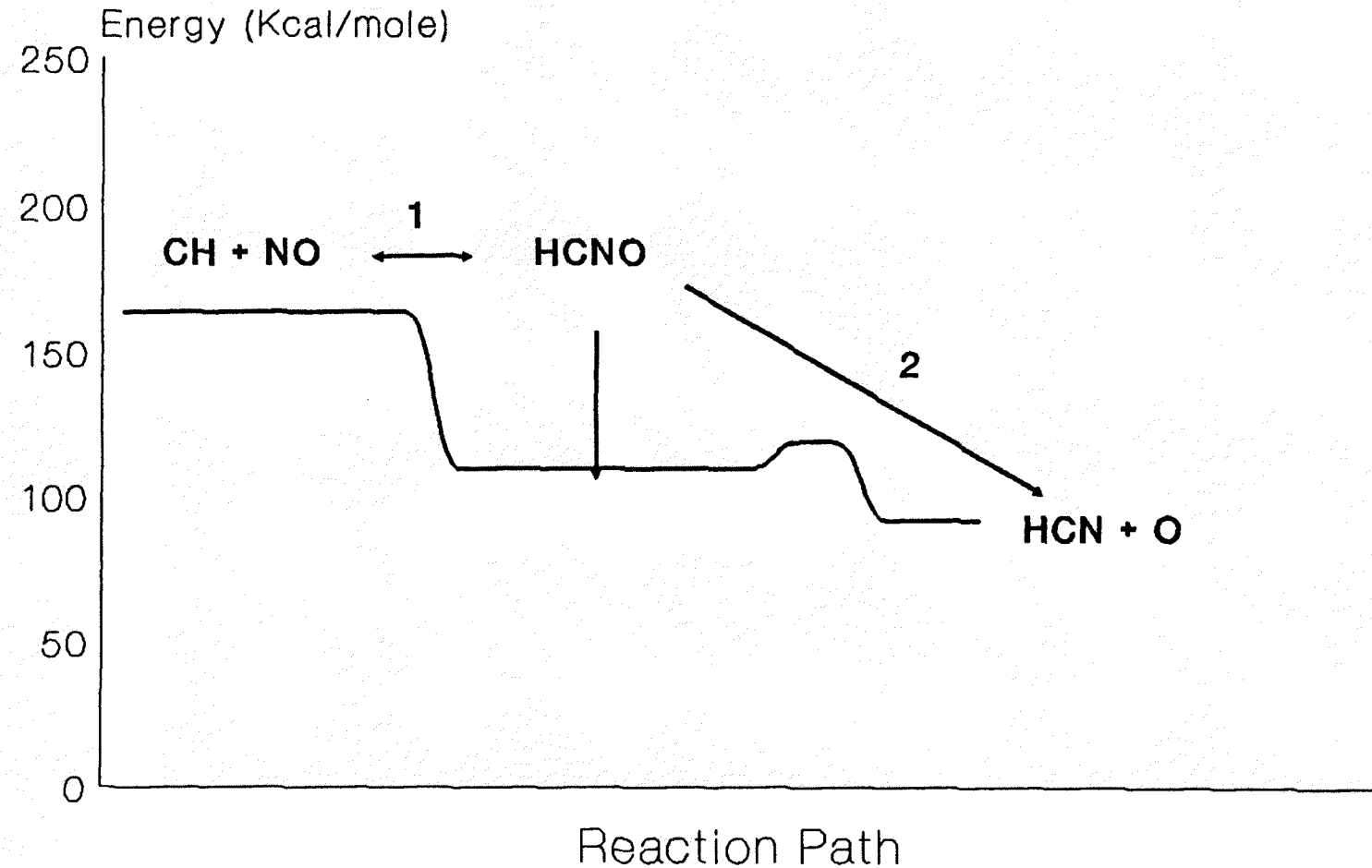
Table A-6 of Appendix respectively. The recently measured high pressure value of Berman is taken for k_1. The A factor and barrier for dissociation of the complex back to reactants were obtained via ΔH_{300} and ΔS_{300}. The thermochemical properties for HCNO are taken from Sandia thermodynamic data base (Kee, Miller 1985). The parameters for the dissociation of the HCNO complex to HCN + O were obtained using an estimate of 1.38E+13 for A_f for the reverse recombination reaction taken from the compilation of Kerr (1981) for O + CH#CH. The geometric mean frequency was calculated from Therm (Ritter, 1989). Lennard Jones collision diameter and well depth were estimated from data for HCCO. The CH radical combines with NO to form the HCNO* adduct. The reaction channels of HCNO* include dissociation back to reactants (k_{-1}), stabilization to HCNO (k_s, well depth equal to 125 Kcal) and dissociation to products (k_2) HCN + O.

The QRRK analysis are illustrated in Figure 5-8. As illustrated in Figure 5-8A there is no temperature dependence of the apparent rate constant in the temperature range of 285-673, and is consistent with the data of Berman (1982). This is because most of the complex formed has sufficient energy to dissociate to the low energy exit channel HCN + O before stabilization occurs. Figure 5-8 shows that stabilization is not important as compared to the low energy exit product channel even at 300 K and pressure of 1 atmp. The low energy exit channel rate starts to fall slightly at high temperature with increasing tempera-

QRRK ANALYSIS: k(app) vs. 10000/T @ 760.
CH + NO -----〉 Products

Figure: Log k apparent vs 10000/Temperature (K), with curves for HCNO and HCN + O.
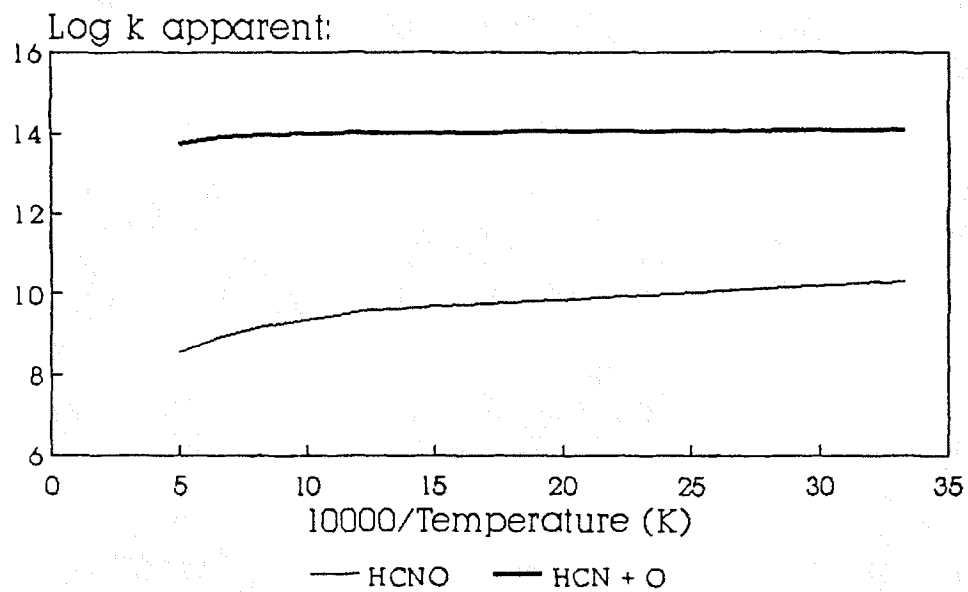
QRRK ANALYSIS: k(app) vs. Log P @ 300 K
CH + NO -----〉 Products

Figure: Log k apparent vs Log P (pressure in torr), with curves for HCNO and HCN + O.
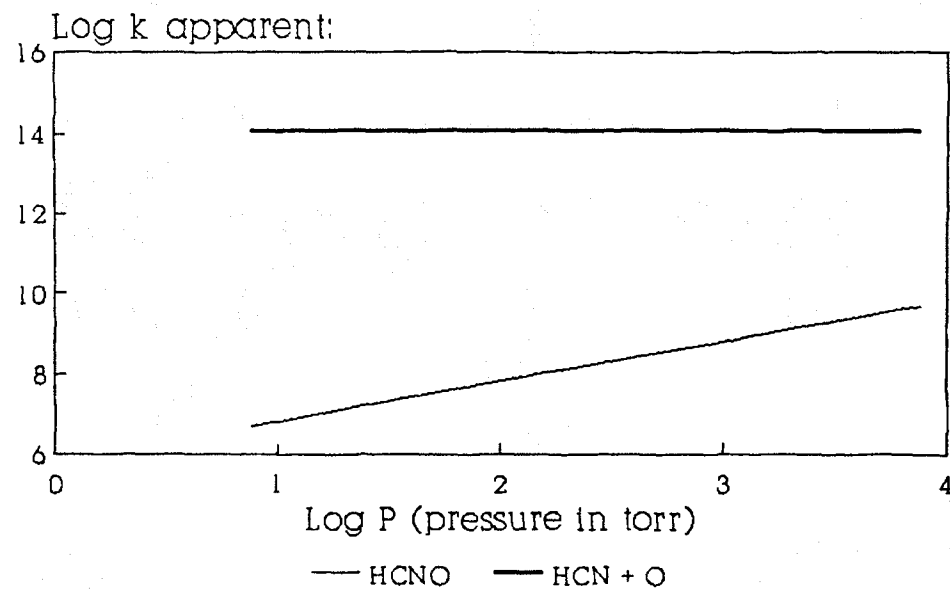
Figure 5.8: Temperature & Pressure dependence

CH + NO -----〉 Products
Comparison of CHEMACT and Experiment:
@ 100 torr

Rate * 1.0E-14

Temperature K

——— Chemact   + Experiment (Berman)
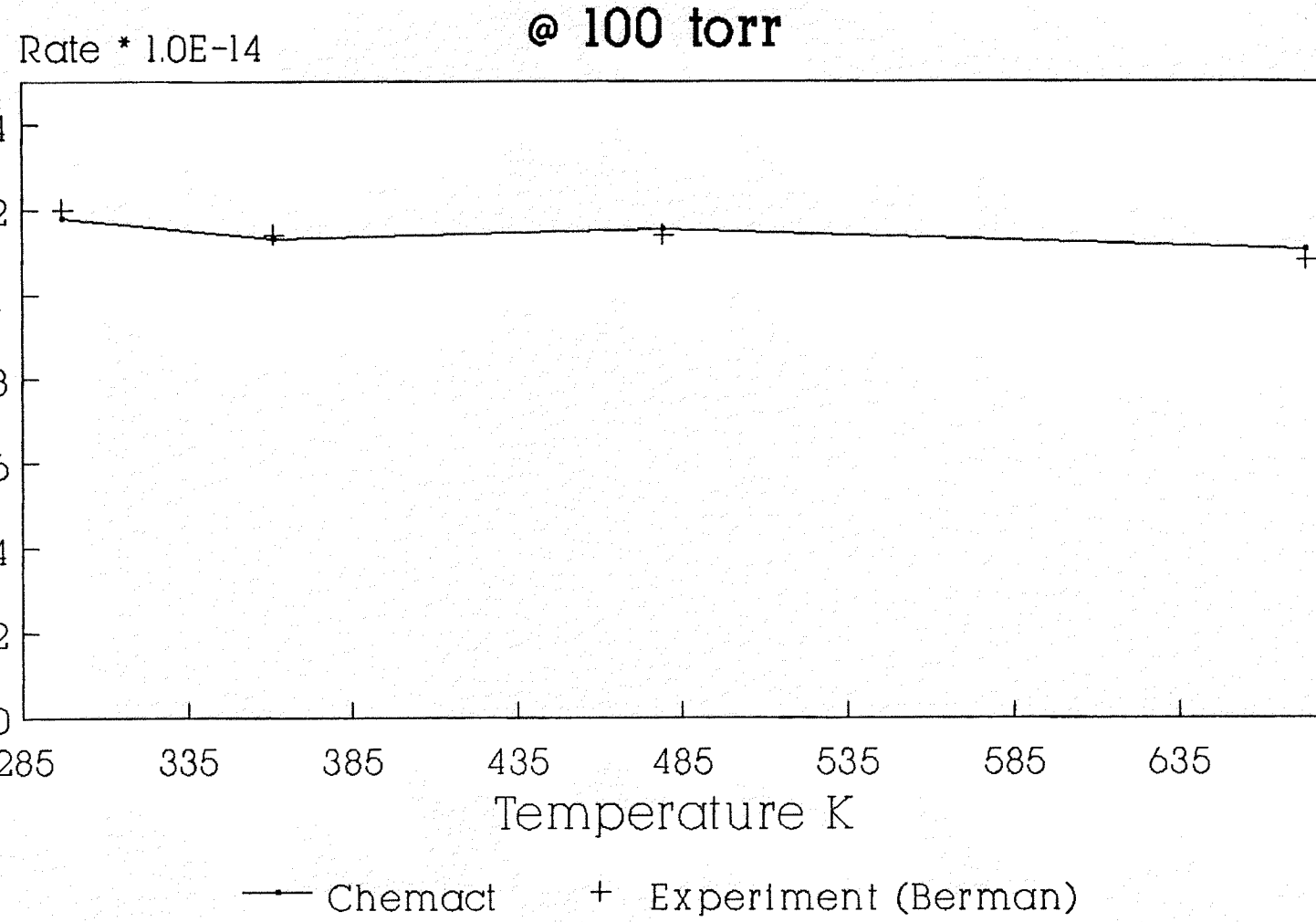
ture. This is because entropy now drives some of the complex HCNO* back to the reactants.

Reaction of CH with Oxygen molecule

This reaction provides a sink for the CH radical due to the relatively high O_2 concentrations. Experimental data for the temperature and pressure dependence of the product distribution is scarce. Messing et al (1979) measured the rate of this reaction by following the LIF signal of the CH radical and by monitoring the chemiluminescence from OH. They obtained a value of 1.98E+13 for the apparent rate constant at 298 K. The temperature dependence of this reaction was investigated by Berman et al (1984), who found no significant variation over the range 297 to 676 K. The rate constant they obtained at room temperature was 3.07E+13 cm^3/mole sec.

The energy level diagram and input parameters for the chemical activation calculation of this reaction are shown in Figure 5-9 and Table A-8 of Appendix respectively. The CH radical combines with O_2 to form the chemically activated adduct HCOO*. The reaction channels of HCOO* include dissociation back to reactants (k_{-1}), stabilization to HCOO (k_s), intramolecular isomerization to $HC(O)O^*$, and dissociation to the low energy exit channel: to HCO + O. $HC(O)O^*$ can then beta scission to H + CO_2 (k_4), be stabilized to $HC(O)O$, isomerize, back to $HCOO_*$ or isomerize forward to HOCO*. The HOCO* can then beta scission to H + CO_2 (k_7) or undergo

Figure 5.9 P.E. diagram for CH + O2

ENERGY (Kcal/mole)
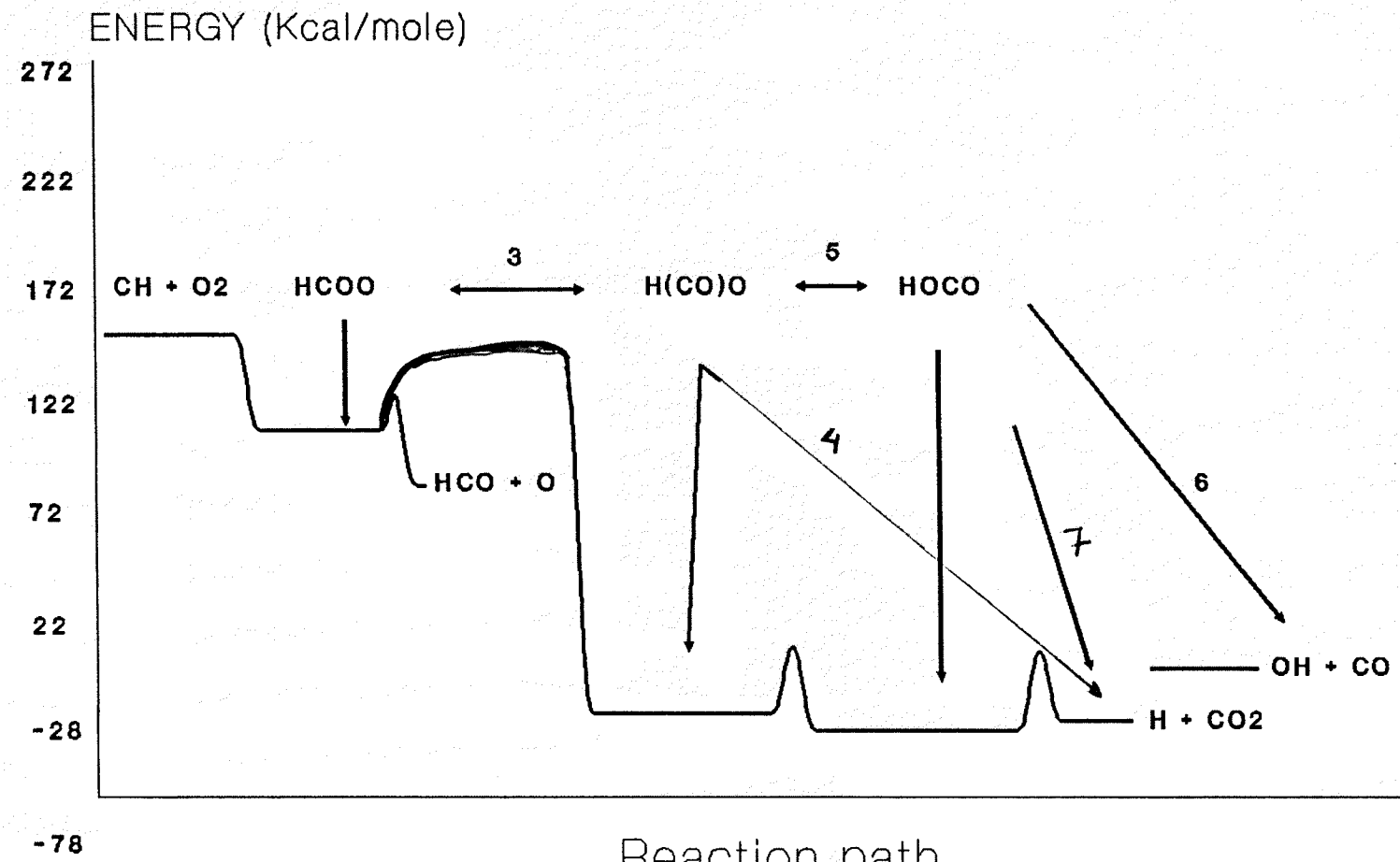
Reaction path

simple fission to OH + CO.

A plot of "Log k vs 10000/T" for the various apparent rate constants at 760 torr are shown in Figure 5-10. The data illustrate that even at high pressures and low temperatures more of the complex $HCOO^*$ dissociates to the HCO + O products then stablize, or isomerize. This is due low barrier and high A factor of this exit channel. The temperature independence as illustrated in Figure 5-10A of this reaction in the temperature range of 127 to 676 K is completely consistent with the Berman data.

A second way to analyze this CH + O_2 reaction is to consider that CH + O_2 inserts into O_2 to form complex $H(CO)O^*$, is shown in Figure 5-11. The $H(CO)O^*$ now formed can dissociate back to reactants (k_{-1}), isomerize to $HOCO^*$ (k_4), beta scission to H + CO_2 (k_3), or dissociate to HCO + O (k_2). The channel to form HCO + O from $H(CO)O_*$ requires now a higher barrier relative to the stabilized H(CO)O than the formation of HCO + O from $HCOO^*$, in the previous case. Here a C--O bond is breaking rather than the relatively weak O--O bond. The $HOCO^*$ complex can now isomerize backward(k_{-4}), decompose to OH + CO (k_6), or it can beta scission to H + CO_2. Figure 5-12 illustrates that OH + CO becomes a dominant channel rather than HCO + O. This is because the barrier as shown in Figure 5-11 for the channel HCO + O is now higher compared to the isomerization channel (where in previous case the isomerization barrier was higher) and as a result most of the complex $H(CO)O^*$ now

QRRK ANALYSIS: k(app) vs. 10000/T @ 760.
CH + O2 -----〉 Products

Log k apparent:

10000/Temperature (K)

—— HCOO   —— HCO + O   ······· H + CO2   - - - OH + CO

QRRK ANALYSIS: k(app) vs. Log P @ 1800 K
CH + O2 -----〉 Products

Log k apparent:

Log P (pressure in torr)

—— CHO2   —— HCO + O   ······· H + CO2   ·- - OH + CO
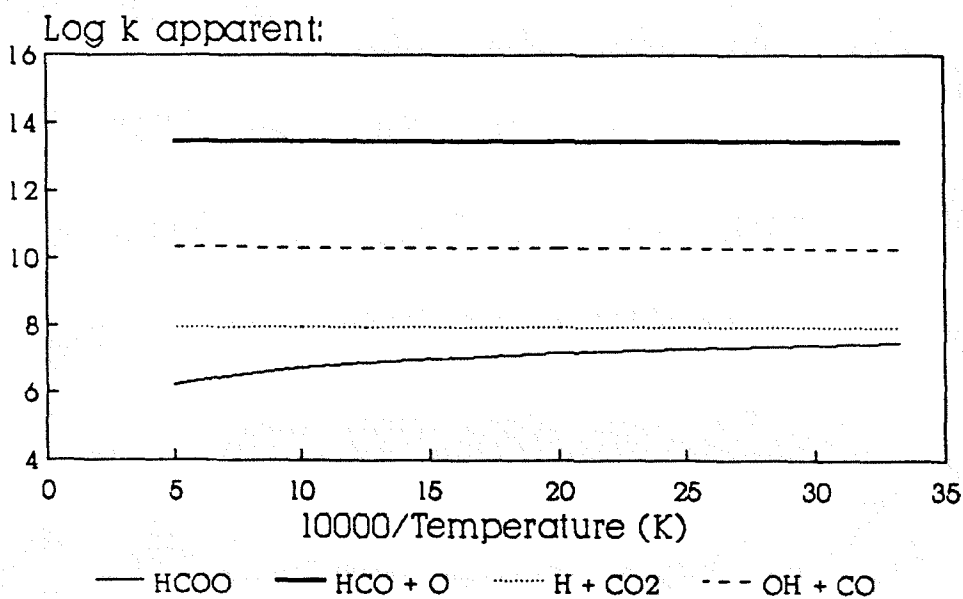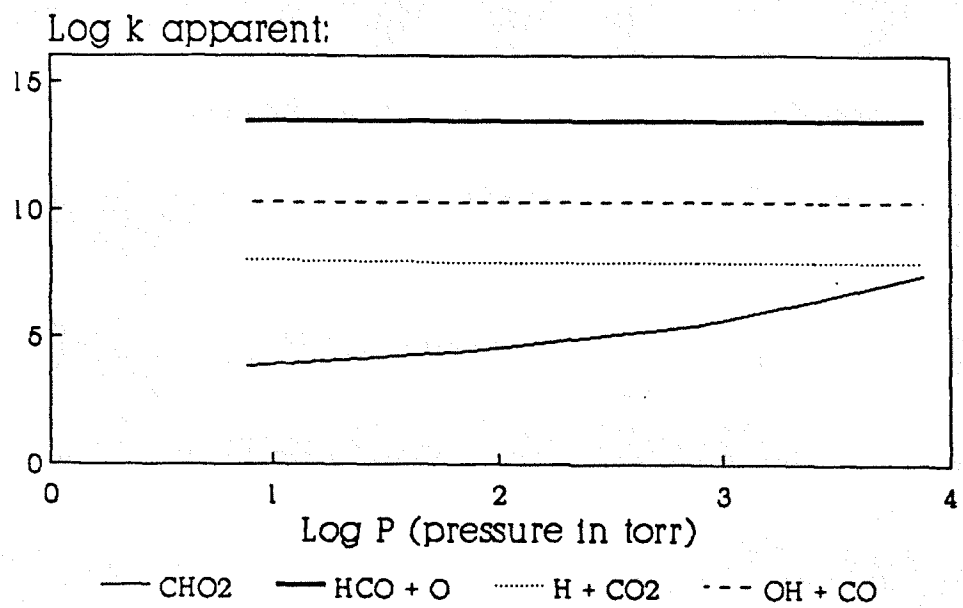
Figure 5.10: Temperature & Presure dependence

CH + O2 -----) Products
Comparison of QRRK and Experiment:
@ 100 torr

Rate Constant * 1.0E-13
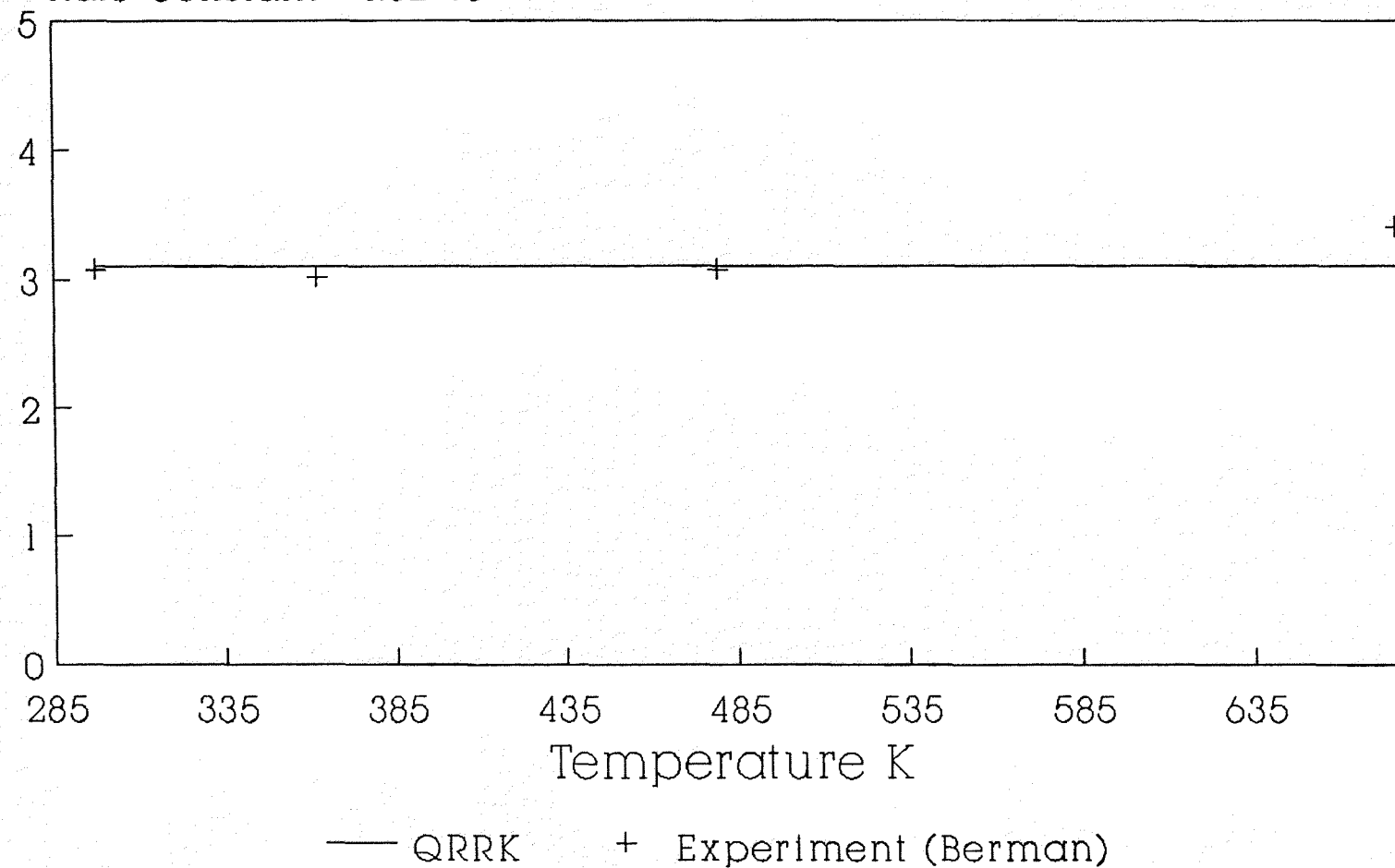
Figure 5.10A: Temperature dependence Comparison

Figure 5.11 P.E. diagram for CH + O2
Alternate attack

ENERGY (Kcal/mole)
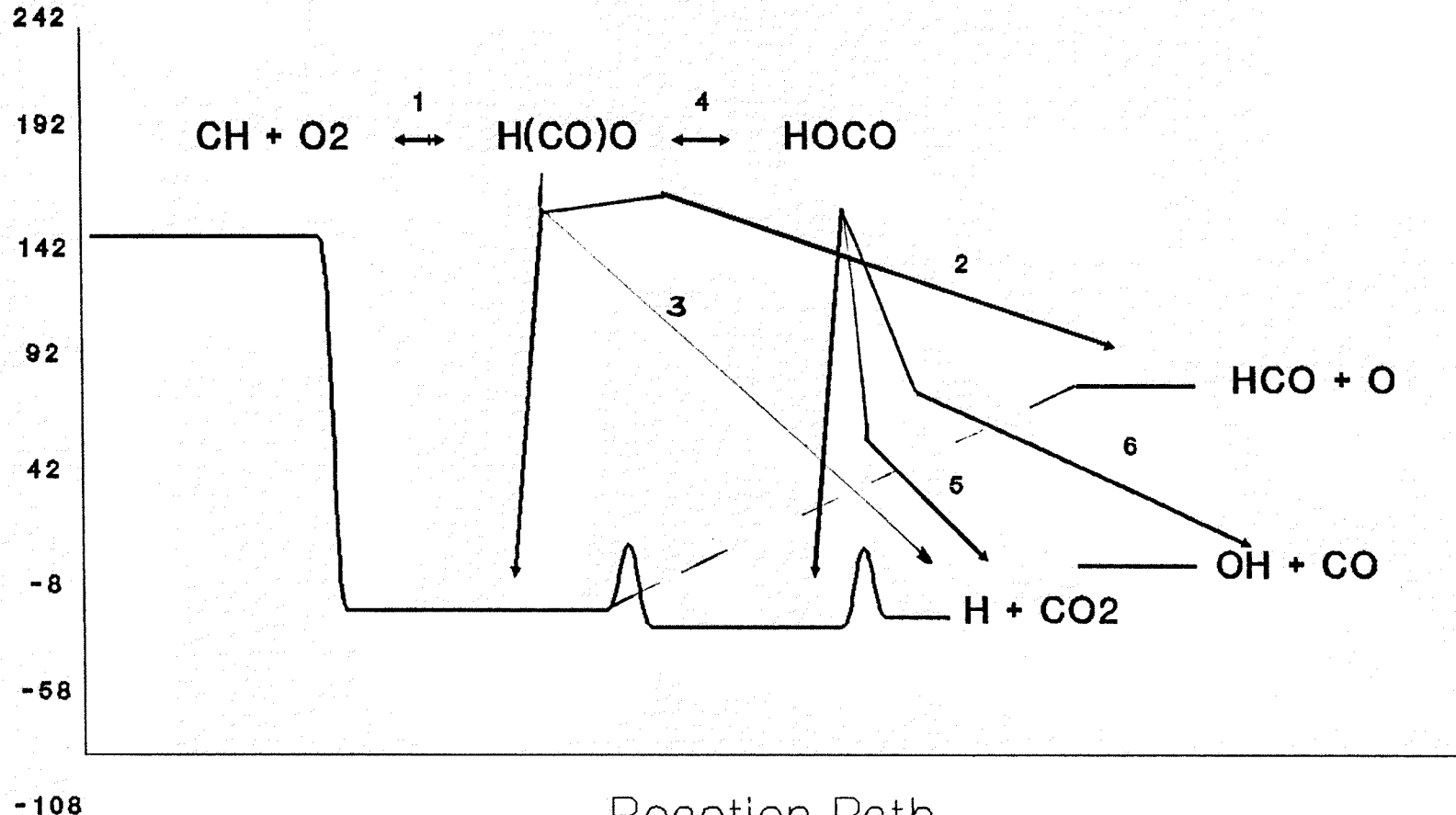
QRRK ANALYSIS: k(app) vs. 10000/T @ 760.
CH + O2 -----〉 Products

Log k apparent:

10000/Temperature (K)

— HCOO ⎯ HCO + O ·········· H + CO2 - - - OH + CO

QRRK ANALYSIS: k(app) vs. Log P @ 1800 K
CH + O2 -----〉 Products

Log k apparent:

Log P (pressure in torr)

— CHO2 ⎯ HCO + O ·········· H + CO2 - - - OH + CO
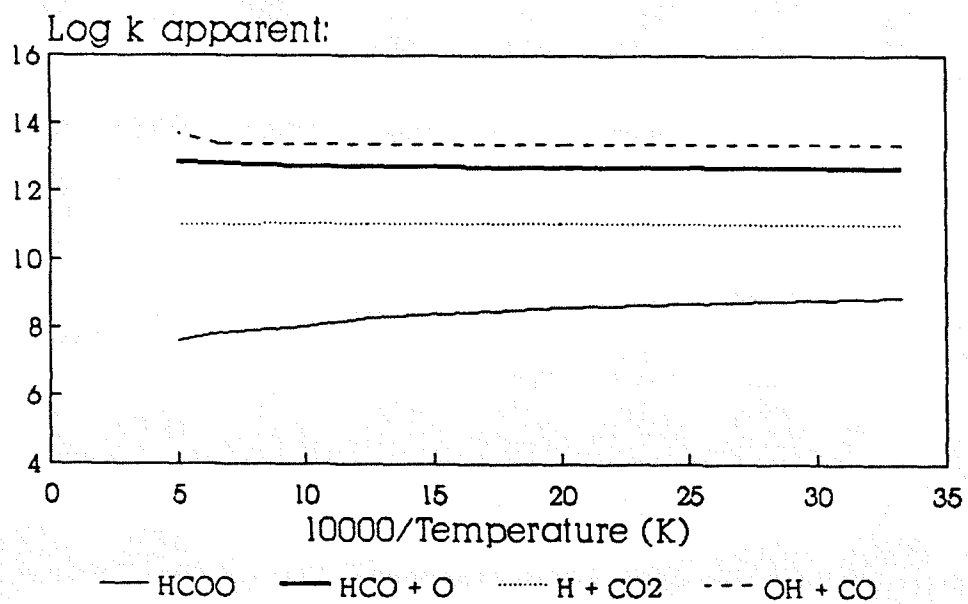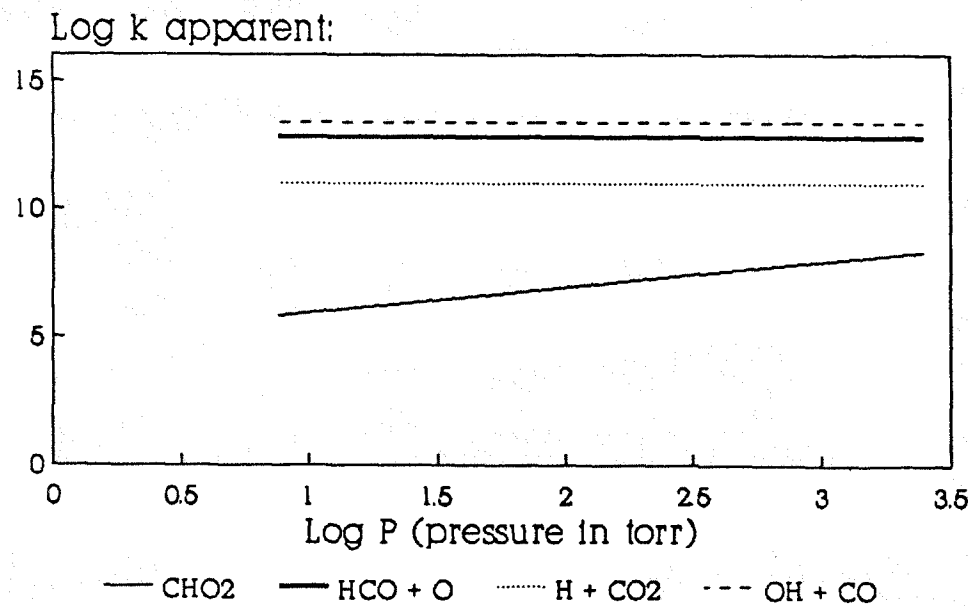
Figure 5.12 Temperature & Pressure dependence

forms complex HOCO[*]. The competition between OH + CO and H + CO_2 is dominated by the channel OH + CO because of its low barrier and high A factor in comparison to the high barier and low A factor (tighter Transition state) for the Beta scission channel.

Experimental data on product distribution is necessary to determine the favored pathways. Experiments carried out by Messing (1979) favors the OH + CO channel for the room temperature rate only.

Reaction of CH with Methane

In fuel rich flames the existence of excess hydrocarbons makes it important to consider CH + CH_4 reaction. Several groups have had studied this reaction at room temperature and the results vary widely. The more recent study of Berman (1983) produced result which is in good agreement with Butler et al (1981). However the Berman determined rate is three times larger than that reported by Bosnali and Perner (1971) and forty times larger than that of Braun (1967). Berman et al observed a negative temperature dependence in the temperature range of 167 K to 652 K and observed no pressure dependence at 297 K in the range of 25 to 200 torr.

The energy level diagram and input parameters for the chemical activation calculation of this reaction are shown in Figure 5-14 and table A-12 of the Appendix respectively. The CH radical combines with CH_4 to form the chemically

Figure 5.14 P.E. diagram for CH + CH4
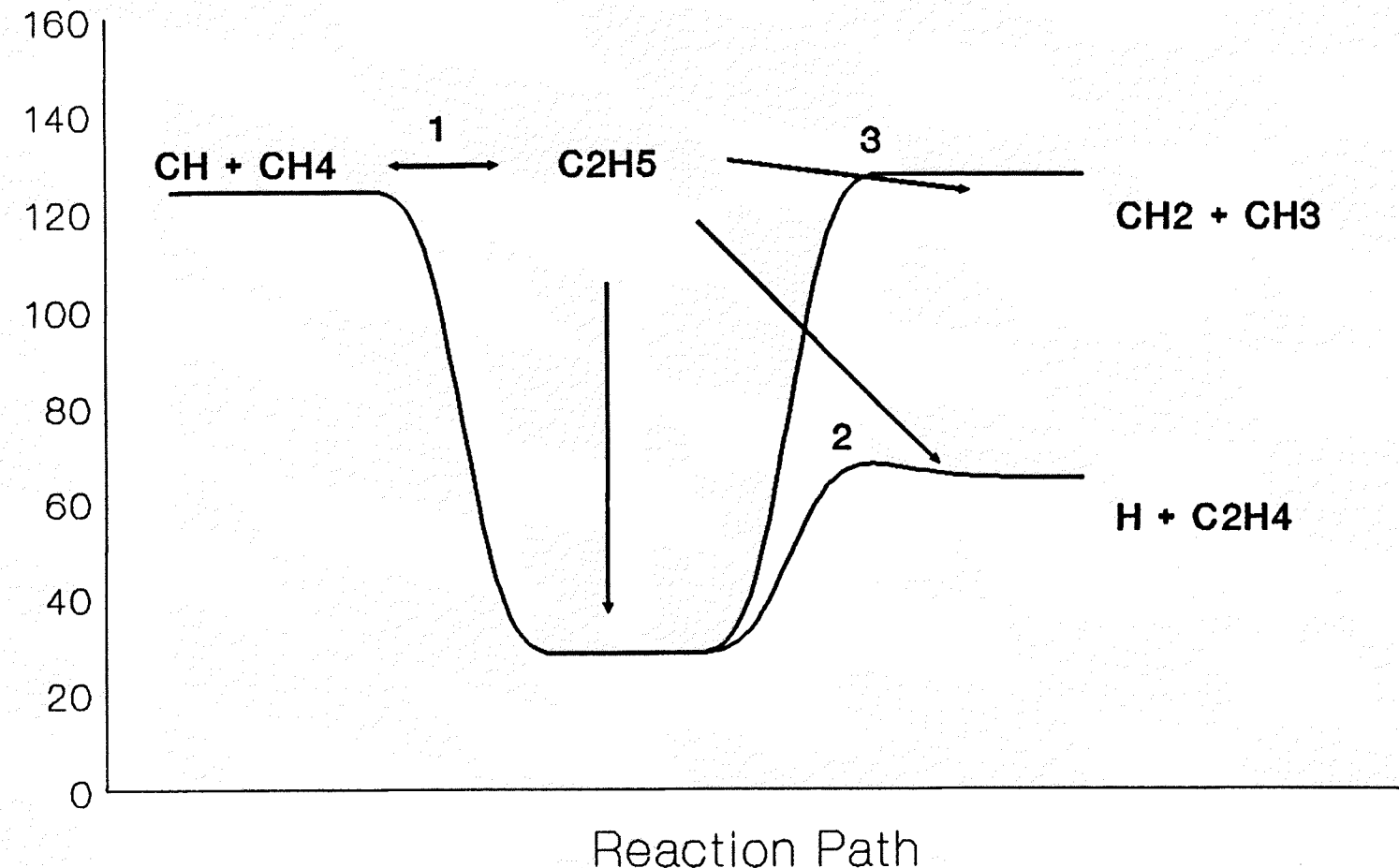
activated adduct $C_2H_5{}^*$. The reaction channel for this com

plex include dissociation to CH_2 + CH_3 (k_3),stabilization

(k_s), or a low energy exit channel through beta scission to

H + C_2H_4.

Calculated QRRK apparent rate constants at 760 torr are

shown in Figure 5-15. The figure illustrates the dominance

of low energy exit channel even in low temperatures and high

pressures range. It also illustrates no temperature depend-

ence in the temperature range of Bermans data which is

contrary to his finding. The possibility of the ambiguity

being result of uncertainty in choosing the QRRK parmeter is

there.

More experimental data is needed to resolve this dis-

crepancy. The negative temperature dependence of this

reaction as demonstrated by Berman data is inconsistent with

the   CH reactions with NO and O_2 discussed earlier where

low energy channels similar to H + C_2H_4 dominate and show

no temperature dependence in the temperature range of 157 to

680 K.

Similar problem is faced with the QRRK result for CH +

C_2H_6. This reaction is not included in the mechanism because

of the probability of this reaction occuring is very low.

Reaction of CH radical with OH

Experimental data on the reaction CH + OH does not

exist. The input parameters and potential energy diagram for

QRRK ANALYSIS: k(app) vs. 10000/T @ 760.
CH + CH4 -----〉 Products

k apparent:

10000/Temperature (K)

—— C2H5   —— H + C2H4   ······· CH2 + CH3
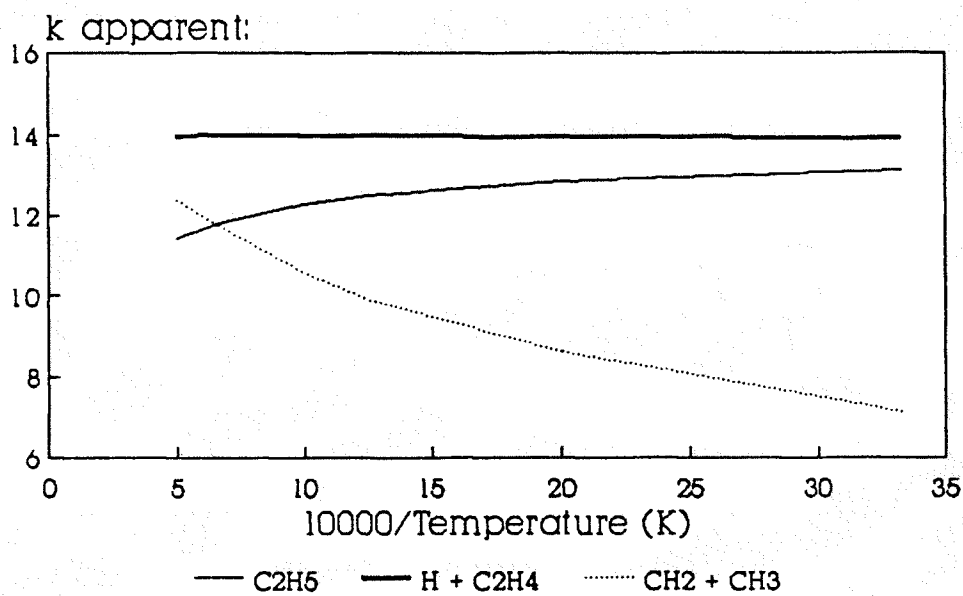
QRRK ANALYSIS: k(app) vs. Log P @ 1800 K
CH + CH4 -----〉 Products

k apparent:

Log P (pressure in torr)

—— C2H5   —— H+C2H5   ······· CH2+CH3
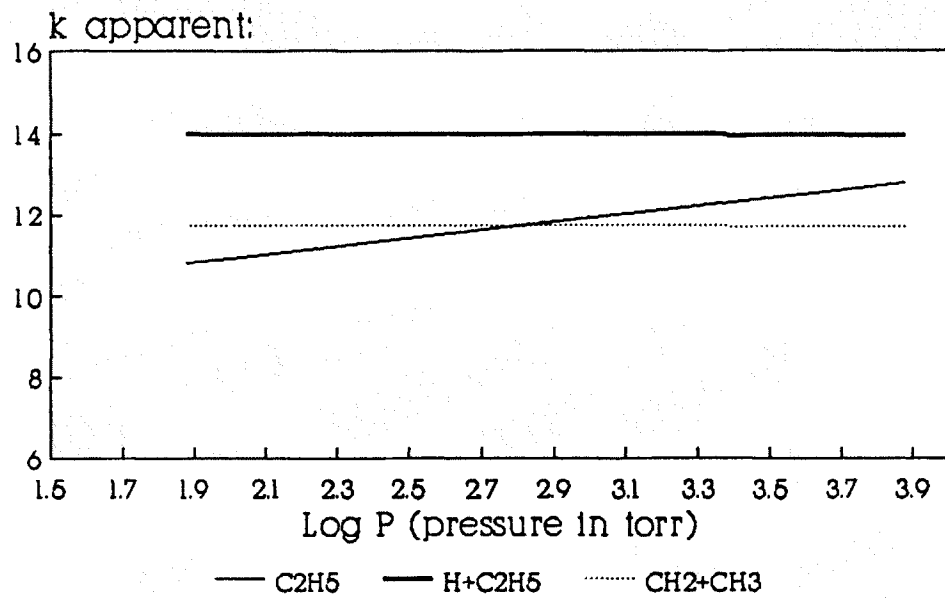
Figure 5.15: Temperature & Pressure dependence

the chemical activation analysis of this reaction are given in Table A-16 of Appendix and Figure 5-16 respectively.

The CH radical can recombine with OH to form HCOH*, as shown or CH_2O via insertion. The complex CHOH* can dissociate back to CH + OH reactants (k_{-1}), or it can go to HCO + H by simple fission. The barrier for this was estimated from the data of Page (1989) for H addition CH_2O. QRRK analysis illustrates in Figure 5-17 that low energy exit channel HCO + H dominates even at high pressures and low temperatures. This is because the complex has an extra 89 Kcal/mole of energy above the H + HCO product. The apparent rate for the product channel H + HCO starts to fall at high temperature because entropy drives some of the complex backwards to reactants.

Instead of adding CH can also insert and form CH_2O^* which has deeper well than previous complex CHOH*. This complex will also lead to the same low energy exit product channel which dominates at high pressures and high temperatures.

We also note that the HCO formed may have upto 89 kcal of energy in excess (depending on how much of the 89 Kcal is assigned to H) to the ground state. This is upto 71 Kcal more than the 18 Kcal it needs to dissociate by beta Scission to CO + H. Therefore this overall reaction while proceeding through several steps might be written as CH + OH --> CO + H + H

CH$_2$ with Nitrogen molecule

This reaction was proposed as a possible important contributor for the formation of prompt NO (Miyachi, 1977). In an attempt to use the correct rate constant at the pressure and temperature of the flame system and then access the importance of this reaction a QRRK calculation was carried out.

The energy level diagram and input parameters for the chemical activation calculation are shown in Figure 5-18 and table A-18 of Appendix respectively. The CH$_2$ radical adds to N$_2$ to form the chemically activated adduct CH$_2$N$_2$*. The major reaction channel of CH$_2$N$_2$* include dissociation back to reactant (k$_{-1}$), stabilization to CH$_2$N$_2$ (k$_s$), and a high energy exit channel to HCN + NH. The channel to CH$_2$N + N is even high in endothermicity and is not considered.

The QRRK calculated apparent rate constant at 760 torr are shown in Figure 5-19. At the flame conditions of the present study stabilization exceeds slightly the high energy exit channel. However at higher temperatures above 1500K and in lower pressures upto 100 torr, the high energy exit channel dominates. The stabilized CH$_2$N$_2$ adduct well is relatively shallow. Dissociation out of the well, back to reactants will be rapid at flame conditions. No experimental data is available to compare and calibrate the chemical activated analysis for this system.

A chemical activated analysis for the CH$_2$ + N$_2$ predicts

Figure 5.16 P.E. diagram for CH + OH
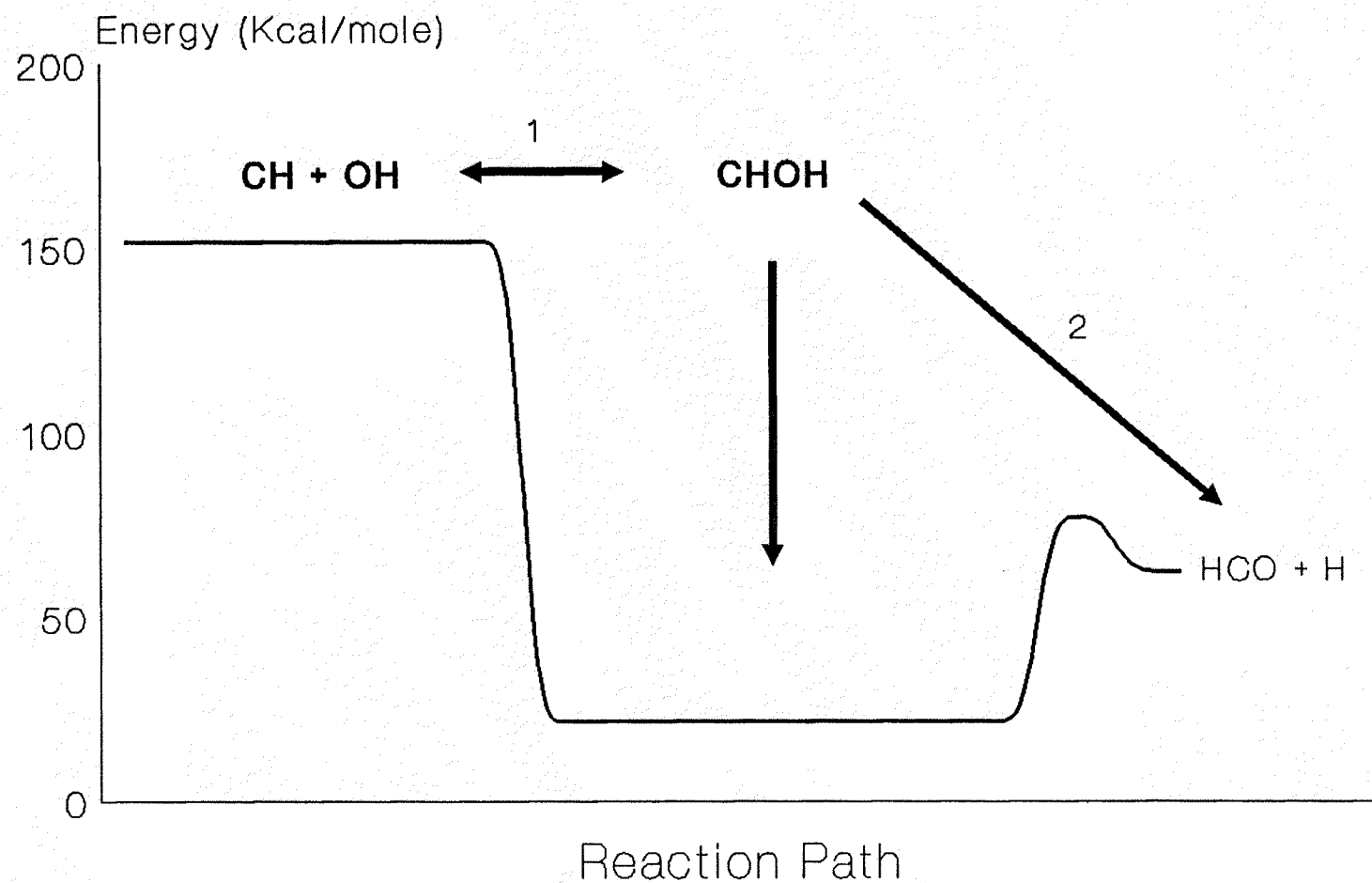
QRRK ANALYSIS: k(app) vs. Log P @ 300 K
CH + OH ----) Products

Log k apparent:

Log P (pressure in torr)
— HCOH   — HCO + H
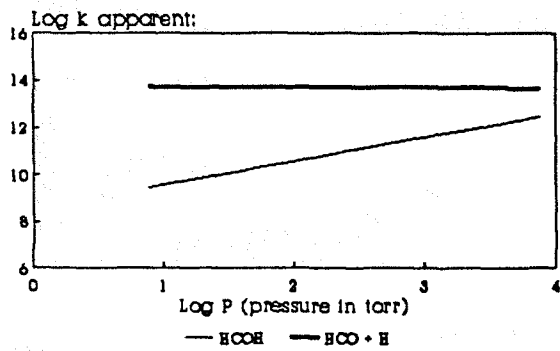
QRRK ANALYSIS: k(app) vs. Log P @ 1800 K
CH + OH ----) Products

Log k apparent:

Log P (pressure in torr)
— HCOH   — HCO + H
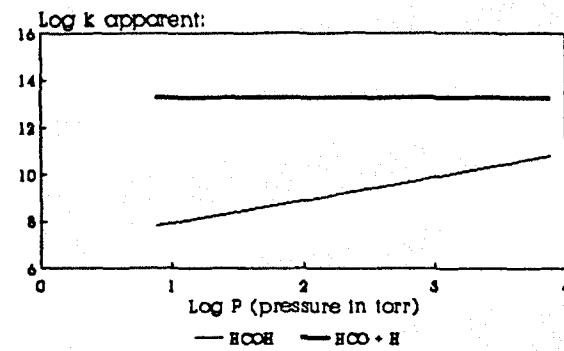
QRRK ANALYSIS: k(app) vs. 10000/T @ 760.
CH + OH---) Products

Log k apparent:

10000/Temperature (K)

——— CHOH   ——— HCO + H
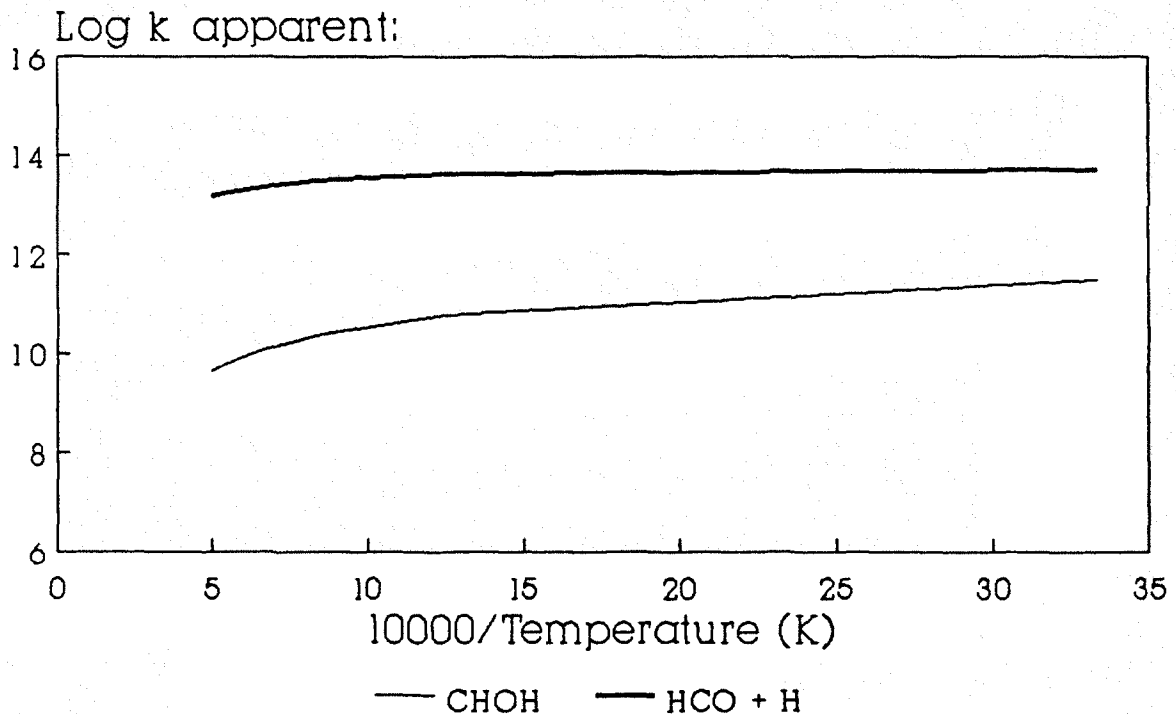
Figure 5.17: Temperature & Presure dependence

Fig: 5.18 P.E. diagram for CH2(t) + N2

Energy (Kcal/mole)

^{3}CH2 + N2 $\xleftarrow{\quad 1 \quad}$ CH2N2   HCN + NH

Reaction Path
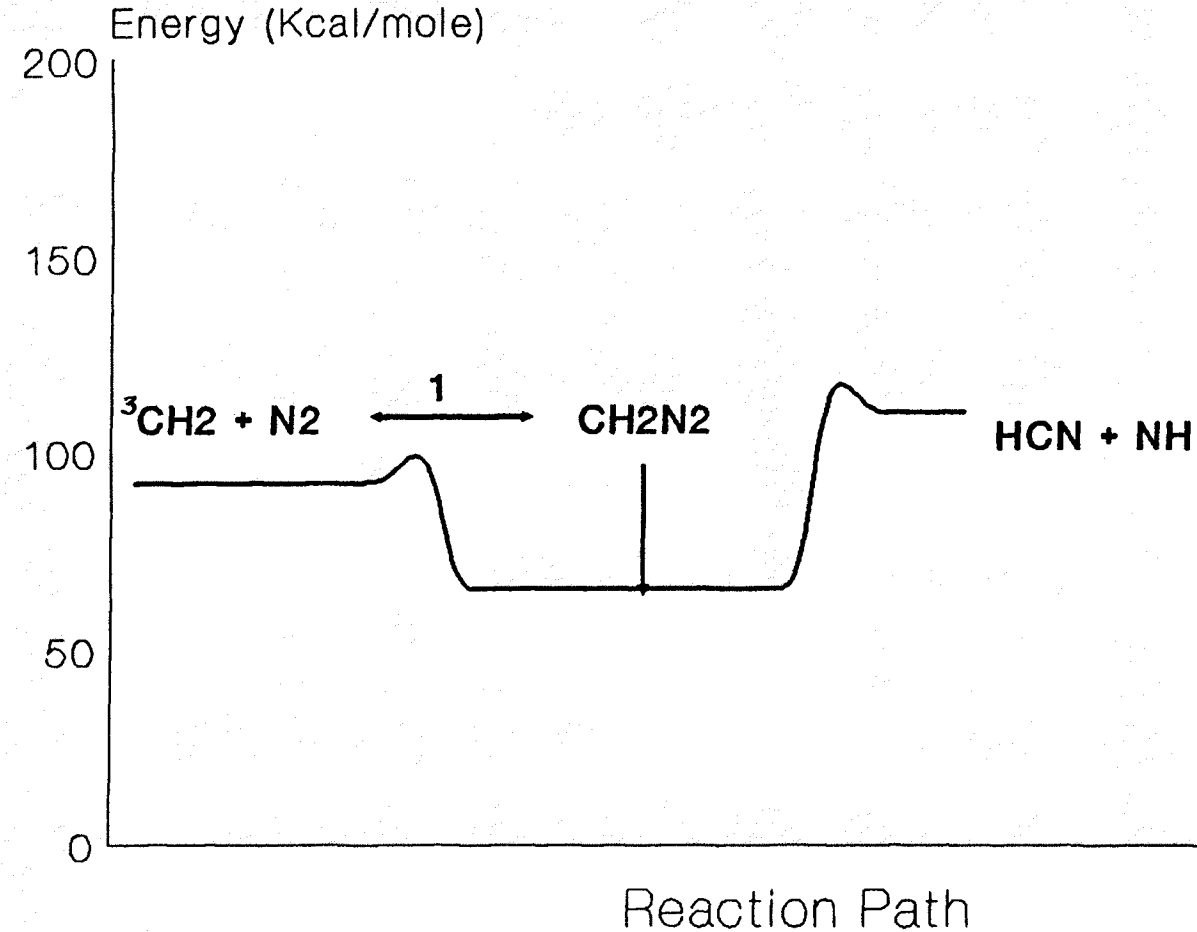
QRRK ANALYSIS: k(app) vs. 10000/T @ 760.
CH2 + N2-----) Products

Log k apparent:

- CH2N2   - HCN + NH
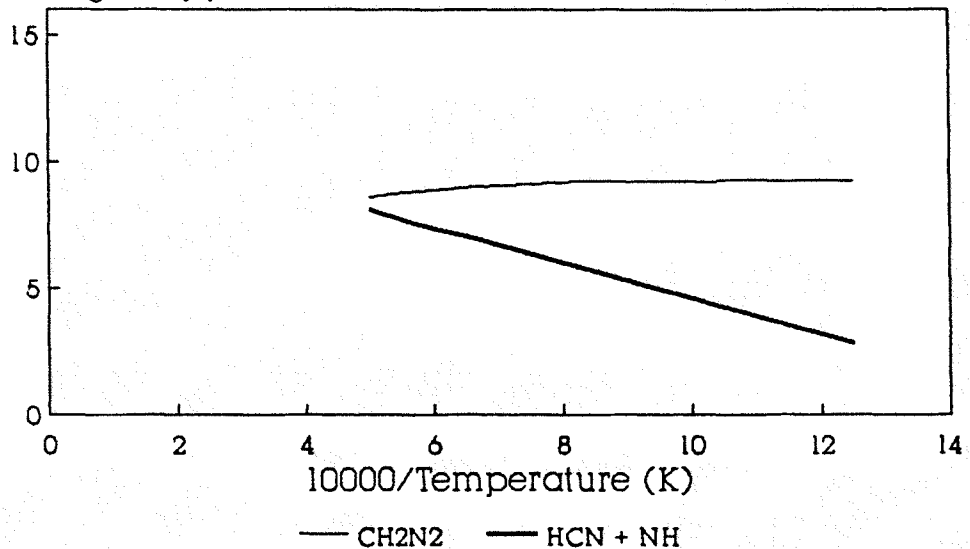
QRRK ANALYSIS: k(app) vs. Log P @ 1800 K
CH2 + N2------) Products

Log k apparent:

- H2CN2   - HCN + NH
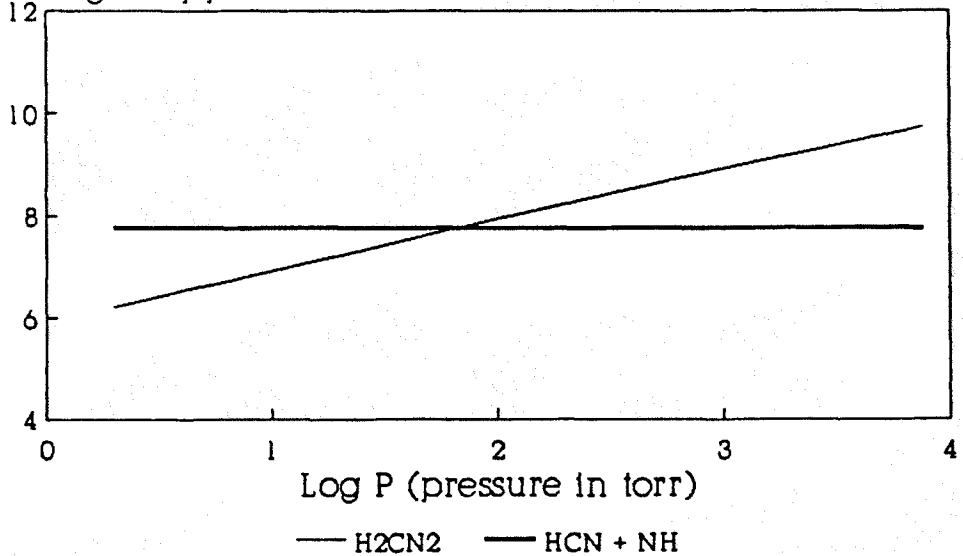
Figure 5-19 Temperature & Pressure dependence

result similar to the results of CH_2 + N_2 but of higher apparent rate constant values because the endothermicity is reduced by 9 Kcal/mole.

Reaction of CH_2 with nitric oxide

Significant rates of NO reduction in fuel rich acetelyne flame were observed by Taylor (1984) in his study. He attributed this reduction of NO to reaction with the CH_2 radical and proposed a rate constant of 1.3E+13. In this study reduction of NO is also observed. To study the relative importance of CH_2 radical in NO destruction, a chemical activation analysis of was performed.

The energy level diagram and important input parameters are given in Figure 5-20, and in table A-20 of Appendix respectively.

The CH_2 (triplet) can combine with the NO at the Nitrogen to form CH_2NO^*. This adduct has sufficient energy over the well depth to isomerize: a hydrogen shift. The A factor for the recombination is taken from recent study of Darwin (1989). The well depth for H_2CNO is taken from Melius (1989). The A factor and barrier for isomerization is based on Transition state Theory and Melius respectively. The $HCNOH^*$ can Beta scission to the HCN + OH a low energy exit channel. Figure 5-22 illustrates that this channel dominates in the flame condition of this study.

Another possible way to look at this reaction for the addition to occur on the oxygen forming the complex CH_2ON^*.

Figure 5.20 P.E. diagram for CH2 + NO

Energy (Kcal/mole)

^{3}CH2 + NO —1→ H2CNO —2→ HCNOH

HCN+OH

Reaction Path
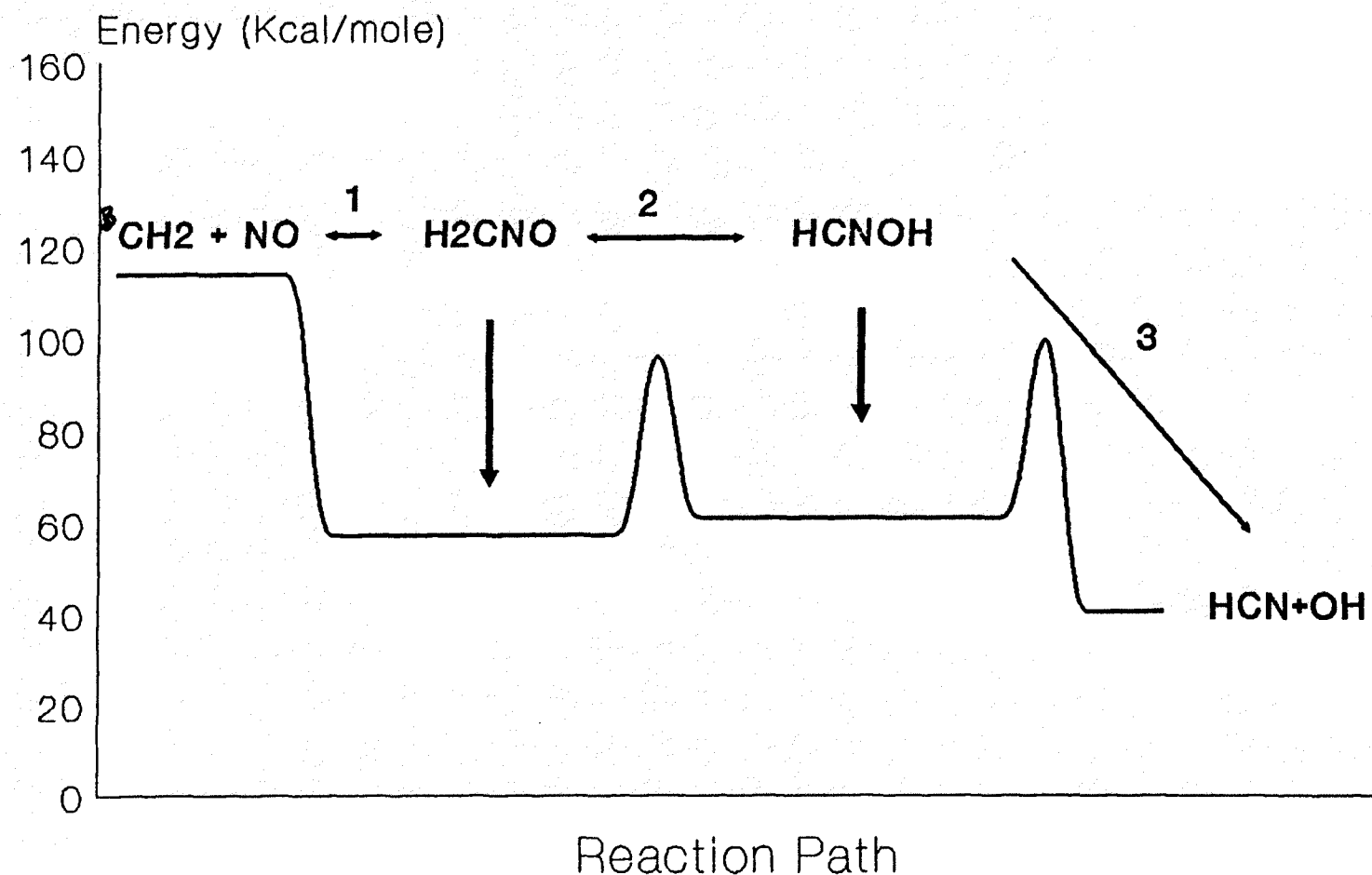
QRRK ANALYSIS: k(app) vs. Log P @ 300 K
CH2 + NO -----) Products

Log k apparent:

Log P (pressure in torr)
— H2CNO — HCN + OH
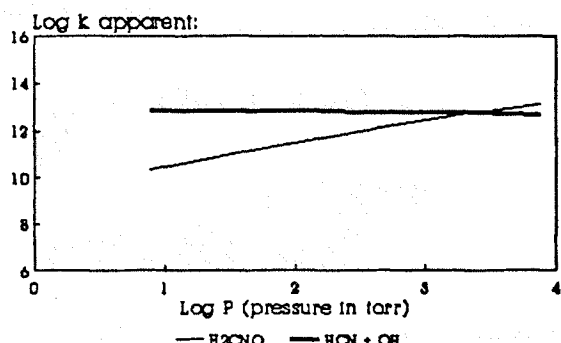
QRRK ANALYSIS: k(app) vs. Log P @ 1800 K
CH2 + NO -----) Products

Log k apparent:

Log P (pressure in torr)
— H2CNO — HCN + OH
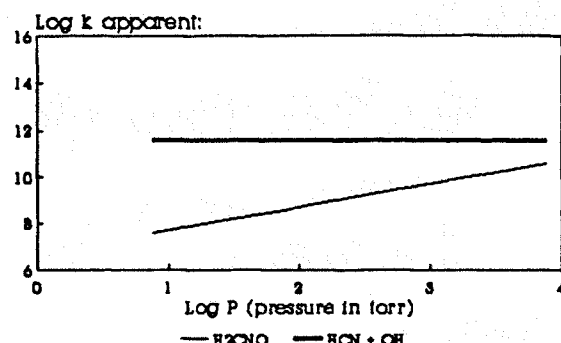
QRRK ANALYSIS: k(app) vs. 10000/T @ 760.
CH2+ NO -----) Products

Log k apparent:

10000/Temperature (K)

— H2CNO — HCN + OH
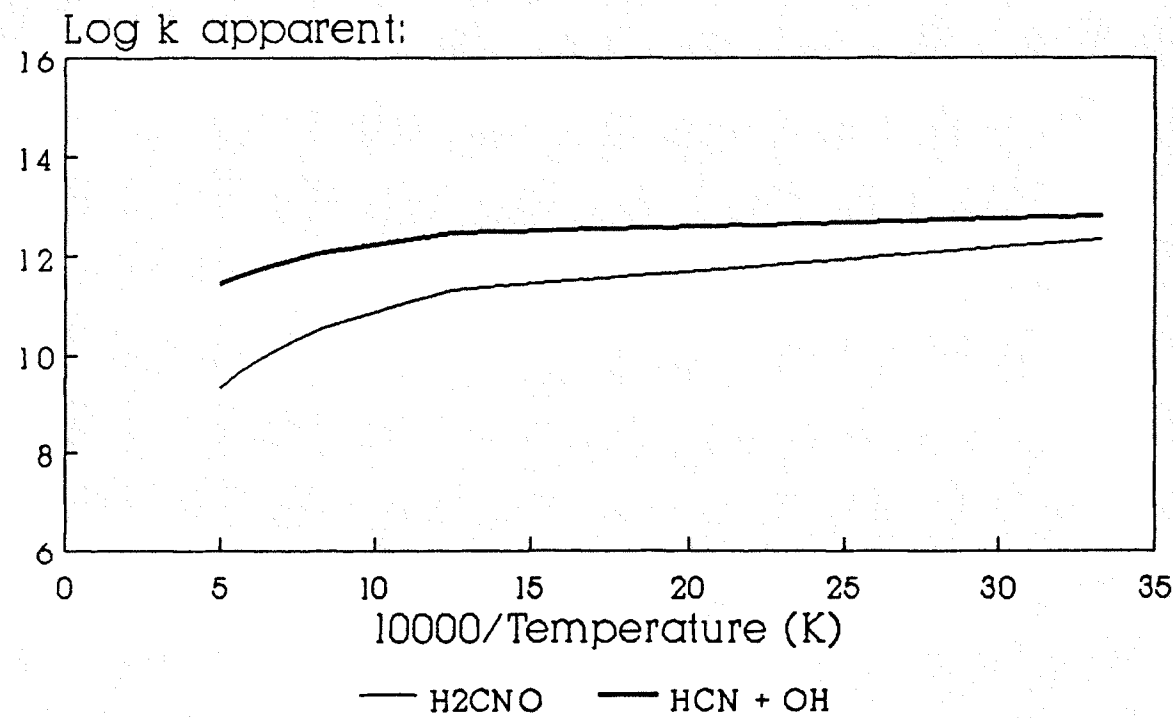
Figure 5-21: Temperature & Pressure dependence

This can stabilize or dissociate to CH_2O + N. Due to the unfavorable thermodynamics of this pathway relative to CH_2 addition to the nitrogen this reaction is not considered.

Discussion of Results

This study was motivated by an interest in the inter-action of hydrocarbon radicals and nitrogeneous species in flames, particularly the formation and destruction of prompt NO in flames. Previous study by Miller and Bowman (1989) established that prompt NO formation involves three separate kinetic issues:

a. The CH concentration and how it is established .

b. The rate of N_2 fixation by hydrocarbon radi-cals.

c. The rates of interconversion among fixed nitro-gen fragments.

So the approach towards understanding the above men-tioned kinetic interactions between hydrocarbon and nitrogen species builds on earlier works which considers these sys-tems separately [Warnatz 1983, Miller and Bowman, 1989, Dean and Chou, 1982]. The mechanism as outlined in Figure 6.1 consist of three reaction subsets, a C_1/C_2 oxidation set, an HCN oxidation set, and an ammonia oxidation set.

The C_1/C_2 oxidation model started as an adaptation of Warnatz (1983). The modifications (stated later) on the Warnatz C_1/C_2 oxidation mechanism are extensive. The modi-fied mechanism which forms the C_1/C_2 oxidation set for the model along with the HCN and NH_3 oxidation set is described in the Table A-1 of the Appendix.

COMPONENTS OF OVERALL MECHANISM

73

CH$_4$

HCN
Doped
Flames

NH$_3$
Flames
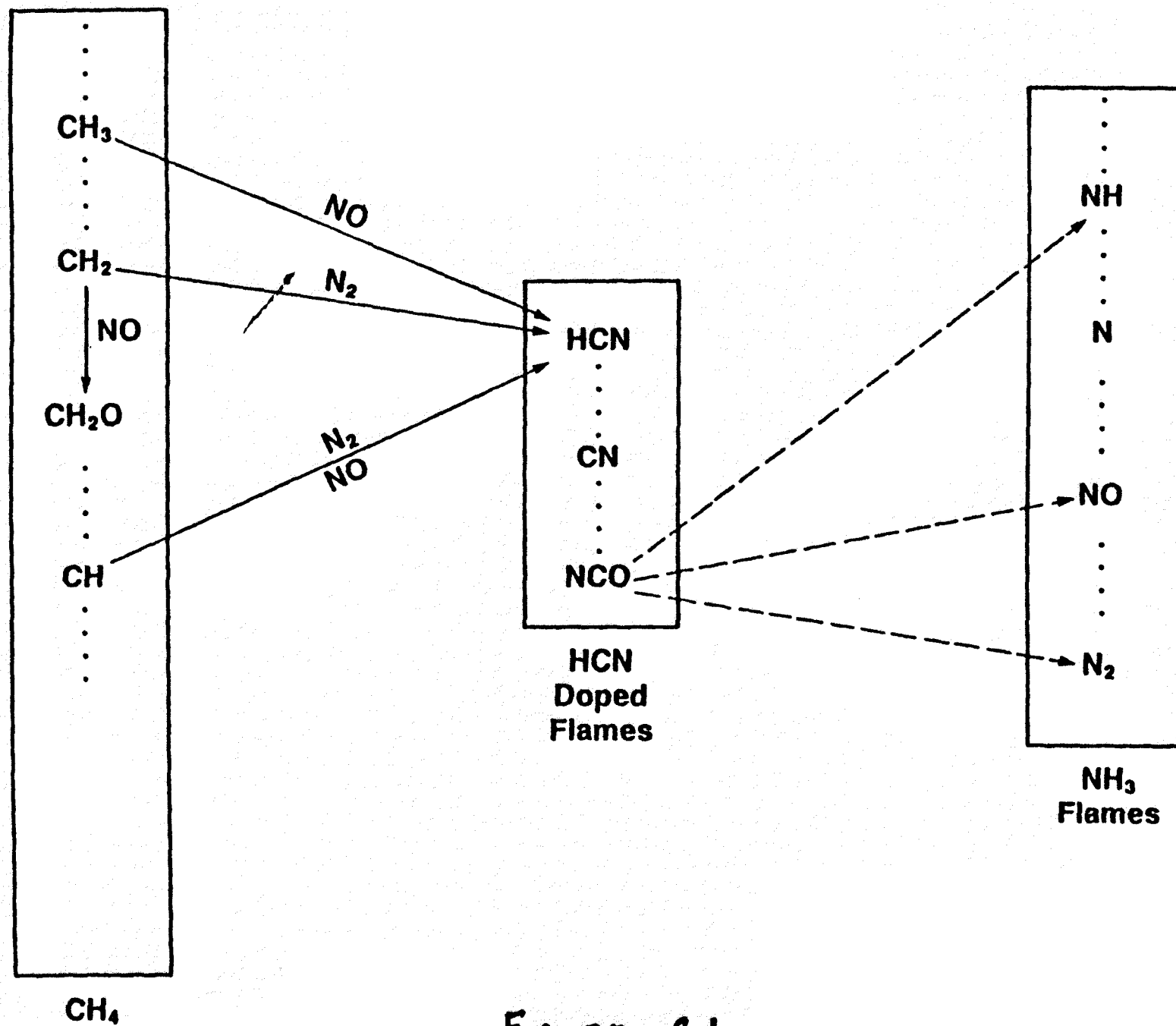
FIGURE 6·1

The modification include results of QRRK treatment of radical recombination and addition reactions, in addition to fall of for unimolecular dissociations. Additional modifications include addition and hydrogen rearrangement for allyl radical reactions with O_2 to form olefin + HO_2. Transition state theory analysis for A and T^n factor for hydrogen transfer reactions. Evans Polanyi plot were utilized for energy of activation for these hydrogen transfer reaction.

Further modification on C_1/C_2 oxidation mechanism of Warnatz (1983) were based upon recent kinetic information in the literature (Gutman,1988) and were oriented towards improved prediction of OH and CH radicals while retaining the good predictive capability it already had for the mainstream hydrocarbon species (CH_4, C_2H_4, C_2H_2 and radicals CH_3, CH_2). The rate constants for CH_3 reactions with O_2, O, OH, (reaction R-20 to R-26 in the the mechanism described in Table A-1 of the Appendix) were based on QRRK from Dean and Westmoreland (1987), but were modified with updated species thermodynamics for the higher temperatures of flame. The rate constant for C_2H_5 reacting with molecular oxygen (R-60 and R-61) were taken from Bozzelli and Dean (1990).

The rate constants for the reaction mainly responsible for CH generation (reverse of R-38), and CH reaction with OH, O_2, CH_4, C_2H_5, (R-44, R-46, R-47, R-50, R-51,) are all from QRRK treatment described in the previous chapter.

The rate constants for the nitrogen fixation by CH, CH_2 (R-94, R-95, R-96), and for NO decomposition by CH,and CH_2 (

R-99, R-100) are also from the QRRK analysis.

A distinction is made in the present mechanism between CH_2, singlet and CH_2 triplet. The generation and decomposition rate constants for the CH_2 are primarily from Miller and Bowman (1989).

The NH_3 and HCN oxidation mechanism are from earlier work on ammonia by Dean and Chou (1982).

The complete listing of the models detailed elementary reaction mechanism developed for the flames studied is given in table A-1 of the Appendix. This elementary reaction mechanism was developed for the undoped flame 2 and doped flame 5. Experimental conditions for these two flames are given in Table 6-1.

The results obtained for flame 2 and flame 5 from the flame code (Kee, Miller, Smooke, Grcar,1989), using the developed elementary reaction mechanism are given in Table B-1 and B-2 in the Appendix.

The OH results in Figure 6-2 indicates very good agreement between model and experimental results. The calculated peak is little higher than observed but it is within the experimental uncertainity. The OH decay is more rapid at larger distance for the calculated profile. The cause of this inconsistency is still unclear. Studies by Dean and Chou (1982) for rich ammonia flame indicate similar problem. The calculation for the OH profile as illustrated in Figure 6-2 in flame 2 undoped and in flame 5 doped are identical, in accordance with the observation. Inspite of the calcu-

Comparison of OH Profile
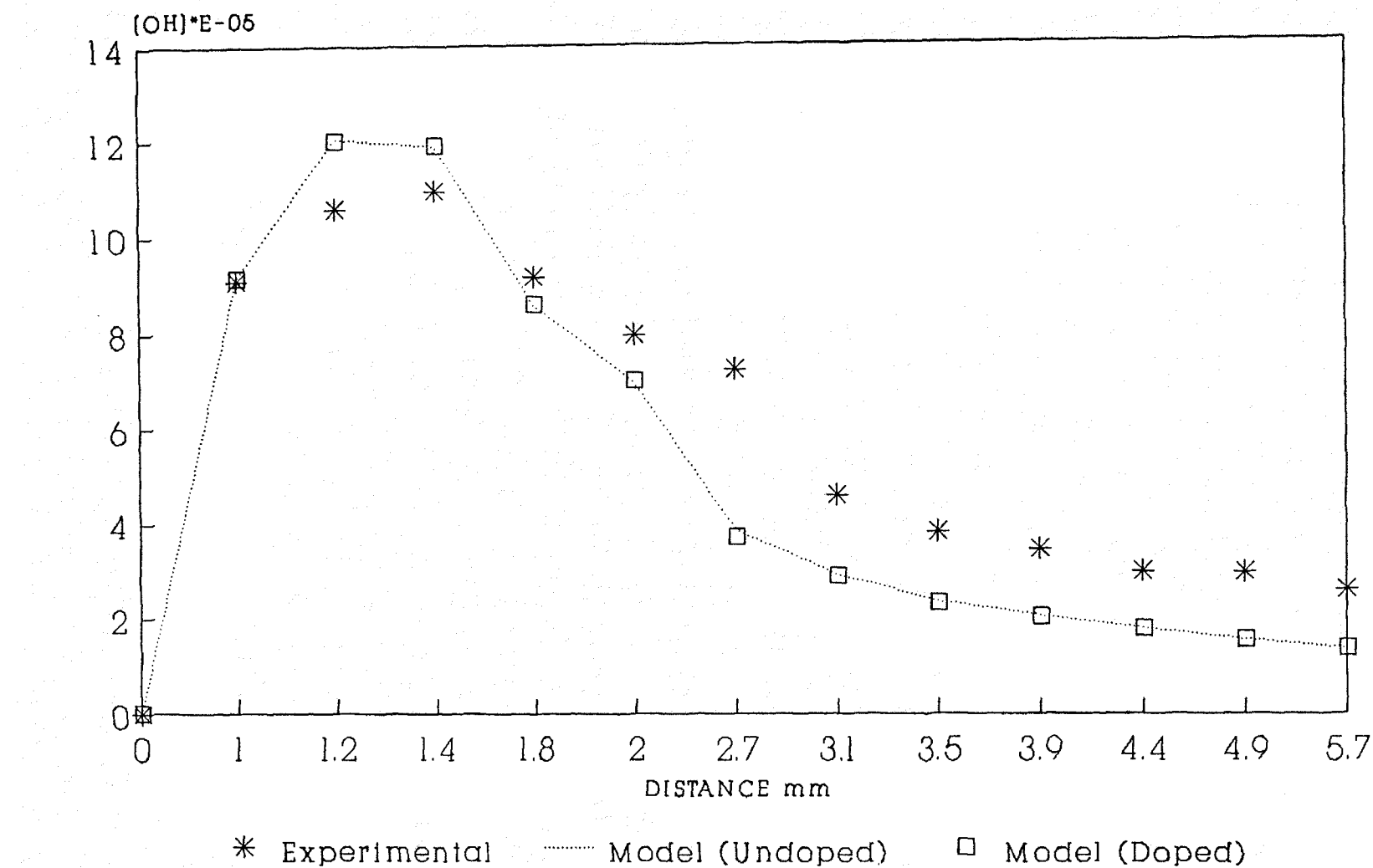
Figure 6.2 Comparison between model & experiment

lated more rapid decay the overall behaviour is encouraging and suggests that the model does a rather good job of describing the mainstream hydrocarbon oxidation kinetics in flame.

The CH result in Figure 6-3 indicated a calculated peak of a factor of 1.8 higher than observed. Given the larger uncertainity (a factor of 2) in the CH experimental concentration assignment during measurement, the prediction is very encouraging. Since CH is so strongly involved in coupling the hydrocarbon mechanism to that of nitrogen system, it is essential to have a good prediction of CH profile.

Sensitivity analysis from figure 6-4 shows that CH comes mainly from the CH_2 (triplet) by the reaction (reverse of R-38) :

$$^3CH_2 + H \longleftrightarrow CH + H_2 \qquad (-R-38)$$
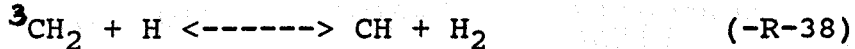
Methylene comes mainly from the C_2 route rather than C_1 route. This is evident by the large sensitivity of CH for the reactions R-55 and R-60:

$$CH_3 + CH_3 \longleftrightarrow C_2H_4 + H2 \qquad (R-55)$$

$$C_2H_5 + O_2 \longleftrightarrow C_2H_4 + HO_2 \qquad (R-60)$$
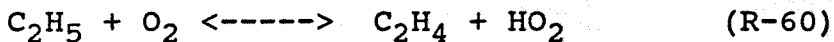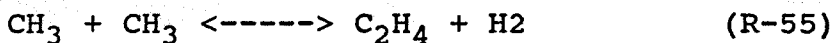
which forms ethylene and for reaction R-69:

$$C_2H_2 + O \longleftrightarrow CH_2 + CO \qquad (R-69)$$
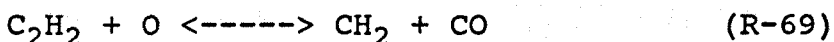
which react C_2H_2 with O to yield CH_2.

Comparison of CH Profile
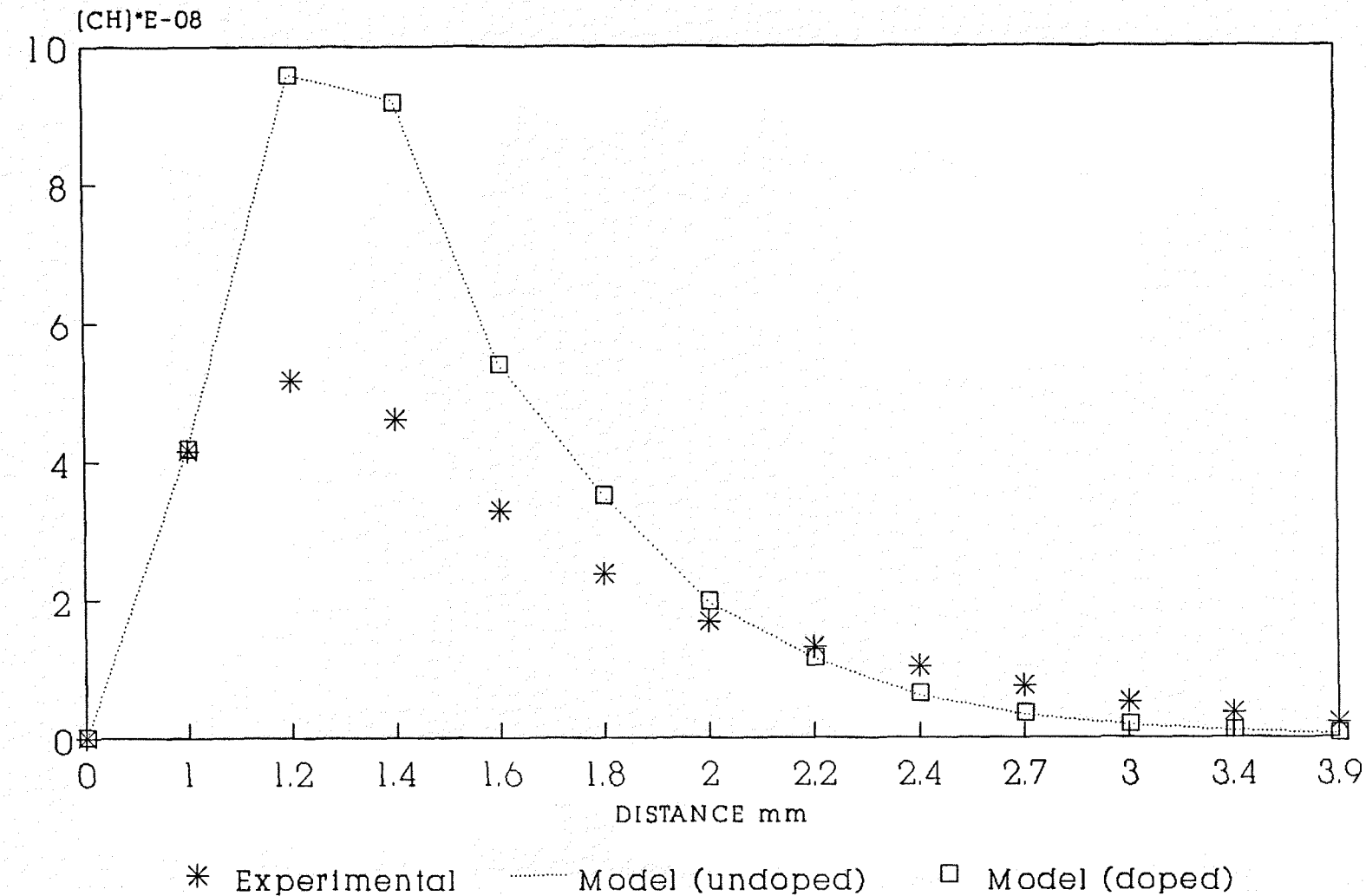
Figure 6.3 Comparison between model & experiment

Fig 6.4 Sensitivity of CH formation

Sensitivity

Distance (mm)

- CH+H2=CH2+H   + CH3+CH3=C2H4+H2

* C2H5+O2=C2H4+HO2   □ C2H2+O=CH2+CO
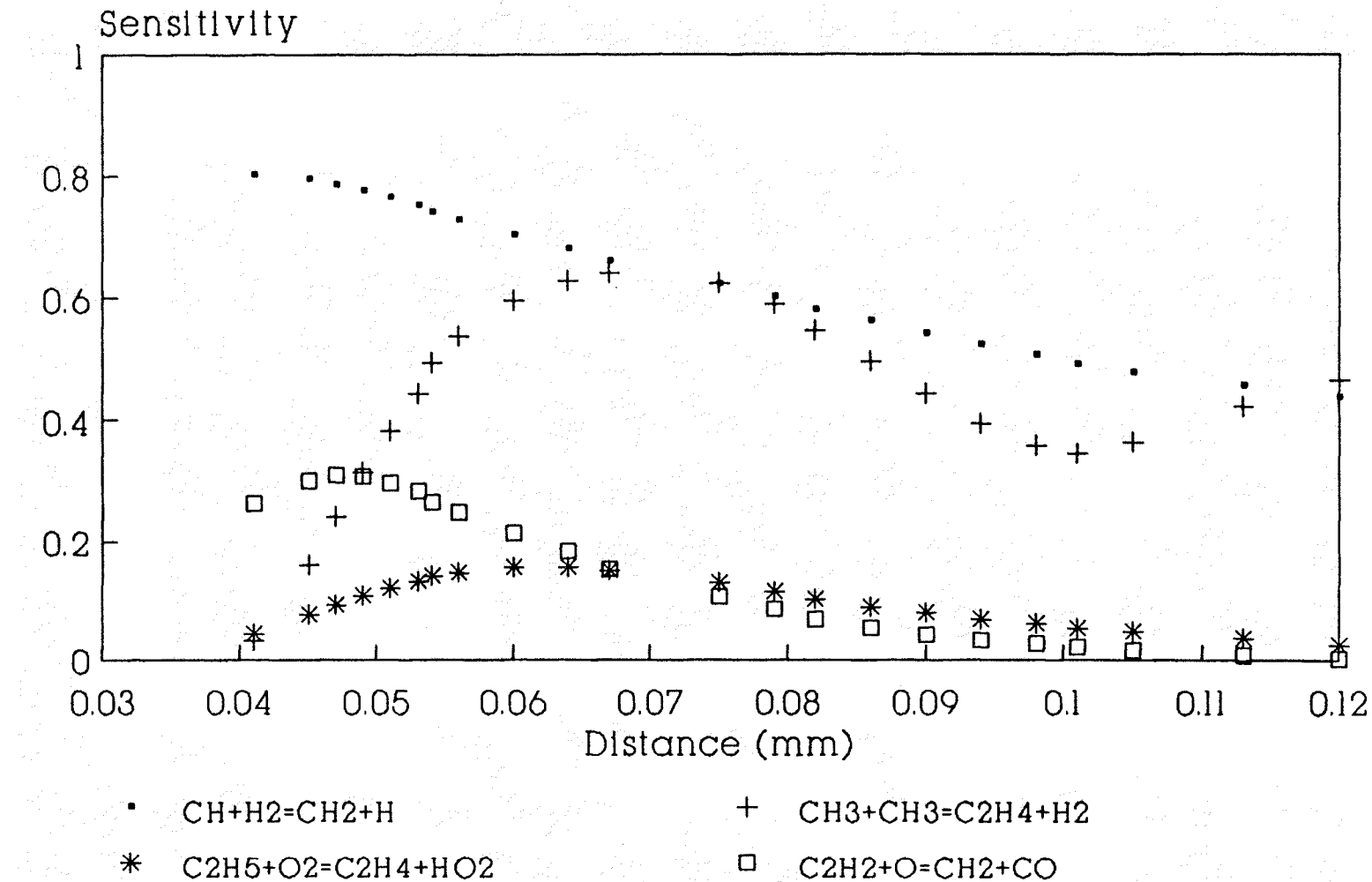
Acetylene decomposition to $^3CH_2$ occurs by reaction with O (R-69), rather than with OH via CH_2CO:

$$C_2H_2 + OH \longleftrightarrow CH_2CO + H \qquad \text{(R-70)}$$

$$CH_2CO + M \longleftrightarrow {}^3CH_2 + CO + M \qquad \text{(R-80)}$$
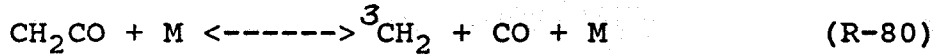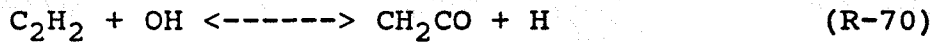
The contribution of additional CH_2 source involving the singelet species:

$$CH_3 + H \longleftrightarrow {}^1CH_2 + H_2 \qquad \text{(-R-185)}$$

$${}^1CH_2 + M \longleftrightarrow {}^3CH_2 + M \qquad \text{(R-181)}$$
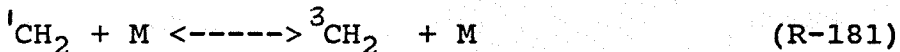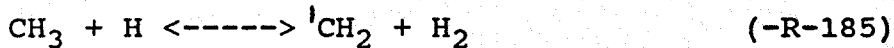
is negligible. The CH profile is not affected by the presence of singlet $^1CH_2$.

The reaction most important for CH consumption in the present mechanism are :

$$CH + H_2O \longleftrightarrow CH_2O + H \qquad \text{(R-48)}$$

$$CH + O_2 \longleftrightarrow HCO + OH \qquad \text{(R-47)}$$
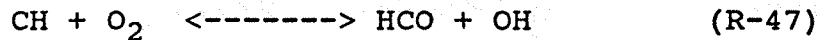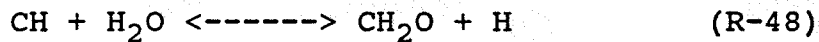
Large negative sensitivity results in for this two channel from these two reactions.

It is important to remember that the amount of nitrogen fixation by CH via reaction R-98 is determined by the rate constant of this reaction and the CH concentration in the flame. But the CH concentration profile and CH depletion does not depend on the rate constant of this channel. The CH profile as illustrated in Figure 6-3 remains nearly un-changed for the doped flame 5. This indicates that there is no interaction between fuel nitrogen (700 ppm of NH_3).

conversion to NO and CH in the flame systems studied. The prediction of NO concentration from the model for undoped flame 2 is shown in Figure 6.5. The Prediction for the model is a order of magnitude less.

The model have the following reaction for N_2 fixation reactions:

$$CH + N_2 \longleftrightarrow HCN + N \qquad (R-98)$$

$$CH_2 + N_2 \longleftrightarrow HCN + NH \qquad (R-194)$$

$$CH_2 + N_2 \longleftrightarrow HCN + NH \qquad (R-195)$$
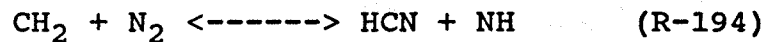
and the following NO destruction path:

$$CH + NO \longleftrightarrow HCN + O \qquad (R-99)$$

$$CH_2 + NO \longleftrightarrow HCN + OH \qquad (R-100)$$

$$CH_3 + NO \longleftrightarrow HCN + H_2O \qquad (R-102)$$
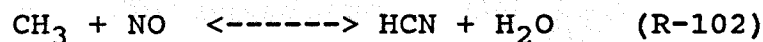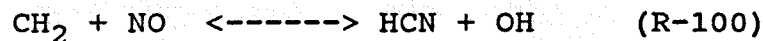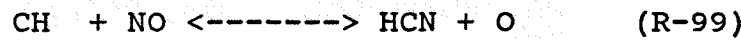
Figure 6-6 shows sensitivity co-efficients for NO formation for model applied to the undoped flame. Large sensitivity coefficient for the reaction R-98 and for the reactions generating CH indicates that CH is mainly responsible to fix nitrogen in the flame environment. The rate coefficents, for this reaction is taken from the QRRK analysis of $CH + N_2$ system (described in earlier chapter) with a barrier of 17.3 for the abstration like channel of HCN + N (R-98). This rate coefficient is consistent with the recent Dean and Bowman (1990) high temperature shock tube data. The contribution of R-100 towards the formation of NO is neglibible in this flame because of low CH_2 concentration.

FLAME 2: NO Conc.
Undoped flame
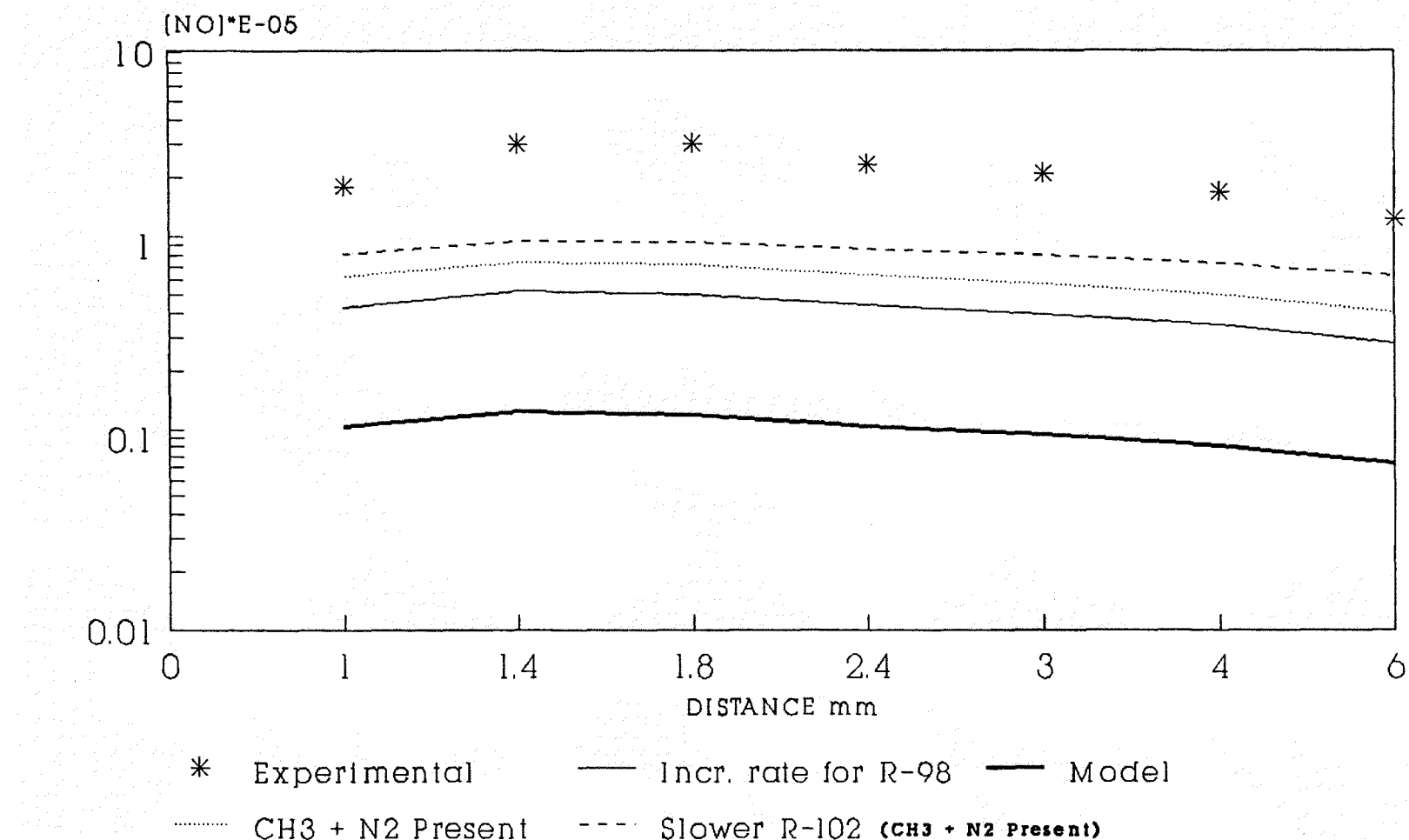
Figure 6.5 Comparisons between models & experimental

The rate constant used in reaction R-100 is order of two magnitude higher than Miller and Bowman (1989) but consistent with Sanders and Lin (1987). This value of rate constant is near an upper limit to the rate constant that reaction R-100 can have. The reason for this differnce is the barrier used in the reaction R-100.

The introduction of CH_2 singlet reaction with N_2 does not have any effect on the NO profile even though its rate constant is higher than the reaction involving triplet species.

Large sensitivity coefficients of NO for the reaction R-104, R-106 and R-160 suggest that HCN is mainly decomposed in this fuel rich flame by :

$$HCN + O \longleftrightarrow NCO + H \qquad (R-104)$$
$$NH + O_2 \longleftrightarrow HNO + O \qquad (R-160)$$

to form NCO. The sensitivity of NO to R-160 indicates that NCO is decomposed to NH by reaction with hydrogen atom (R-110):

$$NCO + H \longleftrightarrow NH + CO \qquad (R-110)$$
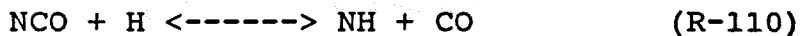
NH can then form HNO by reaction with O_2 (R-160). The HNO now formed can decompose to NO unimolecular decomposition and abstraction reaction of the H.

There is a obvious recycle of HCN in the flame via R-102. This is because of a relatively large concentration of CH_3. The rate constant for this reaction is from flame data

Figure 6.6
NO sensitivity in undoped flame

- • CH2+H=CH+H2 + CH3+CH3=C2H4+H2 ✳ CH+N2=HCN+N □ HCN+O=NCO+H
- ✕ CN+O2=NCO+O ◇ N+O2=NO+O △ NH+O2=HNO+O ⊠ CH3+NO=HCN+H2O
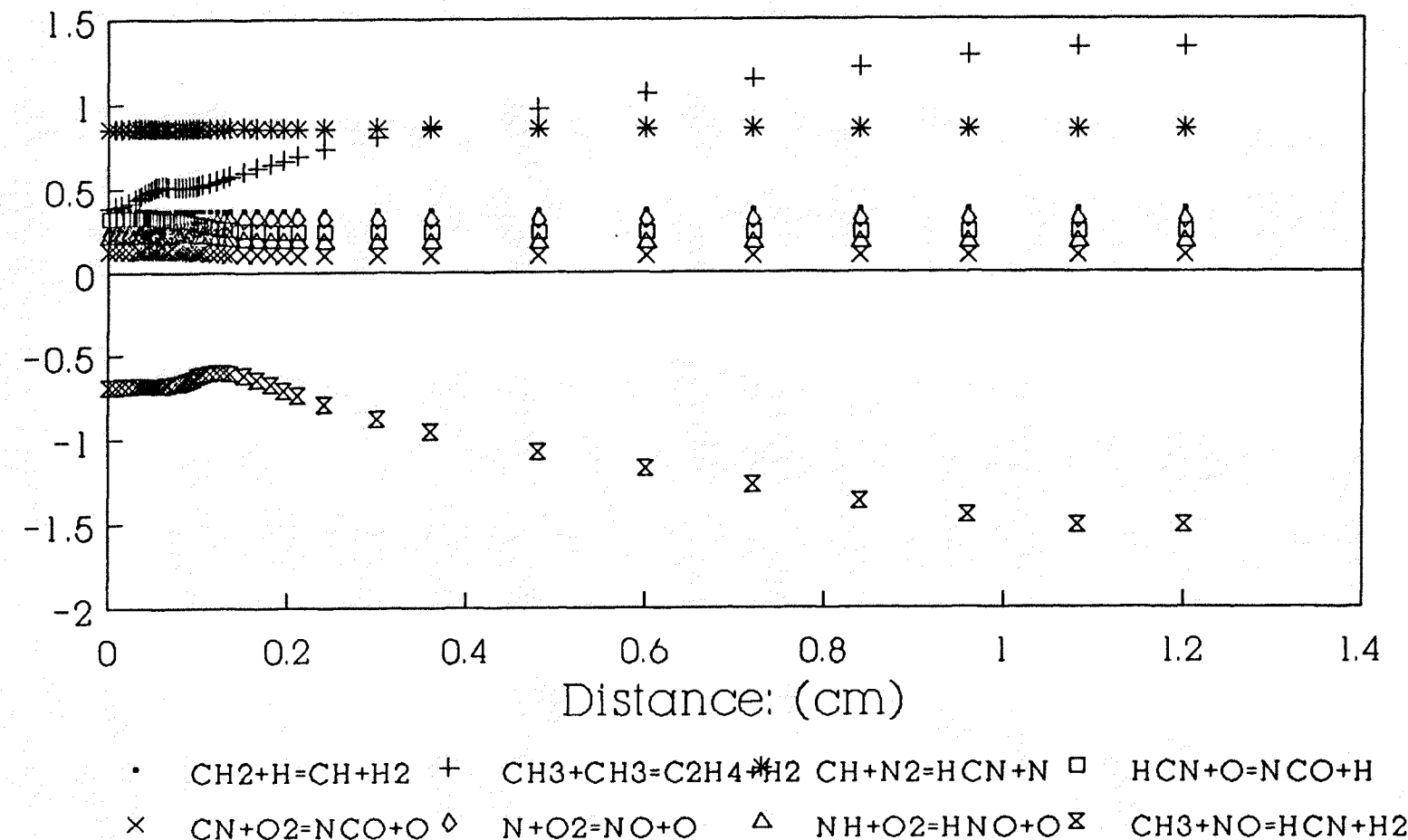
of J.M. Levy (1980), which is nearly two order of magnitude higher than the value recommended by Miller and Bowman (1989). Hilaire et al (1984) had proposed a higher value for R-102 from analysis of slightly fuel rich low pressure CH_4/O_2 flames. Slowing down or omitting this reaction will result in a plateau for the NO profile which is contrary to the observation. The contribution of the other two HCN recycle reactions R-99 and R-100 is negligible, and their omission in the model does not affect HCN and NO concentration predictions due to the low concentration of CH_2 and CH.

Fortuitously the predicted NO profile illustrated in Figure 6-7 for the doped flame 5 by model is very good. This is not because the model is modeling the fixation of N_2 properly in the doped flame 5, rather most of the added NH_3 is converted to NO instead of CN. As a result the CN peak illustrated in Figure 6.8, calculated by Model is a factor of 3 less than the observed. The experimental peak of CN is observed to occurs later than the NO, peak indicating conversion of some of NO to CN. The model prediction qualitatively is very good.

The predicted NH profile shown in Figure 6-9 by the model is a factor of 1.5 higher than observed. The calculated peak is reached earlier and its decay is more rapid than experimentaly observed. The addition of the NH_i + NH_i (i=1,2) reactions are of little importance. This is not surprising since the probability of these bimolecular reactions are very low due to the low concentrations of NH_i. It

Flame 5: NO Conc.
doped flame

Conc.* (10**-5)

Distance (mm)

| * | experimental | —— | Incr. rate R-98 | —— | Model |

············ CH3 + N2 Present.   ---- Slower R-102 **(CH3 + N2 Present)**
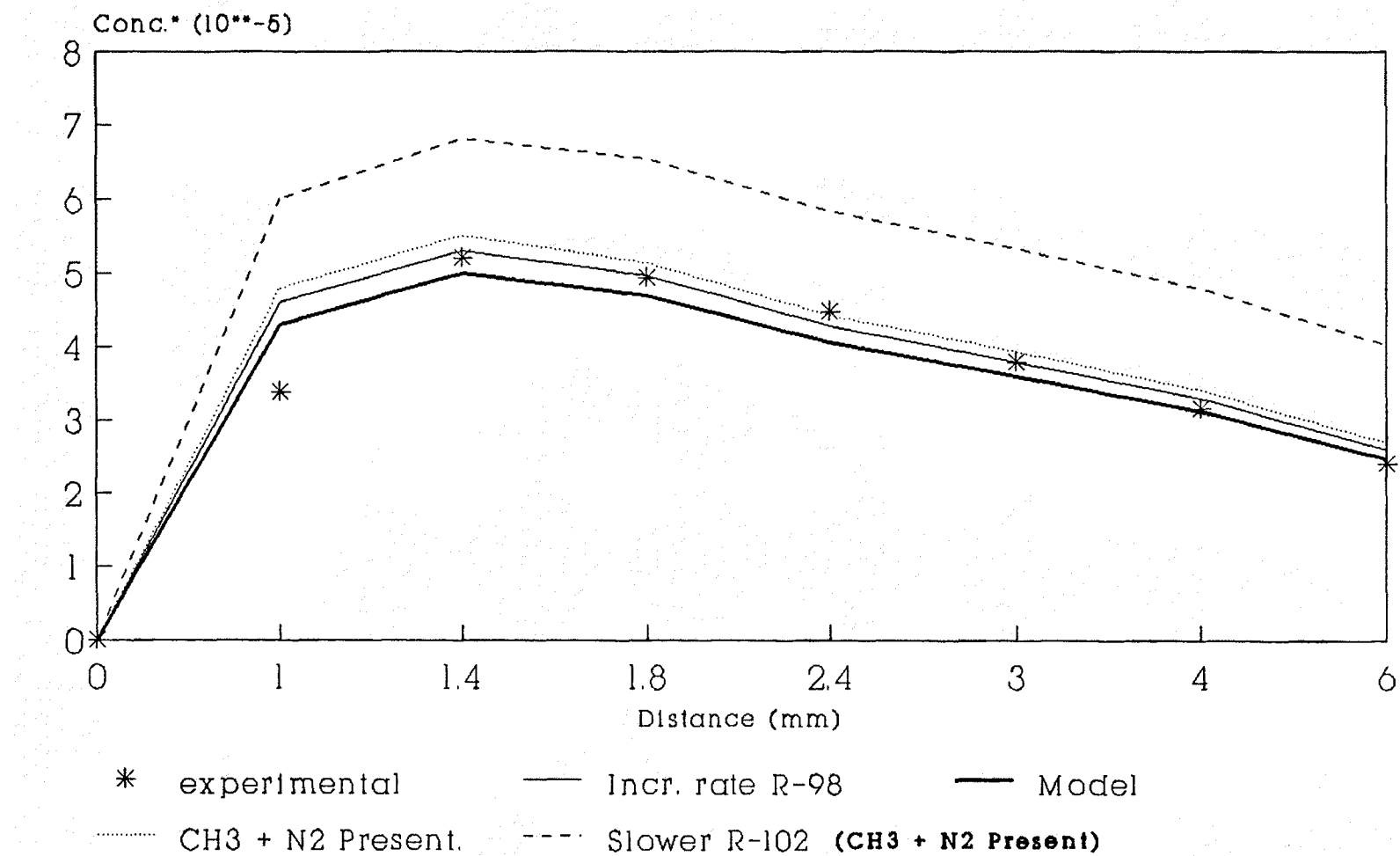
Figure 6.7 Comparison between models & experimental

Flame 5: CN Conc.

Conc.* (10**-8)

* experimental   —— Incr. rate R-98   —— Model

·········· CH3 + N2 Present   - - - Slower R-102   **(CH3 + N2 Present)**

Distance (mm)
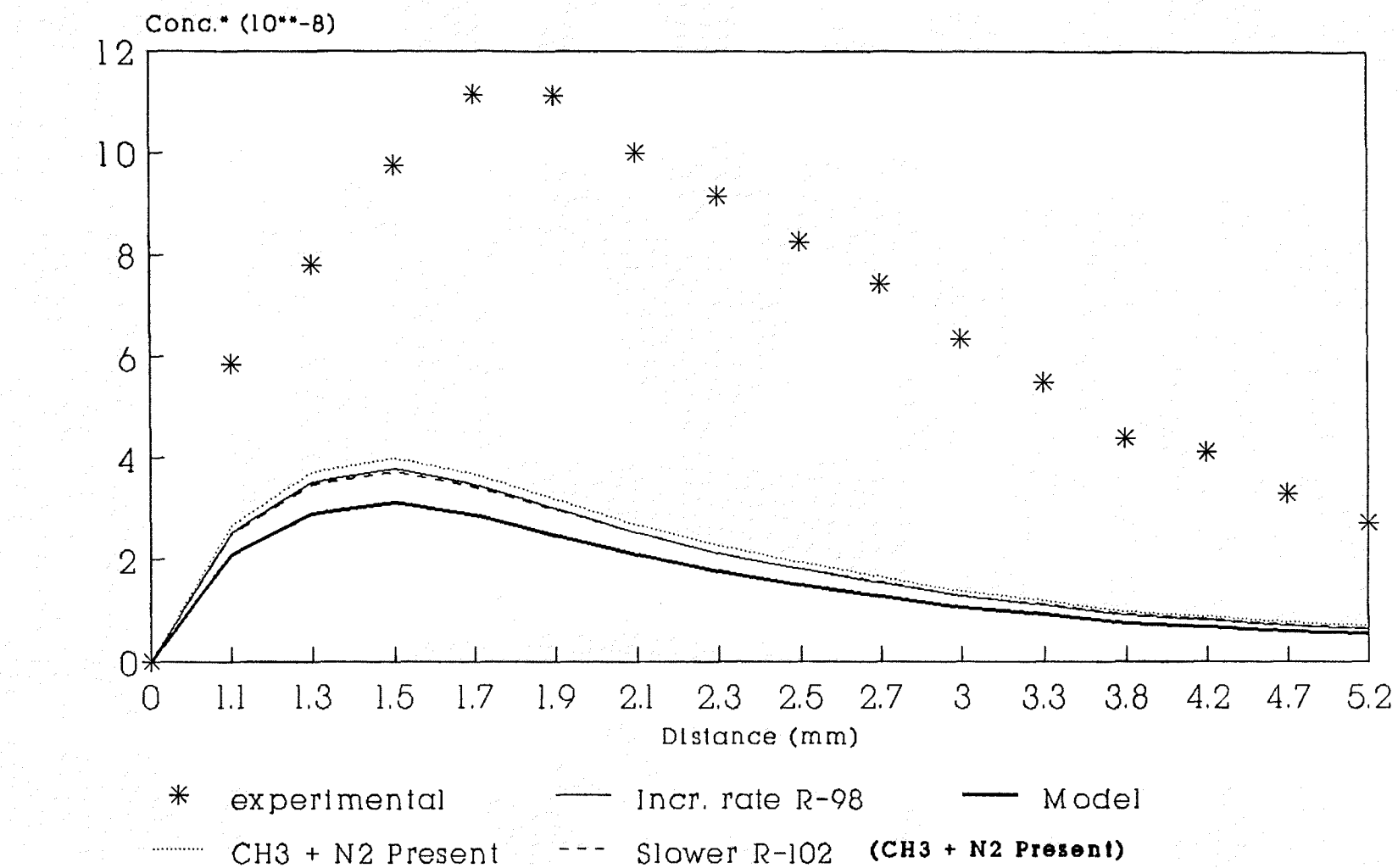
Figure 6.8 Comparisons between model & experimental

Flame 5: NH Conc.

Conc.* (10**-7)

Distance (mm)

- experimental   —— Incr. rate R-98   —— Model

········· CH3 + N2 Present   --- Slower R-102 **(CH3 + N2 Present)**
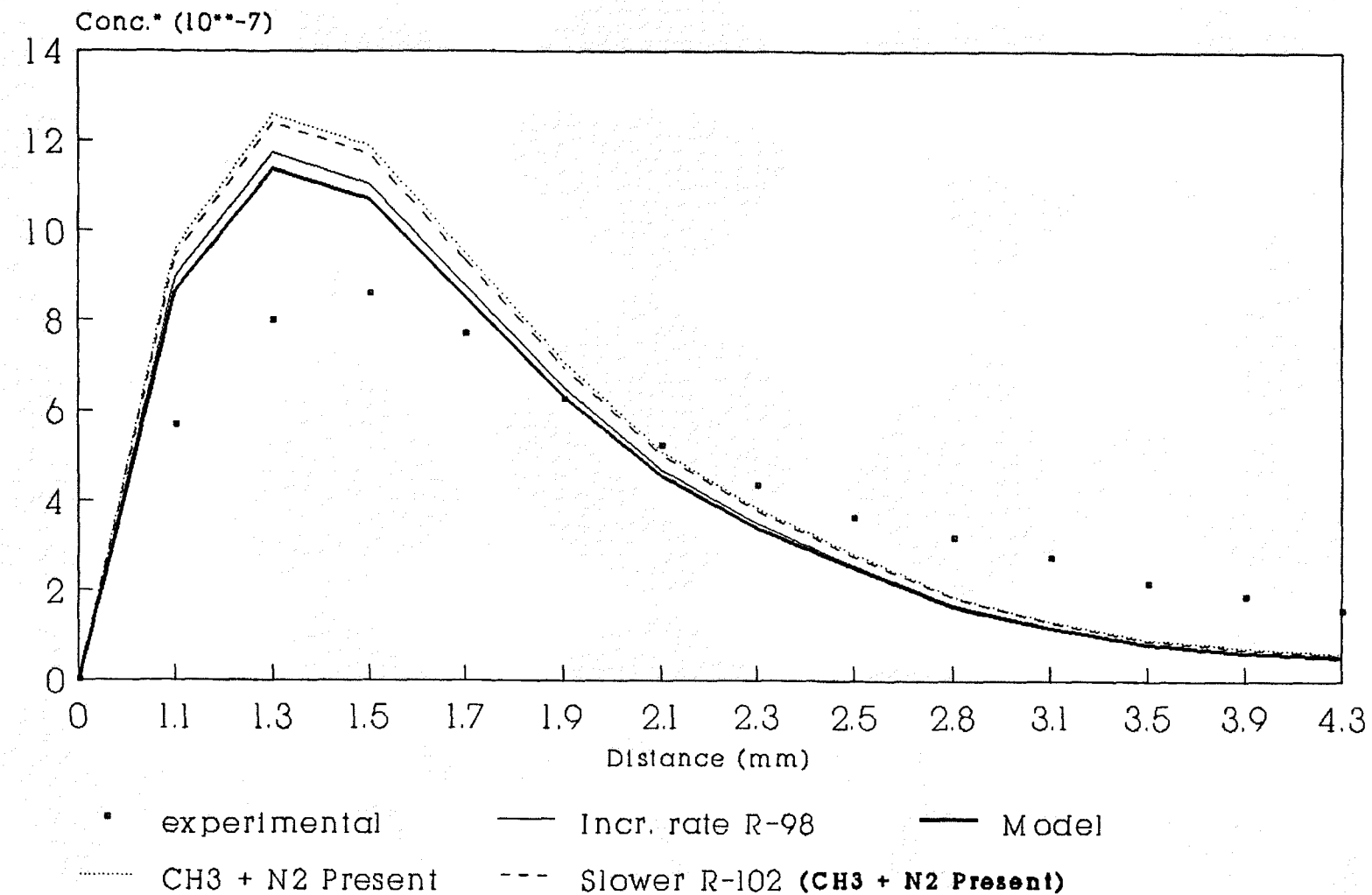
Figure 6.9 Comparison between models & experimental

is interesting to note that the model predicted a drop in the NH concentration by an order of magnitude when going to the undoped flame, which is consistent with the experiment since NH concentration was just at the detection limit in the undoped flame.

To improve the model prediction of NO concentration the simple expedient was to increase the nitrogen fixation rate by reaction R-98. When this was done by reducing the barrier from 17 Kcal to 10 Kcal for the abstraction like channel HCN + N in QRRK calculation, the result is an increase in rate constant for the R-98 reaction by nearly a magnitude. This resulted in increase in NO peak by a factor of 4.5 in undoped flame as demonstrated in Figure 6-5. But it only increases a NO concentration in doped flame by a factor of 1.2, making for a good representation of all the experimental data as shown in Figure 6-7. The predicted CN concentration was better than earlier due to a larger amount of N_2 fixation by R-98.

Since the predicted concentration was still much lower than experimentally observed values in undoped flame the next step was to investigate the following reaction for N_2 fixation in addition to the reactions R-98 in Model :

$$CH_3 + N_2 \longleftrightarrow HCN + NH2$$
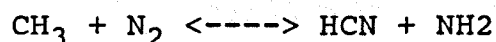
This reaction is 43 Kcal endothermic. An A factor of 3.0E+13 with an E_a of 55 Kcal/mole was used with the 12 Kcal being a

reasonable upper limit for barrier to addition of NH_2 to HCN. A QRRK analysis for this was not performed due to unavailibility of the thermodynamic data for the intermediates involved. It was with the rationale that little would be achieved by doing an QRRK with estimated thermo where error could be high, a generic value was used. Even with such a high E_a it was found that this reaction was contributing towards the formation of NO in addition to reaction R-98. This was because of the preponderance of CH_3 and N_2 concentration. Using this reaction channel, the results for NO concentration in undoped flame as illustrated in figure 6.5 predicted by model shows a increase of factor of 6.0 over the basic model where this above mentioned N_2 fixation by CH_3 was not present. The NO concentration in doped flame as predicted in this case is a now factor of 1.2 higher than experimental value. The CN profile is also improved over the model where this N_2 fixation reaction by CH_3 is not present.

The effect of reduction of rate constant for the reaction of CH_3 with NO (R-102) was investigated for the where reaction between CH_3 + N_2 was there in the mechanism. An activation energy of 1.5 Kcal was added to the value of Levy (1980) rate constant. This increases the NO profile both for undoped and doped flame as illustrated in Figure 6-5 and 6-7 respectively, in comparison to the prediction for the model where R -102 had a faster rate and also had CH_3 + N_2 reaction. There is also a decrease of CN profile due to

slower rate of NO conversion to HCN by reaction R-102.

CONCLUSION

A detailed reaction mechanism based upon fundamental thermochemical kinetic principles has been developed to describe the concentration profiles of OH, CH, NH, CN, and NO including prompt NO radicals in laminar flow, fuel rich methane flames as well as flames doped with 700 ppm ammonia. A one dimensional laminar flat flame code which incorporated diffusion, and the detailed reaction mechanism was used to predict the radical concentration profiles from the model. These calculated values are compared to experimental data of Dean (1984).

The model consist of two reaction subsets, hydrocarbon oxidation set and an ammonia oxidation set. The reactions most important for coupling the two subset are :

$$CH + N_2 \longleftrightarrow HCN + N \qquad (1)$$

$$CH_2 + N_2 \longleftrightarrow HCN + NH \qquad (2)$$

$$CH_3 + NO \longleftrightarrow HCN + H_2O \qquad (3)$$

The mechanism shows good agreement (within experimental error) with experimental concentration as function of distance above the burner, except for NO. The mechanism predicts that reaction (1) is mainly responsible for nitrogen fixation in the fuel rich flame studied. The contribution to the nitrogen fixation by reaction (2) and the Zeldovich (1948) mechanism are negligible.

A rate constant for reaction (1) (from QRRK) consistent with the shock tube data of Bowman (1990) results in under prediction of the NO concentration by a order of magnitude.

A higher value corresponding to a barrier of 10 Kcal for reaction (1) increases the NO peak by a factor of 4.5. Inclusion of the following reaction :

$$CH_3 + N_2 <-----> HCN + NH_2 \qquad\qquad (4)$$

improves the NO profile by a factor of six.

NO decomposition in the flames studied takes place mainly through reaction (3).

A higher value for rate constant for reaction 2 relative to the shock tube data of Bowman and Dean (1990) and an nitrogen fixation reaction in the form of (4) is needed to properly account for the observed nitrogen fixation.

APPENDIX A

Table A-1 Reactions in Mechanism

#	Reaction	Reference	A	n	E
1.	H+O2=O+OH	(Warnatz. Ref 75)	0.120E+18	-0.91000	16490.
2.	H2+O=H+OH	(Warnatz. Ref 75)	0.150E+08	2.0000	7540.0
3.	OH+H2=H2O+H	(Warnatz. Ref 75)	0.100E+09	1.6000	3290.0
4.	OH+OH=O+H2O	(Warnatz. Ref 75)	0.150E+10	1.1400	0.00000E+00
5.	H+H+M=H2+M	(Warnatz. Ref 75)	0.180E+19	-1.0000	0.00000E+00
	H2O	ENHANCED BY	6.500E+00		
	CO2	ENHANCED BY	1.500E+00		
	CO	ENHANCED BY	7.500E-01		
	O2	ENHANCED BY	4.000E-01		
	N2	ENHANCED BY	4.000E-01		
6.	H+OH+M=H2O+M	(Warnatz. Ref 75)	0.220E+23	-2.0000	0.00000E+00
	H2O	ENHANCED BY	6.500E+00		
	CO2	ENHANCED BY	1.500E+00		
	CO	ENHANCED BY	7.500E-01		
	O2	ENHANCED BY	4.000E-01		
	N2	ENHANCED BY	4.000E-01		
7.	H+O2+M=HO2+M	(Warnatz. Ref 75)	0.200E+19	-0.80000	0.00000E+00
	H2O	ENHANCED BY	6.500E+00		
	CO2	ENHANCED BY	1.500E+00		
	CO	ENHANCED BY	7.500E-01		
	O2	ENHANCED BY	4.000E-01		
	N2	ENHANCED BY	4.000E-01		
8.	HO2+H=OH+OH	(Warnatz. Ref 75)	0.150E+15	0.00000E+00	1000.0
9.	HO2+H=H2+O2	(Warnatz. Ref 75)	0.250E+14	0.00000E+00	700.00
10.	HO2+O=OH+O2	(Warnatz. Ref 75)	0.200E+14	0.00000E+00	0.00000E+00
11.	HO2+OH=H2O+O2	(Warnatz. Ref 75)	0.200E+14	0.00000E+00	0.00000E+00
12.	CO+OH=CO2+H	(Warnatz. Ref 75)	0.440E+07	1.5000	-740.00
13.	CH3+H=CH4	(Warnatz. Ref 75)	0.190E+37	-7.0000	9060.0
14.	CH4+H=CH3+H2	(TSANG & WARNATZ)	0.220E+05	3.0000	8740.0
15.	CH4+O=CH3+OH	(TSANG & WARNATZ)	0.102E+08	1.5000	8600.0
16.	CH4+OH=CH3+H2O	(MILLER, Ref 57)	0.160E+07	2.1000	2460.0
17.	CH4+O2=CH3 + HO2	(MILLER, Ref 57)	0.790E+14	0.00000E+00	56000.
18.	CH3+O=CH2O+H	(CHEMACT)	0.700E+14	-0.20000E-01	20.000
19.	CH3+HO2=CH3O+OH	(MILLER, Ref 57)	0.200E+14	0.00000E+00	0.00000E+00
20.	CH3+O2=CH3O2	(CHEMACT)	0.336E+35	-7.4300	5960.0
21.	CH3+O2=O+CH3O	(CHEMACT)	0.789E+15	-0.46000	31150.
22.	CH3+O2=OH+CH2O	(CHEMACT)	0.158E+12	0.30000E-01	10420.
23.	CH3+OH=CH3OH	(CHEMACT)	0.645E+42	-8.5700	13230.
24.	CH3+OH=CH2OH+H	(Warnatz. Ref 75)	0.282E+16	-0.69000	6610.0
25.	CH3+OH=CH2+H2O	(MILLER, Ref 57)	0.750E+07	2.0000	5000.0
26.	CH3O2=OH+CH2O	(DISSOC)	0.465E+29	-5.8100	44460.
27.	CH2OH+M=CH2O+H+M	(MILLER, Ref 57)	0.100E+15	0.00000E+00	25000.
28.	CH3O+M=CH2O+H+M	(MILLER, Ref 57)	0.100E+15	0.00000E+00	25000.
29.	CH2O+H=HCO+H2	(DEAN)	0.440E+15	2.5400	2000.0
30.	CH2O+O=HCO+OH	(TSANG)	0.180E+14	0.00000E+00	3080.0
31.	CH2O+OH=HCO+H2O	(Warnatz. Ref 75)	0.300E+14	0.00000E+00	1200.0
32.	HCO+H=CO+H2	(Warnatz. Ref 75)	0.200E+15	0.00000E+00	0.00000E+00
33.	HCO+O=CO+OH	(Warnatz. Ref 75)	0.300E+14	0.00000E+00	0.00000E+00
34.	HCO+O=CO2+H	(Warnatz. Ref 75)	0.300E+14	0.00000E+00	0.00000E+00
35.	HCO+OH=CO+H2O	(Warnatz. Ref 75)	0.500E+14	0.00000E+00	0.00000E+00
36.	HCO+O2=CO+HO2	(Warnatz. Ref 75)	0.300E+13	0.00000E+00	0.00000E+00
37.	HCO+M=H+CO+M	(Warnatz. Ref 75)	0.710E+15	0.00000E+00	16780.
	H2O	ENHANCED BY	6.500E+00		
	CO2	ENHANCED BY	1.500E+00		
	CO	ENHANCED BY	7.500E-01		
	O2	ENHANCED BY	4.000E-01		
	N2	ENHANCED BY	4.000E-01		
38.	CH+H2=CH2+H (CHEMACT)		0.329E+17	-0.65000	4810.0
39.	CH2+O=CO+H+H	(Warnatz. Ref 75)	0.500E+14	0.00000E+00	0.00000E+00

#	Reaction	Reference	A	n	Ea
42.	CH2+OH=CH + H2O	(CHEMACT)	0.270E-02	3.9400	-2450.0
43.	CH2+OH=CH2O+H	(CHEMACT)	0.185E+15	-0.21000	210.00
44.	CH+OH=H+HCO	(CHEMACT)	0.137E+20	-1.7500	1510.0
45.	CH+O=CO+H	(Warnatz. Ref 75)	0.400E+14	0.00000E+00	0.00000E+00
46.	CH+O2=CO+OH	(Warnatz. Ref 75)	0.789E+10	0.13000	-100.00
47.	CH+O2=HCO+O	(Warnatz. Ref 75)	0.326E+14	-0.10000E-01	10.000
48.	CH+H2O=CH2O+H	(MILLER, Ref 57)	0.300E+14	0.00000E+00	0.00000E+00
49.	CH+CO2=HCO+CO	(MILLER, Ref 57)	0.340E+13	0.00000E+00	690.00
50.	CH+CH4=C2H4+H	(CHEMACT)	0.392E+14	-0.18000	290.00
51.	CH+C2H4=C*C*C+H	(Warnatz. Ref 75)	0.130E+15	0.00000E+00	-344.00
52.	CH+C2H2 = C3H3	(Warnatz. Ref 75)	0.190E+14	0.00000E+00	0.00000E+00
53.	CH3+CH3=C2H6	(Warnatz. Ref 75)	0.170E+54	-12.000	19400.
54.	CH3+CH3=C2H5+H	(Warnatz. Ref 75)	0.800E+15	0.00000E+00	26500.
55.	CH3+CH3=C2H4+H2	(Warnatz. Ref 75)	0.100E+17	0.00000E+00	32000.
56.	C2H6+H=C2H5+H2	(Warnatz. Ref 75)	540.	3.5000	5200.0
57.	C2H6+O=C2H5+OH	(Warnatz. Ref 75)	0.300E+08	2.0000	5110.0
58.	C2H6+OH=C2H5+H2O	(Warnatz. Ref 75)	0.630E+07	2.0000	640.00
59.	O+C2H5=CH3CHO+H	(Warnatz. Ref 75)	0.500E+14	0.00000E+00	0.00000E+00
60.	C2H5+O2=C2H4+HO2	(BOZZELLI)	0.100E+28	-4.8260	9468.0
61.	C2H5+O2=C2H5O+O	(BOZZELLI)	0.110E+14	-0.21000	27934.
62.	C2H4+O=CH3+HCO	(Warnatz. Ref 75)	0.160E+10	1.2000	740.00
63.	C2H4+OH=C2H3+H2O	(Warnatz. Ref 75)	0.700E+14	0.00000E+00	3000.0
64.	C2H4+H=C2H3+H2	(Warnatz. Ref 75)	0.150E+15	0.00000E+00	10190.
65.	C2H3+H=C2H2+H2	(Warnatz. Ref 75)	0.200E+14	0.00000E+00	0.00000E+00
66.	C2H3+O2=C2H2+HO2	(Warnatz. Ref 75)	0.100E+13	0.00000E+00	0.00000E+00
67.	C2H3+O2=HCO+CH2O	(GUTMAN)	0.398E+13	0.00000E+00	-250.00
68.	C2H3=C2H2+H	(Warnatz. Ref 75)	0.160E+33	-5.5000	46200.
69.	C2H2+O=CH2+CO	(Warnatz. Ref 75)	0.794E+14	0.00000E+00	15000.
70.	C2H2+OH=CH2CO+H	(Warnatz. Ref 75)	0.170E+35	-6.7500	9900.0
71.	CH3CHO+H=CH3CO+H2	(DEAN)	0.220E+06	2.5400	1000.0
72.	CH3CHO+O=CH3CO+OH	(DEAN)	0.900E+13	0.00000E+00	3080.0
73.	CH3CO=CH3+CO	(Warnatz. Ref 75)	0.195E+14	0.00000E+00	21505.
74.	CH3CHO+OH=CH3CO+H2O	(DEAN)	0.700E+13	0.00000E+00	1500.0
75.	CH2CO+H=CH3+CO	(BOZZELLI EST.)	0.700E+13	0.00000E+00	2600.0
76.	CH2CO+H=HCCO+H2	(BOZZELLI EST)	0.650E+06	2.5300	12200.
77.	CH2CO+O=HCCO+OH	(MILLER, Ref 57)	0.100E+13	0.00000E+00	8000.0
78.	CH2CO+O=CH2O+CO	(BOZZELLI EST.)	0.170E+13	0.00000E+00	1350.0
79.	CH2CO+OH=CH2O+HCO	(Warnatz. Ref 75)	0.100E+14	0.00000E+00	0.00000E+00
80.	CH2CO+M=CH2+CO+M	(BOZZELLI EST)	0.300E+15	0.00000E+00	75980.
	H2O	ENHANCED BY 1.860E+00			
	CO2	ENHANCED BY 4.000E+00			
	CO	ENHANCED BY 2.000E+00			
	O2	ENHANCED BY 1.100E+00			
	N2	ENHANCED BY 1.100E+00			
81.	C2H2+O=HCCO+H	(Warnatz. Ref 75)	0.435E+15	0.00000E+00	12100.
82.	HCCO+H=CH2+CO	(BOZZELLI)	0.100E+15	0.00000E+00	0.00000E+00
83.	HCCO+O=HCO+CO	(BOZZELLI)	0.300E+14	0.00000E+00	0.00000E+00
84.	HCCO+O2=HCO+CO2	(BOZZELLI)	0.300E+13	0.00000E+00	0.00000E+00
85.	C2H+H2=C2H2+H	(DEAN)	0.100E+14	0.00000E+00	0.00000E+00
86.	C2H2+OH=C2H+H2O	(DEAN)	0.300E+14	0.00000E+00	11000.
87.	C2H+O=CO+CH	(MILLER/BOZZELLI)	0.400E+14	0.00000E+00	0.00000E+00
88.	C2H+O2=HCO+CO	(BOZZELLI)	0.300E+12	0.00000E+00	0.00000E+00
89.	CH2+C2H2=C3H3+H	(Warnatz. Ref 75)	0.180E+13	0.00000E+00	0.00000E+00
90.	C3H3+O=C2H+CH2O	(BOZZELLI)	0.350E+13	0.00000E+00	0.00000E+00
91.	C3H3+O2=CH2CO+HCO	(BOZZELLI)	0.300E+13	0.00000E+00	0.00000E+00
92.	C3H3+H=C#CC	(Warnatz. Ref 75)	0.270E+14	0.00000E+00	0.00000E+00
93.	C#CC+H=CH3+C2H2	(WARNATZ, Ref 75)	0.200E+14	0.00000E+00	2390.0
94.	OH+C#CC=H2O+C3H3	(DEAN)	0.100E+14	0.00000E+00	500.00
95.	C2H+C2H2=C4H2+H	(Warnatz. Ref 75)	0.350E+14	0.00000E+00	0.00000E+00
96.	C4H2+OH=C4H2O+H	(Warnatz. Ref 75)	0.300E+14	0.00000E+00	0.00000E+00
97.	C4H2O+OH=C2H2+CO+CO+H	(Warnatz. Ref 75)	0.100E+15	0.00000E+00	0.00000E+00
98.	CH+N2=HCN+N	(QRRK)	0.193E+15	-0.49000	14390.
99.	CH+NO=HCN+O	(QRRK)	0.349E+18	-1.1100	990.00
100.	CH2+NO=HCN+OH	(CHEMACT)	0.647E+24	-3.6500	2720.0
101.	CH2+NO=CH2O+N		0.160E+13	0.00000E+00	7000.0
102.	CH3+NO=HCN+H2O		0.100E+12	0.00000E+00	0.00000E+00

103.	HCN+OH=CN+H2O		0.440E+13	0.00000E+00	9000.0
104.	HCN+O=NCO+H		0.126E+08	1.8700	6800.0
105.	HCN+O=CN+OH		0.436E+14	0.00000E+00	14823.
106.	CN+O2=NCO+O		0.560E+13	0.00000E+00	0.00000E+00
107.	CN+H2=HCN+H		0.545E+12	0.70000	4885.0
108.	CN+OH=NCO+H		0.500E+14	0.00000E+00	0.00000E+00
109.	O+CN=CO+N		0.180E+14	0.00000E+00	0.00000E+00
110.	NCO+H=NH+CO		0.500E+14	0.00000E+00	0.00000E+00
111.	O+NCO=NO+CO		0.200E+14	0.00000E+00	0.00000E+00
112.	N+NCO=N2+CO		0.200E+14	0.00000E+00	0.00000E+00
113.	OH+NCO=NO+CO+H		0.100E+14	0.00000E+00	0.00000E+00
114.	NO+NCO=N2O+CO		0.100E+14	0.00000E+00	0.00000E+00
115.	NH+NO=N2+OH		0.120E+14	0.00000E+00	0.00000E+00
116.	NH+OH=N+H2O		0.500E+12	0.50000	2000.0
117.	NH+OH=HNO+H		0.500E+12	0.50000	2000.0
118.	NH+H=N+H2		0.300E+14	0.00000E+00	0.00000E+00
119.	NH+O=NO+H		0.630E+12	0.50000	0.00000E+00
120.	NH+O=N+OH		0.630E+12	0.50000	8000.0
121.	H+NH=NH2	(CHEMACT)	0.761E+18	-2.3600	820.00
122.	N2O+H=NH+NO		0.380E+15	0.00000E+00	34500.
123.	NH+N=N2+H		0.630E+12	0.50000	0.00000E+00
124.	N+NO=N2+O		0.160E+14	0.00000E+00	0.00000E+00
125.	N+O2=NO+O		0.640E+10	1.0000	6300.0
126.	N+OH=NO+H		0.630E+12	0.50000	0.00000E+00
127.	N2O+M=N2+O+M		0.270E+15	0.00000E+00	54100.
128.	N2O+H=N2+OH		0.760E+14	0.00000E+00	15100.
129.	N2O+O=N2+O2		0.100E+15	0.00000E+00	28020.
130.	N2O+O=NO+NO		0.100E+15	0.00000E+00	28020.
131.	HO2+NO=NO2+OH		0.343E+13	0.00000E+00	-260.00
132.	NH3+M=NH2+H+M	(Bozzelli)	0.251E+17	0.00000E+00	93790.
133.	NH3+H=NH2+H2	(MICHAEL)	0.182E+15	0.00000E+00	16030.
134.	NH3+O=NH2+OH		0.200E+14	0.00000E+00	8883.0
135.	NH3+OH=NH2+H2O		0.545E+14	0.00000E+00	8058.0
136.	NH2+H=NH+H2		0.190E+14	0.00000E+00	0.00000E+00
137.	NH2+O=NH+OH	(760.200 -1900 N2)(BOZZELLI, Ref 14)	0.690E+12	0.35600	-0.20100
138.	NH2+O=HNO+H	(200-1900 2 CHNLS)(BOZZELLI, Ref 14)	0.150E+16	-0.48900	326.00
139.	NH2+OH=NH2O+H	(1.00A 300.-2100.N2)(BOZZELLI, Ref 14)	0.318E+16	-0.59600	15100.
140.	NH2+OH=H2O+NH	(1.00A 300.-2100.N2)(BOZZELLI, Ref 14)	0.722E+18	-1.3680	4901.0
141.	NH2+O2=HNO+OH	(760.200-1800 N2)(BOZZELLI, Ref 14)	0.472E+15	-1.0520	27500.
142.	NH2+O2=NH2O+O	(760.200-1800)(BOZZELLI, Ref 14)	0.000E+18	-1.3300	33600.
143.	NH2+NO=H2O+N2	(3WELL CHEMACT 1.2->1.8)	0.186E+32	-5.8000	6970.0
144.	NH2+NO=NH2NO	(3WELL CHEMACT)	0.126E+30	-5.7200	3410.0
145.	NH2+NO=HNNOH	(3WELL CHEMACT)	0.626E+37	-8.1100	7580.0
146.	NH2+HNO=NH3+NO		0.351E+14	0.00000E+00	0.00000E+00
147.	NH2+HNO= NNH+H2O	(760. 300.-2500X10)	0.145E+19	-1.3750	4253.0
148.	NH2+HO2= NH2O+OH	(760.300.-1900. N2)(BOZZELLI, Ref 14)	0.195E+14	-0.23900E-01	22.000
149.	NH2+HO2= NH3+O2	(BOZZELLI, Ref 14)	0.245E+14	0.00000E+00	0.00000E+00
150.	NH2+NO2=NH2O+NO		0.350E+13	0.00000E+00	7500.0
151.	NNH+M=N2+H+M		0.200E+15	0.00000E+00	19870.
152.	NNH+O2=HO2+N2		0.250E+13	0.00000E+00	3020.0
153.	HNO+M=NO+H+M		0.178E+17	0.00000E+00	48690.
154.	HNO+O=OH+NO		0.550E+14	0.00000E+00	0.00000E+00
155.	HNO+OH=NO+H2O		0.650E+14	0.00000E+00	1800.0
156.	HNO+O2=HO2+NO		0.100E+13	0.00000E+00	3000.0
157.	HNO+HO2=H2O2+NO		0.290E+14	0.00000E+00	1500.0
158.	HNO+HNO=NH2O+NO		0.100E+14	0.00000E+00	1500.0
159.	NH+O2=NO+OH	(IS)	0.857E+14	-0.94300	777.00
160.	NH+O2=HNO+O	(IS)	0.100E+14	0.00000E+00	10000.
161.	NH+NH2O=NH2+HNO	(ESTIMATED)	0.432E+14	0.00000E+00	0.00000E+00
162.	NH+HNO=NNH+OH	(ESTIMATED)	0.307E+14	0.00000E+00	1500.0
163.	NH2O=HNO+H		0.159E+14	0.00000E+00	62418.
164.	NH2O+O2=HNO+HO2	(ESTIMATED)	0.111E+13	0.00000E+00	13900.
165.	NH2O+O=HNO+OH		0.530E+14	0.00000E+00	1350.0
166.	NH2O+OH=H2O+HNO		0.651E+14	0.00000E+00	1300.0
167.	HONO=OH+NO	(KREV 1.7E13EA2)	0.545E+16	0.00000E+00	49600.
168.	HONO+O=OH+NO2		0.200E+14	0.00000E+00	4500.0

169.	HONO+OH=H2O+NO2		0.200E+14	0.00000E+00	3500.0
170.	HONO+NH2=NH3+NO2		0.289E+13	0.00000E+00	4000.0
171.	NO2+H=NO+OH		0.350E+15	0.00000E+00	1470.0
172.	NO2+M=NO+O+M	(M=n2)	0.110E+17	0.00000E+00	65580.0
173.	NO2+O=NO+O2		0.100E+14	0.00000E+00	600.00
174.	HO2+NO2=HONO+O2		0.200E+13	0.00000E+00	5000.0
175.	O+O+M=O2+M	(M=n2)	0.000E+17	-1.0000	0.00000E+00
176.	HO2+HO2=H2O2+O2	(WARNATZ)	0.200E+13	0.00000E+00	0.00000E+00
177.	H2O2+M=OH+OH+M	(WARNATZ)	0.120E+18	0.00000E+00	45400.
178.	H2O2+OH=H2O+HO2	(WARNATZ)	0.700E+13	0.00000E+00	1430.0
179.	NH2+NO=NNH+OH	(3WELL CHEMACT)	0.542E+24	-3.3000	9230.0
180.	H+HCCO=CH2S+CO	(MILLER, Ref 57)	0.100E+15	0.00000E+00	0.00000E+00
181.	CH2S+M=CH2+M	(MILLER, Ref 57)	0.100E+14	0.00000E+00	0.00000E+00
	H	ENHANCED BY 0.000E+00			
182.	CH2S+CH4=2CH3	(MILLER, Ref 57)	0.400E+14	0.00000E+00	0.00000E+00
183.	CH2S+C2H6=CH3+C2H5	(MILLER, Ref 57)	0.120E+15	0.00000E+00	0.00000E+00
184.	CH2S+O2=CO+OH+H	(MILLER, Ref 57)	0.300E+14	0.00000E+00	0.00000E+00
185.	CH2S+H2=CH3+H	(MILLER, Ref 57)	0.700E+14	0.00000E+00	0.00000E+00
186.	CH2S+H=CH2+H	(MILLER, Ref 57)	0.200E+15	0.00000E+00	0.00000E+00
187.	CH+H=C+H2	(MILLER, Ref 57)	0.150E+15	0.00000E+00	0.00000E+00
188.	C+O2=CO+O	(MILLER, Ref 57)	0.200E+14	0.00000E+00	0.00000E+00
189.	C+OH=CO+H	(MILER, Ref 57)	0.500E+14	0.00000E+00	0.00000E+00
190.	C+CH3=C2H2+H	(MILLER, Ref 57)	0.500E+14	0.00000E+00	0.00000E+00
191.	C+CH2=C2H+H	(MILLER, Ref 57)	0.500E+14	0.00000E+00	0.00000E+00
192.	CH3+OH=CH2S+H2O	(CHEMACT)	0.142E+22	-2.4000	9580.0
193.	CH2+N2=HCN+NH	(CHEMACT)	0.405E+14	-0.54000	33620.
194.	CH2S+N2=HCN+NH	(CHEMACT)	0.154E+17	-1.3200	27100.
195.	CH3+N=CH2N+H	(HANSON)	0.710E+14	0.00000E+00	0.00000E+00
196.	CH3+NO=CH2N+OH	(MILLER, Ref 57)	0.100E+12	0.00000E+00	15000.
197.	CH2N+M=HCN+H+H	(MILLER, Ref 57)	0.300E+15	0.00000E+00	22000.
198.	CH2N+H=N2+CH2	(MILLER, Ref 57)	0.200E+14	0.00000E+00	0.00000E+00

NO ERRORS WERE ENCOUNTERED ON INPUT CARDS.
ALL INPUT WAS PROCESSED, AND THE LINKING FILE CREATED

Experimental Conditions

Flow Rates (slpm)

Flame	CH_4	Air	O_2	NH_3	Equiv. Ratio
#2	2.32	8.66	0.92	---	1.7
#5	2.32	8.66	0.92	0.0083	1.7

Dist. above burner (mm)	T (K)
1.0	1833
2.0	1831
3.0	1823
4.0	1812
5.0	1801
6.0	1792

TABLE A-2

Input Parameters for QRRK Analysis:

$CH + H_2$ ---> Products
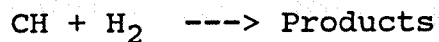
k	A	Ea	source
1	3.0E+14	3.0	a
-1	4.50E+14	107.9	b
2	2.8E+15	109.77	c

$<v> = 1497.0/cm$			d
LJ PARAMETERS :			e
$o^\sim = 3.8$ A		$e/k = 144$ cal	

a. Estimated from Bernan and Lin [10].
b. This study, Ea from Microscopic Reversibility.
c. Estimated from $A_{-2} = 1.2$ E+14 from RRKM calculation
   of Bernan and Lin [10].
d. $<v.>$ estimated by the method of Benson for CH_3 transition
   state [4].

g. Kee et. al [46]
UNITS: cc/mol sec and sec^{-1},   Ea in Kcal/mol

TABLE A-3

Results from CHEMACT calculation

Apparent Rate Constants for CH + H2 ---> Products

Products	A	n	Ea	*	N_2 Bath Gas	
CH_3	1.04E26	-4.56	2650.		76	Torr
	1.25E27	-4.57	2800.		760	Torr
	5.92E28	-4.46	3300.		7600	Torr
CH_2 + H	3.13E16	-0.64	4780.		76	Torr
	3.29E16	-0.65	4810.		760	Torr
	4.58E16	-0.68	5050.		7600	Torr

Valid from 1000 - 1400. K

Best Fit Equation A T^n exp(-Ea/RT) cm^3/mole-sec Units Ea in Cal/mole. Modified Arrhenius Form of the rate constants, k, incorporate changes in Conc [M] with Temp. [M] should not be included in rate expressions.

TABLE A-4

Input Parameters for QRRK Analysis

$CH + N_2 \longrightarrow$ Products
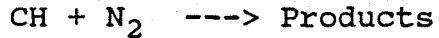
k	A	Ea	source
1	4.0 E+12	0.0	a
-1	1.16 E+14	20.0	b
2	8.80 E+12	15.0	c

$<v>$ = 857.68/cm			d
LJ PARAMETERS :		Ref	e
o˜ = 2.5 A	e/k = 150. cal		

a. High pressure limit Berman [9].
b. This study, Ea from Microscopic Reversibility.
c. Estimated from OH + CH#CH $\approx 10^{12.5}$ E_a from discussion between Benson and Blauwens.
e. Calculated[16] $<v>$ for HCNN = 857.68 cm^{-1}; from $C_p$data. C_p data generated from average of HCCO.
g. Lennard Jones Parameter estimated from HCCO.

o˜ = 2.5 A, e/k 150 °K.

TABLE A-5

Results from CHEMACT calculation

Apparent Rate Constants for CH + N_2 ---> Products

Products	A	n	Ea	*	N_2 Bath Gas
HCNN	4.11E44	-9.15	17920.		7.6 Torr
	4.51E30	-5.02	10630.		760 Torr
	3.16E19	-1.77	4260.		7600 Torr
HCN + N	6.8 E41	-7.62	31290.		7.6 Torr
	4.91E36	-6.0	33070.		760 Torr
	5.04E20	-1.35	27610.		7600 Torr

Valid from 1000 - 1400. K

Best Fit Equation $A \, T^n \exp(-Ea/RT)$ cm^3/mole-sec Units Ea in Cal/mole. Modified Arrhenius Form of the rate constants, k, incorporate changes in Conc [M] with Temp. [M] should not be included in rate expressions.

TABLE A-6

Input Parameters for QRRK Analysis

CH + NO   ---> Products

k	A	Ea	source
1	1.2E+14	0.0	a
-1	9.25E+17	54.58	b
2	7.37E+14	9.8	c

$<v>$ = 935.35/cm   d

LJ PARAMETERS :   Ref   e

o~ = 3.82 A   e/k = 232.4 cal

a. Estimated from Berman et al [7].
b. This study, Ea from Microscopic Reversibility.
c. Estimated from O + CH#CH $\approx 10^{13.14}$ [47]. E_a from Melius.
e. Calculated[16] $<v>$ for HCNO = 935.35 cm^{-1}; from C_p data.
g. Lennard Jones Parameter estimated from HCCO [45] .

o~ = 3.82 A,   e/k 232.4 ^oK.

TABLE A-7

Results from CHEMACT calculation

Apparent Rate Constants for CH + NO ---> Products

Products	A	n	Ea	*	N_2 Bath Gas	
HCNO	7.33E15	-2.91	1290.		76	Torr
	7.33E16	-2.91	1290.		760	Torr
	7.33E17	-2.91	1290.		7600	Torr
HCN + O	3.49E17	-1.11	990.		76	Torr
	3.49E17	-1.11	990.		760	Torr
	3.49E17	-1.11	990.		7600	Torr

Valid from 1000 - 1400. K

Best Fit Equation $A\ T^n\ \exp(-Ea/RT)$ cm^3/mole-sec   Units Ea in Cal/mole. Modified Arrhenius Form of the rate constants, k, incorporate changes in Conc [M] with Temp. [M] should not be included in rate expressions.

TABLE A-8

Input Parameters for QRRK Analysis

CH + O_2 ---> Products
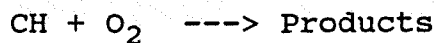
k	A	Ea	source
1	3.1E+13	0.0	a
-1	4.64E+15	45.2	b
2	9.58E+15	4.0	c
3	1.00E+13	9.0	d
-3	7.20E+12	144.0	e
4	1.36E+12	12.8	f
5	5.90E+14	33.0	g
-5	7.27E+13	41.05	h
6	8.4 E+14	29.31	i
7	1.36 E+12	39.1	j

$<v>$ = 1248 /cm   k

LJ PARAMETERS :   l

o^- = 3.9 A e/k = 436 cal

a. Bernan and Lin [7].
b. This study, Ea from Microscopic Reversibility. H_f estimated.
c. Estimated from A_{-2} = $10^{13.16}$ for OH + CO from Kerr and Moss [47]. Barrier estimated from OH addition to CH_2O by Page [59].
d. Estimated from transition state of 1 rotor lost. E_a from vinylidene radical.
e. Estimated from thermo and Microscopic reversibility.
f. Estimated from E_{-5} = $10^{13.3}$ for OH + CO from Kerr and Moss [47]. E_5 from Schatz [68].
g. Estimated from transition state of 1 rotor gain. E_a from

Schatz [68].

h. Estimated from thermo and Microscopic reversibility.
i. Estimated from $A_{-6}= 10^{13.16}$ from Kerr and Moss. E_6
   from Schatz [68].
j. Estimated from $E_{-7}= 0.5*10^{13.3}$ for OH + CO from Kerr and
   Moss. E_7 from Schatz [68].
k. <v.> estimated from CPFIT by THERM .C_p estimated from HCOO
l. Estimated from CH_2CO .

TABLE A-9

Results from CHEMACT calculation

Apparent Rate Constants for CH + O_2 ---> Products

Products	A	n	Ea	*	N_2 Bath Gas	
HCO + O	3.26E13	-0.01	10.		76	Torr
	3.26E13	-0.01	10.		760	Torr
	3.26E13	-0.01	10.		7600	Torr
OH + CO	7.89E09	.13	-100.		76	Torr
	7.89E09	.13	-100.		760	Torr
	7.89E09	.13	-100.		7600	Torr
H + CO_2						
	5.30E07	.07	-50		76	Torr.
	5.30E07	.07	-50		760	Torr.
	5.30E07	.07	-50		7600	Torr.

   Valid from 300 - 2000. K

Best Fit Equation A T^n exp(-Ea/RT) cm^3/mole-sec   Units Ea in
Cal/mole. Modified Arrhenius Form of the rate constants, k,
incorporate changes in Conc [M] with Temp. [M] should not be
included in rate expressions.

TABLE A-10

Input Parameters for QRRK Analysis

$CH + O_2 \longrightarrow$ Products

k	A	Ea	source
1	3.1E+13	0.0	a
-1	2.59E+15	180.24	b
2	5.30E+15	118.64	c
3	1.36E+12	12.8	d
4	5.94E+14	33.0	e
-4	9.35E+13	41.07	f
5	1.27E+12	39.1	g
6	8.40E+14	29.31	h

$<v> = 1283$ /cm			i
LJ PARAMETERS :			j
$o^- = 3.9$ A		$e/k = 436$ cal	

a. Bernan and Lin [7].
b. Ea from Microscopic Reversibility. H_f estimated.
c. From $A_{-2} = 10^{13.16}$ for OH + CO from Kerr and Moss [47].
   Barrier from OH addition to CH_2O by Page [59].
d. From $E_{-5} = 10^{13.3}$ for H + C_2PH_4 from Kerr and Moss.
   E_5 from Schatz [68].
e. Estimated using transition state Theory of 1 rotor gain. E_a
   from Schatz [68].
f. From thermodynamics and Microscopic reversibility.
g. From $A_{-5} = 10^{13.3}$ from Kerr and Moss [47]. E_5
   from Schatz [68].
h. From $A_{-7} = 0.5*10^{13.3}$ for H + C_22H_4 from Kerr and
   Moss. E_7 from Schatz.
i. $<v.>$ estimated from CPFIT by THERM . C_p estimated from H(CO)O
   from Benson [ ].
j. Estimated from CH_2CO .
UNITS: cc/mol sec and sec^{-1},   Ea in Kcal/mol

TABLE A-11

Results from CHEMACT calculation

Apparent Rate Constants for CH + O_2 ---> Products

Products	A	n	Ea	*	N_2 Bath Gas	
HCO + O	3.26E13	-0.01	10.		76	Torr
	3.26E13	-0.01	10.		760	Torr
	3.26E13	-0.01	10.		7600	Torr
OH + CO	7.89E09	.13	-100.		76	Torr
	7.89E09	.13	-100.		760	Torr
	7.89E09	.13	-100.		7600	Torr
H + CO_2						
	5.30E07	.07	-50		76	Torr.
	5.30E07	.07	-50		760	Torr.
	5.30E07	.07	-50		7600	Torr.

Valid from 300 - 2000. K

Best Fit Equation $A\, T^n\, \exp(-Ea/RT)$ cm^3/mole-sec Units Ea in Cal/mole. Modified Arrhenius Form of the rate constants, k, incorporate changes in Conc [M] with Temp. [M] should not be included in rate expressions.

TABLE A-12

Input Parameters for QRRK Analysis

$CH + CH_4 \longrightarrow$ Products

k	A	Ea	source
1	1.0E+14	0.0	a
-1	3.95E+15	95.98	b
2	9.38E+12	39.82	c
3	2.41 E+15	99.28	d

$<v> = 1547$ /cm		e
LJ PARAMETERS :		f
$o^- = 4.3$ A	$e/k = 232.3$ cal	

a. Bernan and Lin. [8]
b. This study, Ea from Microscopic Reversibility.
c. $A_{-2} = 10^{13.3}$ from Allara and Shaw [80].
   $E_{-2} = 3.2$ [80].
d. $A_{-3} =$ Average A of CH_3+CH_3 and $C_2H_5 + C_2H_5$
   addition [80].
   $E_{-2} = 3.3$ [80].
e. <v.> Kee et. al [46].
f. Kee. et al [46].
UNITS: cc/mol sec and sec^{-1},   Ea in Kcal/mol

TABLE A-13

Results from CHEMACT calculation

Apparent Rate Constants for CH + CH_4 ---> Products

Products	A	n	Ea	*	N_2 Bath Gas	
CH_2 + CH_3	2.88E00	3.81	170.		76	Torr
	1.4E-06	5.59	290.		760	Torr
	2.7E-06	5.41	760.		7600	Torr
C_2H_4 + H	3.32E14	-0.16	170.		76	Torr
	3.92E14	-0.18	290.		760	Torr
	2.65E14	-0.12	760.		7600	Torr

Valid from 300 - 2000. K

Best Fit Equation A T^n exp(-Ea/RT) cm^3/mole-sec Units Ea in Cal/mole. Modified Arrhenius Form of the rate constants, k, incorporate changes in Conc [M] with Temp. [M] should not be included in rate expressions.

TABLE A-14

Input Parameters for QRRK Analysis

$CH + C_2H_6 \longrightarrow$ Products
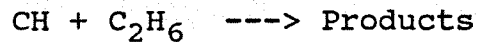
k	A	Ea	source
1	2.7E+14	0.0	a
-1	3.05E+16	101.27	b
2	1.4E+13	38.33	c
3	1.36E+14	33.69	d

$\langle v \rangle$ = 1221 /cm		e
LJ PARAMETERS :		f
o~ = 4.98 A	e/k = 266.8 cal	

a. Bernan and Lin [8].
b. This study, Ea from Microscopic Reversibility.
c. A_{-2} = 6.2E+12 for H addition to CH_3CHCH_2 from Kerr [47].
   E_{-2} = 2.0 [47].
d. A_{-3} = 1.12E+12 for CH_3 addition to C_2H_4 from Kerr [47].
   E_{-2} = 31.76
e. $\langle v. \rangle$ estimated from CPFIT by THERM [63].
f. Kee [46]. et al
UNITS: cc/mol sec and sec^{-1},   Ea in Kcal/mol

TABLE A-15

Results from CHEMACT calculation

Apparent Rate Constants for CH + C_2H_6 ---> Products

Products	A	n	Ea	*	N_2 Bath Gas	
C_3H_7	1.91E23	-4.00	1960.		76	Torr
	2.03E24	-4.00	1990.		760	Torr
	3.08E24	-4.05	2230.		7600	Torr
C_3H_6 + H	5.62E11	.41	-290.		76	Torr
	6.02E11	.40	-260.		760	Torr
	9.66E11	.35	0.00		7600	Torr
C_2H_4 + CH_3	3.10E14	-0.03	20.00		76	Torr
	3.33E14	-0.03	50.00		760	Torr
	5.29E14	-0.09	310.0		7600	Torr

Valid from 300 - 2000. K

Best Fit Equation $A\ T^n\ \exp(-Ea/RT)$ cm^3/mole-sec Units Ea in Cal/mole. Modified Arrhenius Form of the rate constants, k, incorporate changes in Conc [M] with Temp. [M] should not be included in rate expressions.

TABLE A-16

Input Parameters for QRRK Analysis

CH + OH   ---> Products

k	A	Ea	source
1	6.0E+13	0.0	a
-1	8.62E+16	129.9	b
2	1.43E+13	55.61	c

$\langle v \rangle$ = 1394 /cm		e
LJ PARAMETERS :		f
o~ = 3.59 A	e/k = 498.0 cal	

a. Estimated from 3*[OH + $CH_3$3].
b. This study, Ea from Microscopic Reversibility.
c. Estimated from $A_{-2} \approx$ H + C2H4 = 2.7E+13 from Kerr and Moss [47].
   E_{rev} estimated from the barrier of H addition to CH_2O
   Page [59].
d. $\langle v. \rangle$ estimated from CPFIT by THERM [63] from C_p data of HNOH.
g. Estimated from CH_2O
UNITS: cc/mol sec and sec^{-1},   Ea in Kcal/mol

TABLE A-17

Results from CHEMACT calculation

Apparent Rate Constants for CH + OH ---> Products

Products	A	n	Ea	*	N_2 Bath Gas
CHOH	4.94E20	-3.58	1860.	76	Torr
	4.97E21	-3.582	1860.	760	Torr
	5.29E22	-3.59	1900.	7600	Torr
HCO + H	1.36E19	-1.75	1510.	76	Torr
	1.37E19	-1.75	1510.	760	Torr
	1.46E19	-1.75	1550.	7600	Torr

Valid from 1000 - 1400. K

Best Fit Equation $A\ T^n\ exp(-Ea/RT)$ cm^3/mole-sec Units Ea in Cal/mole. Modified Arrhenius Form of the rate constants, k, incorporate changes in Conc [M] with Temp. [M] should not be included in rate expressions.

TABLE A-18

Input Parameters for QRRK Analysis

$CH_2 + N_2$ ---> Products
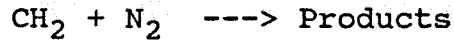
k	A	Ea	source
1	2.2E+12	7.0	a
-1	1.2E+14	27.3	b
2	2.7E+13	52.55	c

$<v> = 1151/cm$			d
LJ PARAMETERS :			e
$o^- = 3.97$ A		$e/k = 436.$ cal	

a. Estimated this study.from $1/2(O + C_2H_4)$.
b. This study, Ea from Microscopic Reversibility. H_f CH_2N_2 from average of Berman [81] and Melius [82]. S_f from S_f of $CH_2CO + 2*R*ln2$ to account for two unpaired electron.
c. Transition State Theory (This Study).
   loss of: 1 rotors, degeneracy 2.
   Ea = 8 Kcal barrier for the addition of NH + HCN
d. <v.> estimated from CPFIT by THERM .C_p estimated from CH_2CO
e. Estimated from CH_2CO .
UNITS: cc/mol sec^2 and sec^{-1}, Ea in Kcal/mol

TABLE A-19

Results from CHEMACT calculation

Apparent Rate Constants for $CH_2 + N_2$ ---> Products

Products	A	n	Ea	*	N_2 Bath Gas
CH_2N_2	1.68E29	-6.18	10660.		76 Torr
	2.50E30	-6.22	11090.		760 Torr
	5.84E29	-5.72	11530.		7600 Torr
HCN + NH	4.02E13	-0.54	33610.		76 Torr
	4.04E13	-0.54	33620.		760 Torr
	4.28E13	-0.54	33650.		7600 Torr

Valid from 300 - 2000. K

Best Fit Equation $A\ T^n\ \exp(-Ea/RT)$ cm^3/mole-sec   Units Ea in Cal/mole. Modified Arrhenius Form of the rate constants, k, incorporate changes in Conc [M] with Temp. [M] should not be included in rate expressions.

TABLE A-20

Input Parameters for QRRK Analysis

$CH_2 + N_2 \quad ---> \quad$ Products

k	A	Ea	source
1	4.0E+12	0.0	a
-1	1.2E+14	29.5	b
2	2.7E+13	52.55	c

$<v> = 1151/cm$		d
LJ PARAMETERS :		e
$o^- = 3.97$ A	$e/k = 436.$ cal	

a. Estimated this study.from $2*({}^3CH_2 + N_2)$
b. This study, Ea from Microscopic Reversibility. H_f CH_2N_2
   from average of Berman [81] and Melius [82]. S_f from S_f of
   $CH_2CO + 2*R*ln2$ to account for two unpaired electron.
c. Transition State Theory (This Study).
   loss of: 1 rotors, degeneracy 2.
   Ea = 8 Kcal barrier for the addition of NH + HCN
d. $<v.>$ estimated from CPFIT by THERM .C_p estimated from CH_2CO
e. Estimated from CH_2CO .
UNITS: cc/mol sec and sec^{-1},   Ea in Kcal/mol

TABLE A-21

Results from CHEMACT calculation

Apparent Rate Constants for $CH_2 + N_2$ ---> Products

Products	A	n	Ea	*	N_2 Bath Gas	
CH_2N_2	2.17E29	-6.26	3690.		76	Torr
	3.05E30	-6.29	3930.		760	Torr
	9.71E30	-6.13	4550.		7600	Torr
HCN + NH	1.53E16	-1.32	27100.		76	Torr
	1.53E16	-1.32	27100.		760	Torr
	1.56E16	-1.32	27110.		7600	Torr

Valid from 300 - 2000. K

Best Fit Equation $A \, T^n \, exp(-Ea/RT)$ cm^3/mole-sec Units Ea in Cal/mole. Modified Arrhenius Form of the rate constants, k, incorporate changes in Conc [M] with Temp. [M] should not be included in rate expressions.

```
------------------------------------------------------------------------------------------
                TABLE B.1 :    RESULT FROM THE MODEL FOR UNDOPED FLAME
------------------------------------------------------------------------------------------

   PREMIX: ONE-DIMENSIONAL STEADY PREMIXED LAMINAR FLAME CODE
       PRODUCTION VERSION 2.4, NOVEMBER 1985

       SINGLE PRECISION

                 WORKING SPACE REQUIREMENTS
                   PROVIDED        REQUIRED
 LOGICAL             160              58
 INTEGER            25000           9011
 REAL              2470700         1075107


       KEYWORD INPUT

       /    flame configuration, burner stabilized with specified temperature
       BURN
       TGIV
       /    in the event of a Newton failure, take 100 timesteps of 1.E-6
       TIME     100   6.00E-6
       /    begin on a uniform mesh of 6 points
       NPTS       6
       /      definition of the computational interval
       XEND 1.20
       XCEN 0.0625
       WMIX 0.1875
       /    pressure and inlet mass flow rate
       PRES  1.00 (atmospheres)
       FLRT  8.00E-03 (g/cm**2-sec)
       /    adaptive mesh criteria
       GRAD  0.25
       CURV  0.7
       /    unreacted mole fractions
       MOLE
       REAC    O2   0.23
       REAC    N2    .5749
       REAC    CH4  0.19496
       /    estimated products
       PROD    N2  0.50
       PROD    CO  0.12
       PROD    H2O 0.20
       PROD    CO2 0.04
       PROD    H2  0.14
       /    estimated intermediate mole fractions
       INTM    CH    1.0E-08
       INTM    OH    1.0E-03
       INTM    H     5.0E-03
       INTM    O     1.0E-04
       INTM    HO2   1.0E-04
       INTM    HO    1.0E-04
       INTM    NNH   1.0E-08
       INTM    N2O   1.0E-08
       INTM    N     5.0E-06
       INTM    NH2   1.0E-06
       INTM    NH    2.0E-06
       INTM    NO    1.0E-04
       INTM    HNO   5.0E-07
       INTM    HCN   1.0E-04
       INTM    CH3   1.0E-02
       INTM    C2H5  3.0E-04
       INTM    C2H3  5.0E-04
```

```
INTM   CH2   1.0E-04
INTM   CN    1.0E-07
INTM   NCO   1.0E-09
/    tolerances for the Newton iteration
ATOL  1.E-09
RTOL  1.E-4
/    tolerances for the time step Newton iteration
ATIM  1.E-5
RTIM  1.E-5
/    print control
PRNT     1
/    given temperature profile
TEMP      0.0  350.0
TEMP      .1   1833.0
TEMP      .150 1836.0
TEMP      .200 1831.0
TEMP      .250 1823.0
TEMP      .300 1823.0
TEMP      .400 1812.0
TEMP      .500 1801.0
TEMP      .600 1792.0
TEMP      1.200 1792.0
/TRANSPORT OPTION TAKING THERMAL DIFFUSION
TDIF
/read the solution from restart file
/RSTR
/ASEN
END
```

CAUTION...REACTANT FRACTIONS SUM TO 0.9998599999999

TWOPNT: TWO-POINT BOUNDARY VALUE PROBLEM SOLVER,
        VERSION 2.05 OF OCTOBER 1986.

        PERMIT TIME STEPPING.
        PERMIT MESH REFINEMENT.

TWOPNT: INITIAL GUESS:

	X	T	V	RHO	CH	NO	OH	NH	CN	H2	NH3
1	0.0000	3.500E+02	8.873E+00	9.017E-04	4.304E-09	4.304E-05	4.304E-04	8.607E-07	4.304E-08	2.316E-02	0.000E+00
2	0.2400	1.825E+03	5.204E+01	1.537E-04	1.113E-11	1.113E-07	1.113E-06	2.226E-09	1.113E-10	1.400E-01	0.000E+00
3	0.4800	1.803E+03	5.143E+01	1.555E-04	4.572E-25	4.572E-21	4.572E-20	9.144E-23	4.572E-24	1.400E-01	0.000E+00
4	0.7200	1.792E+03	5.111E+01	1.565E-04	2.982E-49	2.982E-45	2.982E-44	5.964E-47	2.982E-48	1.400E-01	0.000E+00
5	0.9600	1.792E+03	5.111E+01	1.565E-04	3.089E-84	3.089E-80	3.089E-79	6.178E-82	3.089E-83	1.400E-01	0.000E+00
6	1.2000	1.792E+03	5.111E+01	1.565E-04	5.081-130	5.081-126	5.081-125	1.016-127	5.081-129	1.400E-01	0.000E+00

	X	CH4	O2	N2	H2O	CH2O	CO	CO2	C2H6	C2H4	C2H2
1	0.0000	1.613E-01	1.903E-01	5.583E-01	3.309E-02	0.000E+00	1.985E-02	0.000E+00	0.000E+00	0.000E+00	0.000E+00
2	0.2400	0.000E+00	0.000E+00	5.000E-01	2.000E-01	0.000E+00	1.200E-01	4.000E-02	0.000E+00	0.000E+00	0.000E+00
3	0.4800	0.000E+00	0.000E+00	5.000E-01	2.000E-01	0.000E+00	1.200E-01	4.000E-02	0.000E+00	0.000E+00	0.000E+00
4	0.7200	0.000E+00	0.000E+00	5.000E-01	2.000E-01	0.000E+00	1.200E-01	4.000E-02	0.000E+00	0.000E+00	0.000E+00
5	0.9600	0.000E+00	0.000E+00	5.000E-01	2.000E-01	0.000E+00	1.200E-01	4.000E-02	0.000E+00	0.000E+00	0.000E+00
6	1.2000	0.000E+00	0.000E+00	5.000E-01	2.000E-01	0.000E+00	1.200E-01	4.000E-02	0.000E+00	0.000E+00	0.000E+00

	X	CH2CO	CH3CHO	C*C*C	CH3O2	CH3O	CH3OH	CH2OH	C4H2	CH2	CH3
1	0.0000	0.000E+00	0.000E+00	0.000E+00	0.000E+00	0.000E+00	0.000E+00	0.000E+00	0.000E+00	4.304E-05	4.304E-03
2	0.2400	0.000E+00	0.000E+00	0.000E+00	0.000E+00	0.000E+00	0.000E+00	0.000E+00	0.000E+00	1.113E-07	1.113E-05
3	0.4800	0.000E+00	0.000E+00	0.000E+00	0.000E+00	0.000E+00	0.000E+00	0.000E+00	0.000E+00	4.572E-21	4.572E-19
4	0.7200	0.000E+00	0.000E+00	0.000E+00	0.000E+00	0.000E+00	0.000E+00	0.000E+00	0.000E+00	2.982E-45	2.982E-43
5	0.9600	0.000E+00	0.000E+00	0.000E+00	0.000E+00	0.000E+00	0.000E+00	0.000E+00	0.000E+00	3.089E-80	3.089E-78
6	1.2000	0.000E+00	0.000E+00	0.000E+00	0.000E+00	0.000E+00	0.000E+00	0.000E+00	0.000E+00	5.081-126	5.081-124

	X	HCO	HCN	NCO	C2H5	C2H3	C2H	HCCO	C3H3	C*CC	H
1	0.0000	0.000E+00	4.304E-05	4.304E-10	1.291E-04	2.152E-04	0.000E+00	0.000E+00	0.000E+00	0.000E+00	2.152E-03
2	0.2400	0.000E+00	1.113E-07	1.113E-12	3.339E-07	5.565E-07	0.000E+00	0.000E+00	0.000E+00	0.000E+00	5.565E-06
3	0.4800	0.000E+00	4.572E-21	4.572E-26	1.372E-20	2.286E-20	0.000E+00	0.000E+00	0.000E+00	0.000E+00	2.286E-19

4	0.7200	0.000E+00	2.982E-45	2.982E-50	8.946E-45	1.491E-44	0.000E+00	0.000E+00	0.000E+00	0.000E+00	1.491E-43
5	0.9600	0.000E+00	3.089E-80	3.089E-85	9.267E-80	1.545E-79	0.000E+00	0.000E+00	0.000E+00	0.000E+00	1.545E-78
6	1.2000	0.000E+00	5.081-126	5.081-131	1.524-125	2.541-125	0.000E+00	0.000E+00	0.000E+00	0.000E+00	2.541-124

	x	O	HO2	NO2	HNO	NH2	N	N2O	NNH	C4H2O	NH2O
1	0.0000	4.304E-05	4.304E-05	0.000E+00	2.152E-07	4.304E-07	2.152E-06	4.304E-09	4.304E-09	0.000E+00	0.000E+00
2	0.2400	1.113E-07	1.113E-07	0.000E+00	5.565E-10	1.113E-09	5.565E-09	1.113E-11	1.113E-11	0.000E+00	0.000E+00
3	0.4800	4.572E-21	4.572E-21	0.000E+00	2.286E-23	4.572E-23	2.286E-22	4.572E-25	4.572E-25	0.000E+00	0.000E+00
4	0.7200	2.982E-45	2.982E-45	0.000E+00	1.491E-47	2.982E-47	1.491E-46	2.982E-49	2.982E-49	0.000E+00	0.000E+00
5	0.9600	3.089E-80	3.089E-80	0.000E+00	1.545E-82	3.089E-82	1.545E-81	3.089E-84	3.089E-84	0.000E+00	0.000E+00
6	1.2000	5.081-126	5.081-126	0.000E+00	2.541-128	5.081-128	2.541-127	5.081-130	5.081-130	0.000E+00	0.000E+00

	x	HONO	C2H5O	HNNOH	H2O2	NH2NO	CH3CO	CH2S	C	CH2N
1	0.0000	0.000E+00	0.000E+00	0.000E+00	0.000E+00	0.000E+00	0.000E+00	0.000E+00	0.000E+00	0.000E+00
2	0.2400	0.000E+00	0.000E+00	0.000E+00	0.000E+00	0.000E+00	0.000E+00	0.000E+00	0.000E+00	0.000E+00
3	0.4800	0.000E+00	0.000E+00	0.000E+00	0.000E+00	0.000E+00	0.000E+00	0.000E+00	0.000E+00	0.000E+00
4	0.7200	0.000E+00	0.000E+00	0.000E+00	0.000E+00	0.000E+00	0.000E+00	0.000E+00	0.000E+00	0.000E+00
5	0.9600	0.000E+00	0.000E+00	0.000E+00	0.000E+00	0.000E+00	0.000E+00	0.000E+00	0.000E+00	0.000E+00
6	1.2000	0.000E+00	0.000E+00	0.000E+00	0.000E+00	0.000E+00	0.000E+00	0.000E+00	0.000E+00	0.000E+00

TWOPNT: LOG OF THE BOUNDARY VALUE PROBLEM SOLVER.

ACTIVITY	LOG10 MAX NORM RESIDUAL	LOG10 MAX CONDITION NUMBER	POINTS	STEPS	JACOBIANS	CPU TIME H:MM:SS.F	REMARK
START			6				
NEWTON		15.30		0	1	3.5	FAILURE
TIMSTP	3.80	11.74		100	4	39.4	
NEWTON	-4.15	15.15		27	4	15.2	
REFINE	2.19		11			.0	NEW MESH
NEWTON	-4.51	13.51		25	4	32.9	
REFINE	2.85		14			.0	NEW MESH
NEWTON	-1.68	13.66		15	3	31.7	
REFINE	3.79		18			.0	NEW MESH
NEWTON	-4.30	13.44		26	3	48.9	
REFINE	3.25		25			.0	NEW MESH
NEWTON	-6.14	13.44		10	3	1:01.3	
REFINE	2.75		34			.0	NEW MESH
NEWTON	-6.17	13.38		21	2	58.2	
REFINE	2.35		43			.0	NEW MESH
NEWTON	-1.63	13.76		5	1	35.6	
REFINE	1.73		47			.0	NEW MESH
NEWTON	-1.52	13.73		2	1	38.0	
REFINE			47			.0	

TWOPNT: FINAL SOLUTION:

	x	T	V	RHO	CH	NO	OH	NH	CN	H2	NH3
1	0.0000	3.500E+02	8.978E+00	8.911E-04	3.450E-18	3.076E-08	2.476E-10	1.000E-16	1.352E-19	3.219E-02	7.622E-07
2	0.0075	4.612E+02	1.191E+01	6.715E-04	2.066E-22	3.712E-08	2.807E-10	1.115E-16	1.782E-19	3.794E-02	9.061E-07
3	0.0150	5.724E+02	1.488E+01	5.375E-04	1.176E-25	5.417E-08	4.636E-10	3.841E-15	2.620E-18	4.341E-02	1.045E-06
4	0.0225	6.837E+02	1.789E+01	4.472E-04	4.850E-23	8.320E-08	5.855E-09	7.297E-14	1.436E-16	4.870E-02	1.181E-06
5	0.0300	7.949E+02	2.092E+01	3.823E-04	4.010E-20	1.290E-07	7.533E-08	8.401E-13	5.157E-15	5.383E-02	1.316E-06
6	0.0337	8.505E+02	2.245E+01	3.563E-04	1.228E-18	1.617E-07	1.864E-07	2.964E-12	1.943E-14	5.635E-02	1.384E-06
7	0.0356	8.783E+02	2.322E+01	3.445E-04	5.331E-18	1.812E-07	2.636E-07	5.248E-12	3.333E-14	5.759E-02	1.418E-06
8	0.0375	9.061E+02	2.399E+01	3.335E-04	2.057E-17	2.030E-07	3.576E-07	8.836E-12	5.430E-14	5.883E-02	1.452E-06
9	0.0412	9.617E+02	2.554E+01	3.133E-04	2.320E-16	2.540E-07	6.146E-07	2.193E-11	1.314E-13	6.129E-02	1.520E-06

10	0.0450	1.017E+03	2.709E+01	2.953E-04	2.559E-15	3.165E-07	1.068E-06	5.116E-11	3.174E-13	6.371E-02	1.588E-06
11	0.0469	1.045E+03	2.787E+01	2.871E-04	8.870E-15	3.521E-07	1.433E-06	7.707E-11	5.038E-13	6.492E-02	1.622E-06
12	0.0487	1.073E+03	2.865E+01	2.793E-04	2.889E-14	3.903E-07	1.914E-06	1.127E-10	7.950E-13	6.611E-02	1.656E-06
13	0.0506	1.101E+03	2.943E+01	2.719E-04	8.825E-14	4.308E-07	2.521E-06	1.602E-10	1.239E-12	6.729E-02	1.690E-06
14	0.0525	1.129E+03	3.021E+01	2.648E-04	2.499E-13	4.727E-07	3.249E-06	2.216E-10	1.894E-12	6.847E-02	1.724E-06
15	0.0544	1.156E+03	3.100E+01	2.581E-04	6.510E-13	5.153E-07	4.073E-06	2.983E-10	2.822E-12	6.963E-02	1.758E-06
16	0.0562	1.184E+03	3.178E+01	2.517E-04	1.561E-12	5.575E-07	4.954E-06	3.914E-10	4.090E-12	7.079E-02	1.792E-06
17	0.0600	1.240E+03	3.336E+01	2.398E-04	6.999E-12	6.379E-07	6.755E-06	6.285E-10	7.947E-12	7.307E-02	1.861E-06
18	0.0637	1.295E+03	3.495E+01	2.289E-04	2.439E-11	7.083E-07	8.596E-06	9.390E-10	1.425E-11	7.530E-02	1.930E-06
19	0.0675	1.351E+03	3.653E+01	2.190E-04	7.255E-11	7.685E-07	1.074E-05	1.339E-09	2.440E-11	7.750E-02	1.998E-06
20	0.0750	1.462E+03	3.973E+01	2.014E-04	4.766E-10	8.654E-07	1.734E-05	2.496E-09	6.601E-11	8.176E-02	2.135E-06
21	0.0787	1.518E+03	4.134E+01	1.935E-04	1.152E-09	9.091E-07	2.274E-05	3.385E-09	1.070E-10	8.384E-02	2.203E-06
22	0.0825	1.573E+03	4.295E+01	1.863E-04	2.631E-09	9.513E-07	3.008E-05	4.544E-09	1.702E-10	8.588E-02	2.269E-06
23	0.0862	1.629E+03	4.457E+01	1.795E-04	5.623E-09	9.931E-07	3.969E-05	6.029E-09	2.649E-10	8.790E-02	2.335E-06
24	0.0900	1.685E+03	4.619E+01	1.732E-04	1.110E-08	1.035E-06	5.171E-05	7.873E-09	4.004E-10	8.988E-02	2.398E-06
25	0.0937	1.740E+03	4.782E+01	1.673E-04	2.001E-08	1.076E-06	6.603E-05	1.006E-08	5.849E-10	9.183E-02	2.460E-06
26	0.0975	1.796E+03	4.945E+01	1.618E-04	3.256E-08	1.117E-06	8.203E-05	1.248E-08	8.215E-10	9.373E-02	2.520E-06
27	0.1012	1.033E+03	5.055E+01	1.583E-04	4.681E-08	1.155E-06	9.607E-05	1.490E-08	1.060E-09	9.519E-02	2.578E-06
28	0.1050	1.033E+03	5.058E+01	1.582E-04	5.969E-08	1.192E-06	1.036E-04	1.706E-08	1.217E-09	9.583E-02	2.637E-06
29	0.1125	1.034E+03	5.065E+01	1.579E-04	8.162E-08	1.255E-06	1.144E-04	2.038E-08	1.502E-09	9.695E-02	2.748E-06
30	0.1200	1.034E+03	5.070E+01	1.578E-04	9.629E-08	1.303E-06	1.205E-04	2.246E-08	1.747E-09	9.790E-02	2.851E-06
31	0.1275	1.035E+03	5.075E+01	1.576E-04	1.019E-07	1.337E-06	1.226E-04	2.342E-08	1.938E-09	9.870E-02	2.946E-06
32	0.1350	1.035E+03	5.079E+01	1.575E-04	9.923E-08	1.356E-06	1.217E-04	2.343E-08	2.067E-09	9.939E-02	3.033E-06
33	0.1500	1.036E+03	5.085E+01	1.573E-04	7.849E-08	1.360E-06	1.127E-04	2.130E-08	2.133E-09	1.005E-01	3.187E-06
34	0.1650	1.034E+03	5.083E+01	1.574E-04	5.421E-08	1.337E-06	9.929E-05	1.789E-08	2.020E-09	1.014E-01	3.319E-06
35	0.1800	1.833E+03	5.080E+01	1.575E-04	3.521E-08	1.301E-06	8.557E-05	1.437E-08	1.828E-09	1.022E-01	3.431E-06
36	0.1950	1.031E+03	5.077E+01	1.576E-04	2.239E-08	1.261E-06	7.316E-05	1.127E-08	1.616E-09	1.029E-01	3.525E-06
37	0.2100	1.029E+03	5.072E+01	1.577E-04	1.424E-08	1.221E-06	6.246E-05	8.735E-09	1.412E-09	1.035E-01	3.604E-06
38	0.2400	1.025E+03	5.059E+01	1.581E-04	6.190E-09	1.147E-06	4.649E-05	5.331E-09	1.081E-09	1.044E-01	3.722E-06
39	0.3000	1.023E+03	5.057E+01	1.582E-04	1.853E-09	1.035E-06	3.061E-05	2.500E-09	7.323E-10	1.059E-01	3.860E-06
40	0.3600	1.816E+03	5.040E+01	1.587E-04	7.529E-10	9.506E-07	2.218E-05	1.392E-09	5.384E-10	1.070E-01	3.945E-06
41	0.4800	1.803E+03	5.006E+01	1.598E-04	2.939E-10	8.298E-07	1.556E-05	7.487E-10	3.837E-10	1.085E-01	4.045E-06
42	0.6000	1.792E+03	4.976E+01	1.608E-04	1.807E-10	7.358E-07	1.278E-05	5.436E-10	3.185E-10	1.097E-01	4.120E-06
43	0.7200	1.792E+03	4.978E+01	1.607E-04	1.557E-10	6.574E-07	1.207E-05	4.926E-10	3.045E-10	1.107E-01	4.184E-06
44	0.8400	1.792E+03	4.980E+01	1.607E-04	1.495E-10	5.913E-07	1.184E-05	4.817E-10	3.021E-10	1.116E-01	4.243E-06
45	0.9600	1.792E+03	4.981E+01	1.606E-04	1.482E-10	5.382E-07	1.177E-05	4.820E-10	3.030E-10	1.122E-01	4.294E-06
46	1.0800	1.792E+03	4.981E+01	1.606E-04	1.480E-10	5.036E-07	1.175E-05	4.841E-10	3.042E-10	1.126E-01	4.327E-06
47	1.2000	1.792E+03	4.981E+01	1.606E-04	1.480E-10	5.036E-07	1.175E-05	4.841E-10	3.042E-10	1.126E-01	4.327E-06

	x	CH4	O2	N2	H2O	CH2O	CO	CO2	C2H6	C2H4	C2H2
1	0.0000	1.421E-01	1.757E-01	5.511E-01	6.842E-02	5.515E-07	2.210E-02	6.121E-03	4.517E-04	2.686E-04	1.237E-03
2	0.0075	1.329E-01	1.645E-01	5.469E-01	8.050E-02	6.967E-07	2.665E-02	7.742E-03	5.794E-04	3.384E-04	1.549E-03
3	0.0150	1.239E-01	1.535E-01	5.430E-01	9.194E-02	8.497E-07	3.124E-02	9.436E-03	7.145E-04	4.108E-04	1.872E-03
4	0.0225	1.151E-01	1.423E-01	5.396E-01	1.030E-01	1.011E-06	3.592E-02	1.122E-02	8.582E-04	4.863E-04	2.209E-03
5	0.0300	1.062E-01	1.311E-01	5.363E-01	1.138E-01	1.286E-06	4.072E-02	1.309E-02	1.011E-03	5.651E-04	2.563E-03
6	0.0337	1.018E-01	1.254E-01	5.348E-01	1.192E-01	1.677E-06	4.318E-02	1.407E-02	1.091E-03	6.054E-04	2.747E-03
7	0.0356	9.953E-02	1.225E-01	5.340E-01	1.219E-01	1.933E-06	4.442E-02	1.457E-02	1.132E-03	6.257E-04	2.841E-03
8	0.0375	9.730E-02	1.196E-01	5.333E-01	1.246E-01	2.211E-06	4.567E-02	1.508E-02	1.174E-03	6.461E-04	2.936E-03
9	0.0412	9.281E-02	1.138E-01	5.318E-01	1.299E-01	2.752E-06	4.819E-02	1.611E-02	1.259E-03	6.866E-04	3.134E-03
10	0.0450	8.829E-02	1.080E-01	5.305E-01	1.352E-01	3.031E-06	5.074E-02	1.717E-02	1.345E-03	7.259E-04	3.343E-03
11	0.0469	8.602E-02	1.051E-01	5.298E-01	1.378E-01	3.011E-06	5.202E-02	1.772E-02	1.388E-03	7.446E-04	3.457E-03
12	0.0487	8.375E-02	1.021E-01	5.291E-01	1.405E-01	2.908E-06	5.329E-02	1.827E-02	1.431E-03	7.624E-04	3.578E-03
13	0.0506	8.147E-02	9.920E-02	5.284E-01	1.431E-01	2.723E-06	5.455E-02	1.882E-02	1.473E-03	7.792E-04	3.710E-03
14	0.0525	7.918E-02	9.629E-02	5.278E-01	1.457E-01	2.472E-06	5.580E-02	1.939E-02	1.514E-03	7.946E-04	3.855E-03
15	0.0544	7.688E-02	9.338E-02	5.271E-01	1.484E-01	2.181E-06	5.703E-02	1.996E-02	1.554E-03	8.085E-04	4.018E-03
16	0.0562	7.459E-02	9.049E-02	5.265E-01	1.510E-01	1.877E-06	5.823E-02	2.054E-02	1.591E-03	8.206E-04	4.200E-03
17	0.0600	6.999E-02	8.476E-02	5.253E-01	1.561E-01	1.320E-06	6.055E-02	2.171E-02	1.655E-03	8.393E-04	4.626E-03
18	0.0637	6.542E-02	7.912E-02	5.241E-01	1.612E-01	9.132E-07	6.275E-02	2.291E-02	1.696E-03	8.513E-04	5.131E-03
19	0.0675	6.089E-02	7.354E-02	5.229E-01	1.663E-01	6.475E-07	6.484E-02	2.412E-02	1.704E-03	8.589E-04	5.700E-03
20	0.0750	5.201E-02	6.263E-02	5.206E-01	1.760E-01	3.785E-07	6.876E-02	2.659E-02	1.587E-03	8.725E-04	6.984E-03
21	0.0787	4.773E-02	5.735E-02	5.195E-01	1.806E-01	3.133E-07	7.061E-02	2.782E-02	1.450E-03	8.918E-04	7.666E-03
22	0.0825	4.356E-02	5.221E-02	5.185E-01	1.851E-01	2.723E-07	7.239E-02	2.903E-02	1.267E-03	9.230E-04	8.366E-03
23	0.0862	3.954E-02	4.726E-02	5.174E-01	1.894E-01	2.446E-07	7.409E-02	3.022E-02	1.052E-03	9.668E-04	9.077E-03
24	0.0900	3.571E-02	4.256E-02	5.164E-01	1.934E-01	2.237E-07	7.570E-02	3.136E-02	8.262E-04	1.019E-03	9.787E-03
25	0.0937	3.209E-02	3.814E-02	5.154E-01	1.971E-01	2.059E-07	7.722E-02	3.244E-02	6.150E-04	1.071E-03	1.048E-02
26	0.0975	2.875E-02	3.405E-02	5.144E-01	2.006E-01	1.894E-07	7.863E-02	3.345E-02	4.391E-04	1.110E-03	1.115E-02

27	0.1012	2.573E-02	3.034E-02	5.137E-01	2.037E-01	1.713E-07	7.996E-02	3.439E-02	3.138E-04	1.118E-03	1.177E-02
28	0.1050	2.304E-02	2.698E-02	5.136E-01	2.066E-01	1.506E-07	8.125E-02	3.529E-02	2.359E-04	1.089E-03	1.234E-02
29	0.1125	1.854E-02	2.121E-02	5.132E-01	2.116E-01	1.160E-07	8.355E-02	3.688E-02	1.542E-04	9.512E-04	1.330E-02
30	0.1200	1.510E-02	1.658E-02	5.130E-01	2.155E-01	9.029E-08	8.546E-02	3.821E-02	1.084E-04	7.845E-04	1.400E-02
31	0.1275	1.251E-02	1.293E-02	5.127E-01	2.184E-01	7.140E-08	8.703E-02	3.929E-02	7.878E-05	6.288E-04	1.448E-02
32	0.1350	1.058E-02	1.010E-02	5.126E-01	2.206E-01	5.753E-08	8.830E-02	4.018E-02	5.846E-05	4.992E-04	1.478E-02
33	0.1500	8.184E-03	6.364E-03	5.123E-01	2.232E-01	3.996E-08	9.008E-02	4.147E-02	3.503E-05	3.236E-04	1.502E-02
34	0.1650	6.812E-03	4.129E-03	5.122E-01	2.244E-01	2.962E-08	9.124E-02	4.239E-02	2.294E-05	2.213E-04	1.505E-02
35	0.1800	5.990E-03	2.764E-03	5.120E-01	2.250E-01	2.326E-08	9.201E-02	4.307E-02	1.611E-05	1.611E-04	1.498E-02
36	0.1950	5.472E-03	1.902E-03	5.120E-01	2.252E-01	1.916E-08	9.254E-02	4.359E-02	1.194E-05	1.242E-04	1.488E-02
37	0.2100	5.127E-03	1.337E-03	5.119E-01	2.251E-01	1.641E-08	9.292E-02	4.400E-02	9.227E-06	1.003E-04	1.477E-02
38	0.2400	4.745E-03	7.320E-04	5.118E-01	2.247E-01	1.330E-08	9.342E-02	4.460E-02	6.160E-06	7.423E-05	1.456E-02
39	0.3000	4.431E-03	3.035E-04	5.115E-01	2.236E-01	1.095E-08	9.394E-02	4.530E-02	3.422E-06	5.391E-05	1.419E-02
40	0.3600	4.271E-03	1.342E-04	5.114E-01	2.227E-01	9.953E-09	9.429E-02	4.577E-02	2.274E-06	4.571E-05	1.389E-02
41	0.4800	4.117E-03	3.797E-05	5.111E-01	2.211E-01	9.282E-09	9.478E-02	4.639E-02	1.520E-06	4.125E-05	1.341E-02
42	0.6000	4.017E-03	1.022E-05	5.110E-01	2.198E-01	8.977E-09	9.521E-02	4.684E-02	1.251E-06	4.033E-05	1.300E-02
43	0.7200	3.926E-03	2.516E-06	5.108E-01	2.187E-01	8.865E-09	9.563E-02	4.716E-02	1.100E-06	3.894E-05	1.263E-02
44	0.8400	3.845E-03	5.772E-07	5.106E-01	2.177E-01	8.853E-09	9.605E-02	4.741E-02	1.029E-06	3.788E-05	1.230E-02
45	0.9600	3.780E-03	1.280E-07	5.105E-01	2.170E-01	8.876E-09	9.645E-02	4.760E-02	9.880E-07	3.704E-05	1.201E-02
46	1.0800	3.737E-03	3.162E-08	5.104E-01	2.165E-01	8.896E-09	9.673E-02	4.772E-02	9.647E-07	3.646E-05	1.181E-02
47	1.2000	3.737E-03	3.162E-08	5.104E-01	2.165E-01	8.896E-09	9.673E-02	4.772E-02	9.647E-07	3.646E-05	1.181E-02

	X	CH2CO	CH3CHO	C*C*C	CH3O2	CH3O	CH3OH	CH2OH	C4H2	CH2	CH3
1	0.0000	2.224E-05	7.877E-06	5.252E-06	1.399E-05	9.544E-05	1.182E-04	1.395E-07	1.070E-06	2.508E-17	1.809E-11
2	0.0075	2.903E-05	1.031E-05	7.018E-06	1.806E-05	1.210E-04	1.500E-04	1.765E-07	1.507E-06	2.421E-19	2.151E-11
3	0.0150	3.627E-05	1.290E-05	8.964E-06	2.232E-05	1.473E-04	1.827E-04	2.146E-07	2.013E-06	2.591E-17	3.036E-09
4	0.0225	4.399E-05	1.567E-05	1.111E-05	2.648E-05	1.748E-04	2.167E-04	2.541E-07	2.591E-06	2.130E-15	2.373E-07
5	0.0300	5.223E-05	1.863E-05	1.346E-05	2.484E-05	2.034E-04	2.523E-04	2.956E-07	3.250E-06	2.592E-13	4.663E-06
6	0.0337	5.652E-05	2.020E-05	1.472E-05	1.825E-05	2.171E-04	2.707E-04	3.183E-07	3.615E-06	2.091E-12	1.193E-05
7	0.0356	5.870E-05	2.100E-05	1.537E-05	1.449E-05	2.233E-04	2.800E-04	3.306E-07	3.809E-06	4.842E-12	1.674E-05
8	0.0375	6.089E-05	2.182E-05	1.604E-05	1.103E-05	2.288E-04	2.895E-04	3.437E-07	4.011E-06	1.026E-11	2.222E-05
9	0.0412	6.532E-05	2.350E-05	1.743E-05	6.083E-06	2.374E-04	3.087E-04	3.736E-07	4.441E-06	3.885E-11	3.557E-05
10	0.0450	6.977E-05	2.526E-05	1.888E-05	3.628E-06	2.413E-04	3.284E-04	4.122E-07	4.913E-06	1.455E-10	5.602E-05
11	0.0469	7.199E-05	2.616E-05	1.963E-05	2.938E-06	2.410E-04	3.384E-04	4.374E-07	5.169E-06	2.904E-10	7.126E-05
12	0.0487	7.419E-05	2.708E-05	2.039E-05	2.449E-06	2.387E-04	3.484E-04	4.675E-07	5.441E-06	5.689E-10	9.080E-05
13	0.0506	7.637E-05	2.803E-05	2.118E-05	2.085E-06	2.343E-04	3.586E-04	5.036E-07	5.731E-06	1.090E-09	1.156E-04
14	0.0525	7.853E-05	2.899E-05	2.198E-05	1.801E-06	2.274E-04	3.687E-04	5.466E-07	6.043E-06	2.028E-09	1.464E-04
15	0.0544	8.067E-05	2.997E-05	2.280E-05	1.571E-06	2.178E-04	3.789E-04	5.975E-07	6.380E-06	3.640E-09	1.840E-04
16	0.0562	8.278E-05	3.096E-05	2.364E-05	1.377E-06	2.055E-04	3.890E-04	6.566E-07	6.746E-06	6.299E-09	2.289E-04
17	0.0600	8.695E-05	3.290E-05	2.537E-05	1.065E-06	1.734E-04	4.090E-04	7.995E-07	7.579E-06	1.667E-08	3.411E-04
18	0.0637	9.115E-05	3.457E-05	2.717E-05	8.223E-07	1.364E-04	4.281E-04	9.754E-07	8.572E-06	3.892E-08	4.827E-04
19	0.0675	9.554E-05	3.568E-05	2.905E-05	6.328E-07	1.009E-04	4.457E-04	1.190E-06	9.755E-06	8.355E-08	6.528E-04
20	0.0750	1.053E-04	3.528E-05	3.302E-05	3.738E-07	4.889E-05	4.752E-04	1.772E-06	1.276E-05	3.204E-07	1.074E-03
21	0.0787	1.111E-04	3.323E-05	3.513E-05	2.873E-07	3.358E-05	4.848E-04	2.186E-06	1.465E-05	5.992E-07	1.322E-03
22	0.0825	1.176E-04	2.999E-05	3.730E-05	2.197E-07	2.368E-05	4.901E-04	2.686E-06	1.684E-05	1.071E-06	1.581E-03
23	0.0862	1.245E-04	2.586E-05	3.955E-05	1.662E-07	1.736E-05	4.902E-04	3.249E-06	1.934E-05	1.821E-06	1.835E-03
24	0.0900	1.317E-04	2.125E-05	4.184E-05	1.238E-07	1.324E-05	4.845E-04	3.827E-06	2.213E-05	2.915E-06	2.059E-03
25	0.0937	1.388E-04	1.667E-05	4.417E-05	9.048E-08	1.041E-05	4.731E-04	4.349E-06	2.518E-05	4.369E-06	2.233E-03
26	0.0975	1.451E-04	1.257E-05	4.648E-05	6.487E-08	8.386E-06	4.574E-04	4.748E-06	2.836E-05	6.083E-06	2.338E-03
27	0.1012	1.501E-04	9.241E-06	4.876E-05	4.951E-08	7.005E-06	4.406E-04	5.042E-06	3.149E-05	7.695E-06	2.369E-03
28	0.1050	1.535E-04	6.722E-06	5.102E-05	4.338E-08	6.098E-06	4.259E-04	5.287E-06	3.446E-05	8.822E-06	2.340E-03
29	0.1125	1.550E-04	3.602E-06	5.514E-05	3.169E-08	4.622E-06	3.983E-04	5.348E-06	3.965E-05	1.034E-05	2.179E-03
30	0.1200	1.511E-04	1.958E-06	5.848E-05	2.228E-08	3.382E-06	3.696E-04	5.023E-06	4.372E-05	1.103E-05	1.964E-03
31	0.1275	1.438E-04	1.090E-06	6.099E-05	1.534E-08	2.410E-06	3.389E-04	4.495E-06	4.668E-05	1.100E-05	1.737E-03
32	0.1350	1.347E-04	6.175E-07	6.277E-05	1.047E-08	1.689E-06	3.069E-04	3.897E-06	4.868E-05	1.043E-05	1.522E-03
33	0.1500	1.157E-04	2.353E-07	6.460E-05	5.036E-09	8.395E-07	2.426E-04	2.774E-06	5.039E-05	8.447E-06	1.165E-03
34	0.1650	9.946E-05	9.921E-08	6.534E-05	2.543E-09	4.287E-07	1.861E-04	1.921E-06	5.053E-05	6.352E-06	9.010E-04
35	0.1800	8.675E-05	4.616E-08	6.557E-05	1.350E-09	2.277E-07	1.400E-04	1.328E-06	5.002E-05	4.641E-06	7.098E-04
36	0.1950	7.701E-05	2.334E-08	6.560E-05	7.515E-10	1.261E-07	1.042E-04	9.297E-07	4.926E-05	3.371E-06	5.704E-04
37	0.2100	6.954E-05	1.249E-08	6.554E-05	4.364E-10	7.246E-08	7.731E-05	6.620E-07	4.843E-05	2.460E-06	4.669E-04
38	0.2400	5.976E-05	4.549E-09	6.532E-05	1.740E-10	2.818E-08	4.399E-05	3.637E-07	4.680E-05	1.391E-06	3.329E-04
39	0.3000	5.012E-05	1.129E-09	6.486E-05	4.585E-11	7.141E-09	1.764E-05	1.553E-07	4.440E-05	6.143E-07	2.100E-04
40	0.3600	4.475E-05	3.928E-10	6.450E-05	1.497E-11	2.233E-09	8.606E-06	8.328E-08	4.229E-05	3.326E-07	1.506E-04
41	0.4800	3.956E-05	1.483E-10	6.396E-05	3.174E-12	4.481E-10	4.423E-06	4.334E-08	3.889E-05	1.741E-07	1.062E-04
42	0.6000	3.601E-05	9.966E-11	6.352E-05	7.448E-13	1.016E-10	3.296E-06	3.062E-08	3.614E-05	1.237E-07	8.791E-05
43	0.7200	3.327E-05	8.715E-11	6.308E-05	1.700E-13	2.313E-11	2.827E-06	2.684E-08	3.412E-05	1.105E-07	8.153E-05

	x	HCO	HCN	NCO	C2H5	C2H3	C2H	HCCO	C3H3	C#CC	H
44	0.8400	3.150E-05	8.275E-11	6.266E-05	3.763E-14	5.151E-12	2.646E-06	2.543E-08	3.240E-05	1.063E-07	7.868E-05
45	0.9600	3.036E-05	8.061E-11	6.228E-05	8.180E-15	1.147E-12	2.566E-06	2.476E-08	3.096E-05	1.048E-07	7.709E-05
46	1.0800	2.968E-05	7.950E-11	6.200E-05	1.997E-15	3.048E-13	2.528E-06	2.443E-08	2.997E-05	1.042E-07	7.621E-05
47	1.2000	2.968E-05	7.950E-11	6.200E-05	1.997E-15	3.048E-13	2.528E-06	2.443E-08	2.997E-05	1.042E-07	7.621E-05

	x	HCO	HCN	NCO	C2H5	C2H3	C2H	HCCO	C3H3	C#CC	H
1	0.0000	3.101E-12	1.927E-06	3.065E-09	3.650E-09	3.404E-13	1.433E-17	2.013E-17	1.982E-16	5.697E-08	3.866E-15
2	0.0075	3.912E-12	2.441E-06	3.875E-09	4.674E-09	4.270E-13	1.790E-17	2.347E-17	2.510E-16	7.612E-08	1.064E-14
3	0.0150	3.044E-11	2.969E-06	4.727E-09	1.922E-08	4.851E-12	4.242E-16	2.045E-15	6.399E-16	9.723E-08	4.649E-13
4	0.0225	9.373E-10	3.515E-06	5.626E-09	1.116E-07	8.744E-11	3.172E-14	9.377E-14	1.172E-14	1.205E-07	9.245E-11
5	0.0300	1.743E-08	4.084E-06	6.581E-09	6.235E-07	2.755E-09	1.448E-12	2.858E-12	2.087E-13	1.460E-07	6.099E-09
6	0.0337	5.687E-08	4.377E-06	7.081E-09	1.542E-06	1.182E-08	5.966E-12	1.843E-11	6.201E-13	1.597E-07	2.817E-08
7	0.0356	9.558E-08	4.526E-06	7.339E-09	2.349E-06	2.230E-08	1.063E-11	4.556E-11	9.727E-13	1.667E-07	5.429E-08
8	0.0375	1.550E-07	4.676E-06	7.601E-09	3.480E-06	4.040E-08	1.792E-11	1.072E-10	1.479E-12	1.740E-07	1.001E-07
9	0.0412	3.629E-07	4.983E-06	8.140E-09	7.034E-06	1.188E-07	4.579E-11	4.890E-10	3.310E-12	1.888E-07	3.056E-07
10	0.0450	7.788E-07	5.296E-06	8.705E-09	1.341E-05	3.358E-07	1.135E-10	2.086E-09	8.139E-12	2.041E-07	9.200E-07
11	0.0469	1.104E-06	5.455E-06	9.002E-09	1.820E-05	5.565E-07	1.799E-10	4.303E-09	1.373E-11	2.119E-07	1.606E-06
12	0.0487	1.474E-06	5.616E-06	9.312E-09	2.424E-05	8.688E-07	2.816E-10	8.389E-09	2.367E-11	2.196E-07	2.691E-06
13	0.0506	1.846E-06	5.779E-06	9.639E-09	3.171E-05	1.270E-06	4.326E-10	1.562E-08	4.153E-11	2.274E-07	4.323E-06
14	0.0525	2.159E-06	5.944E-06	9.988E-09	4.072E-05	1.726E-06	6.475E-10	2.776E-08	7.336E-11	2.350E-07	6.632E-06
15	0.0544	2.355E-06	6.110E-06	1.037E-08	5.130E-05	2.175E-06	9.399E-10	4.712E-08	1.294E-10	2.424E-07	9.697E-06
16	0.0562	2.408E-06	6.278E-06	1.078E-08	6.339E-05	2.546E-06	1.321E-09	7.666E-08	2.274E-10	2.494E-07	1.353E-05
17	0.0600	2.160E-06	6.620E-06	1.173E-08	9.164E-05	2.903E-06	2.388E-09	1.782E-07	6.555E-10	2.617E-07	2.331E-05
18	0.0637	1.717E-06	6.968E-06	1.285E-08	1.231E-04	2.778E-06	3.995E-09	3.630E-07	1.796E-09	2.688E-07	3.537E-05
19	0.0675	1.325E-06	7.324E-06	1.414E-08	1.547E-04	2.438E-06	6.479E-09	6.729E-07	4.793E-09	2.659E-07	4.978E-05
20	0.0750	8.679E-07	8.056E-06	1.705E-08	2.079E-04	1.761E-06	1.684E-08	1.885E-06	2.769E-08	2.132E-07	8.857E-05
21	0.0787	7.679E-07	8.433E-06	1.847E-08	2.210E-04	1.531E-06	2.736E-08	2.975E-06	6.343E-08	1.628E-07	1.166E-04
22	0.0825	7.146E-07	8.817E-06	1.981E-08	2.230E-04	1.351E-06	4.413E-08	4.485E-06	1.340E-07	1.096E-07	1.519E-04
23	0.0862	6.857E-07	9.209E-06	2.097E-08	2.134E-04	1.205E-06	7.001E-08	6.448E-06	2.650E-07	6.868E-08	1.951E-04
24	0.0900	6.636E-07	9.607E-06	2.191E-08	1.938E-04	1.079E-06	1.082E-07	8.810E-06	4.930E-07	4.409E-08	2.456E-04
25	0.0937	6.366E-07	1.001E-05	2.254E-08	1.680E-04	9.629E-07	1.618E-07	1.141E-05	8.592E-07	3.028E-08	3.016E-04
26	0.0975	5.982E-07	1.042E-05	2.275E-08	1.406E-04	8.492E-07	2.324E-07	1.394E-05	1.384E-06	2.179E-08	3.598E-04
27	0.1012	5.637E-07	1.083E-05	2.235E-08	1.156E-04	8.184E-07	3.018E-07	1.585E-05	2.031E-06	1.952E-08	4.148E-04
28	0.1050	5.480E-07	1.126E-05	2.129E-08	9.477E-05	9.461E-07	3.388E-07	1.673E-05	2.737E-06	2.611E-08	4.620E-04
29	0.1125	4.873E-07	1.210E-05	1.836E-08	6.656E-05	1.164E-06	3.961E-07	1.698E-05	4.377E-06	4.298E-08	5.400E-04
30	0.1200	4.149E-07	1.290E-05	1.549E-08	4.816E-05	1.326E-06	4.344E-07	1.604E-05	6.260E-06	6.356E-08	5.973E-04
31	0.1275	3.450E-07	1.363E-05	1.296E-08	3.542E-05	1.429E-06	4.543E-07	1.445E-05	8.232E-06	8.528E-08	6.339E-04
32	0.1350	2.833E-07	1.429E-05	1.079E-08	2.638E-05	1.478E-06	4.584E-07	1.263E-05	1.013E-05	1.051E-07	6.511E-04
33	0.1500	1.894E-07	1.532E-05	7.559E-09	1.570E-05	1.437E-06	4.310E-07	9.267E-06	1.312E-05	1.290E-07	6.353E-04
34	0.1650	1.281E-07	1.606E-05	5.328E-09	1.004E-05	1.323E-06	3.796E-07	6.684E-06	1.507E-05	1.377E-07	5.831E-04
35	0.1800	8.900E-08	1.657E-05	3.815E-09	6.841E-06	1.176E-06	3.256E-07	4.875E-06	1.622E-05	1.338E-07	5.180E-04
36	0.1950	6.397E-08	1.693E-05	2.783E-09	4.898E-06	1.029E-06	2.765E-07	3.630E-06	1.687E-05	1.240E-07	4.533E-04
37	0.2100	4.767E-08	1.720E-05	2.061E-09	3.641E-06	9.002E-07	2.341E-07	2.761E-06	1.725E-05	1.133E-07	3.948E-04
38	0.2400	2.973E-08	1.752E-05	1.230E-09	2.235E-06	7.013E-07	1.712E-07	1.757E-06	1.743E-05	9.366E-08	3.033E-04
39	0.3000	1.643E-08	1.784E-05	5.983E-10	1.108E-06	4.676E-07	1.104E-07	9.828E-07	1.799E-05	6.688E-08	2.056E-04
40	0.3600	1.122E-08	1.803E-05	3.254E-10	6.555E-07	3.568E-07	7.795E-08	6.458E-07	2.050E-05	6.205E-08	1.537E-04
41	0.4800	7.859E-09	1.827E-05	1.553E-10	3.728E-07	2.774E-07	5.218E-08	4.166E-07	2.990E-05	7.956E-08	1.136E-04
42	0.6000	6.610E-09	1.844E-05	9.964E-11	2.749E-07	2.480E-07	4.109E-08	3.233E-07	4.388E-05	1.161E-07	9.723E-05
43	0.7200	6.191E-09	1.859E-05	8.525E-11	2.367E-07	2.307E-07	3.795E-08	2.860E-07	5.855E-05	1.482E-07	9.312E-05
44	0.8400	6.089E-09	1.873E-05	8.155E-11	2.197E-07	2.229E-07	3.646E-08	2.678E-07	7.038E-05	1.768E-07	9.243E-05
45	0.9600	6.085E-09	1.884E-05	8.081E-11	2.103E-07	2.182E-07	3.555E-08	2.576E-07	7.864E-05	1.979E-07	9.265E-05
46	1.0800	6.098E-09	1.892E-05	8.081E-11	2.051E-07	2.153E-07	3.500E-08	2.519E-07	8.346E-05	2.107E-07	9.292E-05
47	1.2000	6.098E-09	1.892E-05	8.081E-11	2.051E-07	2.153E-07	3.500E-08	2.519E-07	8.346E-05	2.107E-07	9.292E-05

	x	O	HO2	NO2	HNO	NH2	N	N2O	NNH	C4H2O	NH2O
1	0.0000	7.603E-12	1.751E-05	2.281E-07	1.026E-12	2.118E-12	1.287E-17	1.117E-09	2.080E-19	3.621E-07	4.499E-10
2	0.0075	8.600E-12	2.107E-05	2.829E-07	1.236E-12	2.389E-12	1.476E-17	1.414E-09	2.512E-19	5.168E-07	5.701E-10
3	0.0150	4.466E-11	2.987E-05	3.270E-07	2.611E-12	6.456E-12	3.233E-17	1.720E-09	1.886E-18	6.975E-07	6.910E-10
4	0.0225	2.824E-10	4.462E-05	3.600E-07	6.390E-12	1.874E-11	1.350E-16	2.036E-09	1.336E-17	9.063E-07	8.112E-10
5	0.0300	2.008E-09	6.738E-05	3.771E-07	1.619E-11	5.424E-11	8.448E-16	2.364E-09	1.259E-16	1.146E-06	9.251E-10
6	0.0337	6.974E-09	8.308E-05	3.761E-07	2.644E-11	9.631E-11	3.179E-15	2.532E-09	7.347E-16	1.279E-06	9.727E-10
7	0.0356	1.280E-08	9.214E-05	3.725E-07	3.392E-11	1.276E-10	6.366E-15	2.617E-09	1.987E-15	1.350E-06	9.918E-10
8	0.0375	2.263E-08	1.020E-04	3.666E-07	4.349E-11	1.677E-10	1.230E-14	2.703E-09	5.085E-15	1.423E-06	1.007E-09
9	0.0412	6.265E-08	1.234E-04	3.470E-07	7.063E-11	2.828E-10	4.006E-14	2.876E-09	2.520E-14	1.578E-06	1.019E-09
10	0.0450	1.698E-07	1.445E-04	3.151E-07	1.135E-10	4.771E-10	1.342E-13	3.052E-09	1.172E-13	1.747E-06	9.940E-10
11	0.0469	2.797E-07	1.527E-04	2.942E-07	1.432E-10	6.227E-10	2.559E-13	3.140E-09	2.559E-13	1.838E-06	9.617E-10

12	0.0487	4.425E-07	1.583E-04	2.703E-07	1.792E-10	8.069E-10	4.637E-13	3.229E-09	5.157E-13	1.933E-06	9.152E-10
13	0.0506	6.732E-07	1.602E-04	2.438E-07	2.226E-10	1.036E-09	8.081E-13	3.318E-09	9.794E-13	2.033E-06	8.552E-10
14	0.0525	9.830E-07	1.579E-04	2.156E-07	2.745E-10	1.314E-09	1.353E-12	3.407E-09	1.756E-12	2.140E-06	7.837E-10
15	0.0544	1.376E-06	1.512E-04	1.867E-07	3.364E-10	1.642E-09	2.172E-12	3.496E-09	2.976E-12	2.253E-06	7.045E-10
16	0.0562	1.845E-06	1.408E-04	1.584E-07	4.102E-10	2.022E-09	3.343E-12	3.585E-09	4.780E-12	2.374E-06	6.218E-10
17	0.0600	2.965E-06	1.122E-04	1.065E-07	6.016E-10	2.931E-09	6.965E-12	3.760E-09	1.057E-11	2.642E-06	4.594E-10
18	0.0637	4.190E-06	8.320E-05	6.641E-08	8.776E-10	4.031E-09	1.283E-11	3.929E-09	2.000E-11	2.951E-06	3.261E-10
19	0.0675	5.443E-06	5.965E-05	3.866E-08	1.271E-09	5.355E-09	2.200E-11	4.088E-09	3.393E-11	3.308E-06	2.288E-10
20	0.0750	8.000E-06	3.184E-05	1.247E-08	2.494E-09	8.889E-09	5.750E-11	4.365E-09	7.974E-11	4.179E-06	1.258E-10
21	0.0787	9.449E-06	2.400E-05	6.570E-09	3.353E-09	1.141E-08	9.730E-11	4.469E-09	1.166E-10	4.710E-06	1.005E-10
22	0.0825	1.097E-05	1.870E-05	3.484E-09	4.324E-09	1.453E-08	1.663E-10	4.547E-09	1.657E-10	5.311E-06	8.644E-11
23	0.0862	1.249E-05	1.501E-05	1.917E-09	5.309E-09	1.830E-08	2.873E-10	4.592E-09	2.290E-10	5.986E-06	7.906E-11
24	0.0900	1.390E-05	1.233E-05	1.125E-09	6.176E-09	2.269E-08	4.945E-10	4.604E-09	3.070E-10	6.730E-06	7.510E-11
25	0.0937	1.504E-05	1.034E-05	7.148E-10	6.800E-09	2.754E-08	8.300E-10	4.579E-09	3.982E-10	7.533E-06	7.222E-11
26	0.0975	1.577E-05	8.837E-06	4.936E-10	7.135E-09	3.258E-08	1.324E-09	4.520E-09	4.979E-10	8.369E-06	6.900E-11
27	0.1012	1.599E-05	7.777E-06	3.709E-10	7.327E-09	3.737E-08	1.932E-09	4.432E-09	5.909E-10	9.215E-06	6.622E-11
28	0.1050	1.572E-05	7.083E-06	3.007E-10	7.569E-09	4.157E-08	2.552E-09	4.321E-09	6.611E-10	1.005E-05	6.561E-11
29	0.1125	1.435E-05	5.976E-06	2.241E-10	7.706E-09	4.839E-08	3.868E-09	4.027E-09	7.772E-10	1.158E-05	6.322E-11
30	0.1200	1.244E-05	4.976E-06	1.745E-10	7.305E-09	5.339E-08	5.186E-09	3.678E-09	8.638E-10	1.283E-05	5.842E-11
31	0.1275	1.039E-05	4.086E-06	1.385E-10	6.568E-09	5.667E-08	6.342E-09	3.308E-09	9.203E-10	1.376E-05	5.229E-11
32	0.1350	8.444E-06	3.320E-06	1.113E-10	5.692E-09	5.839E-08	7.197E-09	2.945E-09	9.483E-10	1.441E-05	4.578E-11
33	0.1500	5.354E-06	2.193E-06	7.585E-11	3.990E-09	5.779E-08	7.704E-09	2.289E-09	9.294E-10	1.501E-05	3.386E-11
34	0.1650	3.295E-06	1.460E-06	5.430E-11	2.705E-09	5.394E-08	7.043E-09	1.768E-09	8.542E-10	1.511E-05	2.464E-11
35	0.1800	2.025E-06	9.865E-07	4.038E-11	1.826E-09	4.873E-08	5.860E-09	1.371E-09	7.593E-10	1.499E-05	1.799E-11
36	0.1950	1.260E-06	6.789E-07	3.095E-11	1.253E-09	4.326E-08	4.612E-09	1.074E-09	6.644E-10	1.479E-05	1.330E-11
37	0.2100	7.977E-07	4.747E-07	2.421E-11	8.859E-10	3.811E-08	3.517E-09	8.497E-10	5.782E-10	1.455E-05	1.000E-11
38	0.2400	3.576E-07	2.550E-07	1.613E-11	5.057E-10	2.971E-08	2.003E-09	5.619E-10	4.430E-10	1.407E-05	6.113E-12
39	0.3000	1.135E-07	1.000E-07	8.691E-12	2.472E-10	2.044E-08	8.008E-10	2.992E-10	3.000E-10	1.335E-05	3.040E-12
40	0.3600	4.479E-08	4.244E-08	4.775E-12	1.610E-10	1.535E-08	3.832E-10	1.737E-10	2.233E-10	1.273E-05	1.822E-12
41	0.4800	1.510E-08	1.161E-08	1.823E-12	1.091E-10	1.136E-08	1.731E-10	8.436E-11	1.636E-10	1.171E-05	1.080E-12
42	0.6000	8.005E-09	3.102E-09	7.553E-13	8.915E-11	9.732E-09	1.146E-10	5.024E-11	1.389E-10	1.088E-05	8.303E-13
43	0.7200	6.370E-09	7.598E-10	4.198E-13	7.649E-11	9.372E-09	1.004E-10	3.688E-11	1.330E-10	1.027E-05	7.485E-13
44	0.8400	5.974E-09	1.760E-10	3.148E-13	6.868E-11	9.362E-09	9.726E-11	3.156E-11	1.320E-10	9.750E-06	7.224E-13
45	0.9600	5.898E-09	4.061E-11	2.716E-13	6.307E-11	9.442E-09	9.713E-11	2.936E-11	1.323E-10	9.314E-06	7.132E-13
46	1.0800	5.896E-09	1.147E-11	2.503E-13	5.949E-11	9.515E-09	9.756E-11	2.846E-11	1.326E-10	9.014E-06	7.098E-13
47	1.2000	5.896E-09	1.147E-11	2.503E-13	5.949E-11	9.515E-09	9.756E-11	2.846E-11	1.326E-10	9.014E-06	7.098E-13

	X	HONO	C2H5O	HNNOH	H2O2	NH2NO	CH3CO	CH2S	C	CH2N
1	0.0000	4.880E-09	1.030E-06	4.484E-15	7.406E-05	1.944E-14	1.417E-11	4.715E-24	-2.584E-16	2.519E-12
2	0.0075	5.968E-09	1.385E-06	5.244E-15	8.925E-05	2.548E-14	1.852E-11	6.935E-24	-3.452E-20	3.013E-12
3	0.0150	6.916E-09	1.773E-06	5.898E-15	1.019E-04	3.125E-14	9.764E-12	6.868E-21	-8.909E-24	3.508E-12
4	0.0225	7.460E-09	2.199E-06	6.381E-15	1.119E-04	3.655E-14	4.875E-11	1.340E-17	-3.996E-27	4.016E-12
5	0.0300	7.120E-09	2.663E-06	6.548E-15	1.181E-04	4.079E-14	2.358E-10	6.766E-15	1.826E-26	4.635E-12
6	0.0337	6.333E-09	2.911E-06	6.414E-15	1.189E-04	4.206E-14	3.504E-10	5.821E-14	2.225E-24	5.154E-12
7	0.0356	5.753E-09	3.039E-06	6.275E-15	1.185E-04	4.236E-14	3.857E-10	1.334E-13	1.956E-23	5.507E-12
8	0.0375	5.052E-09	3.170E-06	6.084E-15	1.175E-04	4.241E-14	4.085E-10	2.760E-13	1.603E-22	5.941E-12
9	0.0412	3.340E-09	3.442E-06	5.542E-15	1.137E-04	4.159E-14	4.352E-10	9.970E-13	5.607E-21	7.121E-12
10	0.0450	1.641E-09	3.726E-06	4.815E-15	1.067E-04	3.930E-14	4.802E-10	3.624E-12	1.792E-19	9.000E-12
11	0.0469	1.019E-09	3.873E-06	4.412E-15	1.019E-04	3.755E-14	5.199E-10	7.225E-12	1.147E-18	1.031E-11
12	0.0487	5.845E-10	4.024E-06	3.997E-15	9.605E-05	3.540E-14	5.695E-10	1.444E-11	6.364E-18	1.185E-11
13	0.0506	3.239E-10	4.180E-06	3.580E-15	8.935E-05	3.287E-14	6.284E-10	2.865E-11	3.181E-17	1.358E-11
14	0.0525	1.862E-10	4.340E-06	3.174E-15	8.187E-05	3.004E-14	6.957E-10	5.572E-11	1.405E-16	1.545E-11
15	0.0544	1.167E-10	4.505E-06	2.789E-15	7.376E-05	2.698E-14	7.695E-10	1.051E-10	5.464E-16	1.738E-11
16	0.0562	7.922E-11	4.676E-06	2.431E-15	6.524E-05	2.380E-14	8.473E-10	1.913E-10	1.908E-15	1.930E-11
17	0.0600	4.179E-11	5.036E-06	1.812E-15	4.776E-05	1.748E-14	1.006E-09	5.622E-10	1.509E-14	2.296E-11
18	0.0637	2.370E-11	5.420E-06	1.331E-15	3.178E-05	1.207E-14	1.156E-09	1.435E-09	8.438E-14	2.662E-11
19	0.0675	1.436E-11	5.824E-06	9.780E-16	1.890E-05	8.057E-15	1.291E-09	3.304E-09	3.869E-13	3.117E-11
20	0.0750	6.465E-12	6.653E-06	5.647E-16	4.552E-06	3.810E-15	1.519E-09	1.413E-08	4.987E-12	4.685E-11
21	0.0787	4.809E-12	7.015E-06	4.510E-16	1.678E-06	2.776E-15	1.612E-09	2.740E-08	1.722E-11	6.372E-11
22	0.0825	3.759E-12	7.319E-06	3.724E-16	5.109E-07	2.125E-15	1.683E-09	5.060E-08	5.485E-11	9.041E-11
23	0.0862	3.043E-12	7.548E-06	3.148E-16	1.311E-07	1.682E-15	1.721E-09	8.855E-08	1.607E-10	1.318E-10
24	0.0900	2.517E-12	7.693E-06	2.701E-16	3.231E-08	1.360E-15	1.716E-09	1.457E-07	4.247E-10	1.924E-10
25	0.0937	2.104E-12	7.752E-06	2.334E-16	1.093E-08	1.112E-15	1.666E-09	2.240E-07	9.954E-10	2.732E-10
26	0.0975	1.758E-12	7.734E-06	2.030E-16	6.322E-09	9.165E-16	1.573E-09	3.201E-07	2.037E-09	3.671E-10
27	0.1012	1.619E-12	7.654E-06	1.939E-16	5.036E-09	8.459E-16	1.501E-09	4.096E-07	3.583E-09	4.749E-10
28	0.1050	1.802E-12	7.536E-06	2.181E-16	4.678E-09	9.543E-16	1.502E-09	4.599E-07	5.526E-09	6.117E-10

```
29   0.1125   2.085E-12   7.221E-06   2.664E-16   4.232E-09   1.166E-15   1.433E-09   5.188E-07   1.050E-08   8.569E-10
30   0.1200   2.272E-12   6.902E-06   3.044E-16   3.775E-09   1.332E-15   1.317E-09   5.341E-07   1.629E-08   1.032E-09
31   0.1275   2.365E-12   6.618E-06   3.306E-16   3.307E-09   1.446E-15   1.184E-09   5.154E-07   2.167E-08   1.115E-09
32   0.1350   2.372E-12   6.379E-06   3.448E-16   2.852E-09   1.507E-15   1.050E-09   4.744E-07   2.546E-08   1.108E-09
33   0.1500   2.190E-12   6.038E-06   3.406E-16   2.065E-09   1.488E-15   8.186E-10   3.663E-07   2.595E-08   9.120E-10
34   0.1650   1.917E-12   5.820E-06   3.154E-16   1.471E-09   1.379E-15   6.427E-10   2.645E-07   2.071E-08   6.548E-10
35   0.1800   1.625E-12   5.681E-06   2.797E-16   1.042E-09   1.225E-15   5.120E-10   1.871E-07   1.434E-08   4.382E-10
36   0.1950   1.361E-12   5.590E-06   2.428E-16   7.412E-10   1.064E-15   4.150E-10   1.324E-07   9.195E-09   2.847E-10
37   0.2100   1.142E-12   5.529E-06   2.096E-16   5.329E-10   9.207E-16   3.425E-10   9.460E-08   5.691E-09   1.845E-10
38   0.2400   8.275E-13   5.461E-06   1.581E-16   2.965E-10   6.970E-16   2.478E-10   5.176E-08   2.205E-09   8.335E-11
39   0.3000   4.974E-13   5.408E-06   9.902E-17   1.229E-10   4.372E-16   1.577E-10   2.218E-08   5.053E-10   2.768E-11
40   0.3600   3.474E-13   5.383E-06   7.102E-17   6.051E-11   3.154E-16   1.151E-10   1.173E-08   1.644E-10   1.408E-11
41   0.4800   2.347E-13   5.362E-06   4.968E-17   2.632E-11   2.232E-16   8.379E-11   5.943E-09   5.098E-11   8.331E-12
42   0.6000   1.859E-13   5.350E-06   4.043E-17   1.616E-11   1.834E-16   7.127E-11   4.112E-09   2.804E-11   6.854E-12
43   0.7200   1.568E-13   5.338E-06   3.478E-17   1.320E-11   1.578E-16   6.638E-11   3.640E-09   2.303E-11   6.419E-12
44   0.8400   1.385E-13   5.327E-06   3.125E-17   1.238E-11   1.418E-16   6.435E-11   3.480E-09   2.183E-11   6.341E-12
45   0.9600   1.253E-13   5.318E-06   2.869E-17   1.216E-11   1.302E-16   6.331E-11   3.414E-09   2.159E-11   6.355E-12
46   1.0800   1.170E-13   5.312E-06   2.705E-17   1.209E-11   1.227E-16   6.277E-11   3.383E-09   2.158E-11   6.381E-12
47   1.2000   1.170E-13   5.312E-06   2.705E-17   1.209E-11   1.227E-16   6.277E-11   3.383E-09   2.158E-11   6.381E-12
```

TWOPNT: TOTAL CPU TIME.

6:07.6 MINUTES : SECONDS . FRACTION

TWOPNT: PERCENT OF TOTAL CPU TIME.

GRID POINTS	GRID TOTAL	ACTIVITY			EVENT		
		TIMESTEP	NEWTON	REFINE	FUNCTION	JACOBIAN	SOLVE
6	15.8	10.7	5.1	0.0	7.5	8.1	0.3
11	9.0	0.0	9.0	0.0	0.9	8.0	0.0
14	8.7	0.0	8.6	0.0	0.6	8.0	0.0
18	13.4	0.0	13.3	0.0	2.6	10.7	0.1
25	16.8	0.0	16.7	0.0	1.4	15.4	0.0
34	16.0	0.0	15.8	0.0	1.6	14.3	0.1
43	9.9	0.0	9.7	0.0	0.7	9.2	0.0
47	10.5	0.0	10.3	0.0	0.5	10.0	0.0
TOTAL		10.7	88.5	0.0	15.7	83.6	0.5

TWOPNT: AVERAGE CPU TIME.

GRID POINTS	AVERAGE SECONDS			NUMBER OF EVENTS		
	FUNCTION	JACOBIAN	SOLVE	FUNCTION	JACOBIAN	SOLVE
6	0.034	3.293	0.001	817	9	720
11	0.072	7.385	0.003	47	4	48
14	0.094	9.835	0.003	24	3	24
18	0.125	13.107	0.005	76	3	76
25	0.178	18.825	0.006	28	3	28
34	0.248	26.231	0.009	24	2	23
43	0.315	33.658	0.011	8	1	6
47	0.346	36.918	0.013	5	1	3

TWOPNT: SUCCESS. BOUNDARY VALUE PROBLEM SOLVED.

```
------------------------------------------------------------------------------
        TABLE B.2 :  RESULT FROM THE MODEL FOR DOPED FLAME
------------------------------------------------------------------------------



    PREMIX: ONE-DIMENSIONAL STEADY PREMIXED LAMINAR FLAME CODE
    PRODUCTION VERSION 2.4, NOVEMBER 1985

    SINGLE PRECISION

            WORKING SPACE REQUIREMENTS
              PROVIDED      REQUIRED
LOGICAL          160           58
INTEGER        25000         9011
REAL         2470700      1075107


    KEYWORD INPUT

    /   flame configuration, burner stabilized with specified temperature
    BURN
    TGIV
    /   in th5event of a Newton failure, take 100 timesteps of 1.E-6
    TIME    150  6.0E-6
    /   begin on a uniform mesh of 6 points
    NPTS      6
    /       definition of the computational interval
    XEND 1.20
    XCEN 0.0625
    WMIX 0.1875
    /   pressure and inlet mass flow rate
    PRES  1.00 (atmospheres)
    FLRT  8.00E-03 (g/cm**2-sec)
    /   adaptive mesh criteria
    GRAD  0.25
    CURV  0.7
    /   unreacted mole fractions
    MOLE
    REAC    O2   0.229974
    REAC    N2    .57450
    REAC    CH4  0.1948
    REAC    NH3  6.9699E-04
    /   estimated products
    PROD    N2   0.50
    PROD    CO   0.12
    PROD    H2O  0.20
    PROD    CO2  0.04
    PROD    H2   0.14
    /   estimated intermediate mole fractions
    INTM    CH    1.0E-08
    INTM    OH    1.0E-03
    INTM    H     5.0E-03
    INTM    O     1.0E-04
    INTM    HO2   1.0E-04
    INTM    NO    1.0E-04
    INTM    NNH   1.0E-08
    INTM    N2O   1.0E-08
    INTM    N     5.0E-06
    INTM    NH2   1.0E-06
    INTM    NH    2.0E-06
    INTM    NO    1.0E-04
    INTM    HNO   5.0E-07
```

```
INTM   C2H5   3.0E-04
INTM   C2H3   5.0E-04
INTM   CH2    1.0E-04
INTM   CN     1.0E-07
INTM   NCO    1.0E-09
/   tolerances for the Newton iteration
ATOL   5.0E-09
RTOL   1.E-4
/   tolerances for the time step Newton iteration
ATIM   1.E-5
RTIM   1.E-5
/   print control
PRNT    1
/   given temperature profile
TEMP     0.0   350.0
TEMP      .1   1833.0
TEMP     .150  1836.0
TEMP     .200  1831.0
TEMP     .250  1823.0
TEMP     .300  1823.0
TEMP     .400  1812.0
TEMP     .500  1801.0
TEMP     .600  1792.0
TEMP    1.200  1792.0
/TRANSPORT OPTION TAKING THERMAL DIFFUSION
TDIF
/read the solution from restart file
/ASEN
/RSTR
END
```

CAUTION...REACTANT FRACTIONS SUM TO 0.9999709899999

TWOPNT: TWO-POINT BOUNDARY VALUE PROBLEM SOLVER,
          VERSION 2.05 OF OCTOBER 1986.

          PERMIT TIME STEPPING.
          PERMIT MESH REFINEMENT.

TWOPNT: INITIAL GUESS:

	X	T	V	RHO	CH	NO	OH	NH	CN	H2	NH3
1	0.0000	3.500E+02	8.874E+00	9.015E-04	4.304E-09	4.304E-05	4.304E-04	8.607E-07	4.304E-08	2.316E-02	5.765E-04
2	0.2400	1.825E+03	5.204E+01	1.537E-04	1.113E-11	1.113E-07	1.113E-06	2.226E-09	1.113E-10	1.400E-01	0.000E+00
3	0.4800	1.803E+03	5.143E+01	1.555E-04	4.572E-25	4.572E-21	4.572E-20	9.144E-23	4.572E-24	1.400E-01	0.000E+00
4	0.7200	1.792E+03	5.111E+01	1.565E-04	2.982E-49	2.982E-45	2.982E-44	5.964E-47	2.982E-48	1.400E-01	0.000E+00
5	0.9600	1.792E+03	5.111E+01	1.565E-04	3.089E-84	3.089E-80	3.089E-79	6.178E-82	3.089E-83	1.400E-01	0.000E+00
6	1.2000	1.792E+03	5.111E+01	1.565E-04	5.081-130	5.081-126	5.081-125	1.016-127	5.081-129	1.400E-01	0.000E+00

	X	CH4	O2	N2	H2O	CH2O	CO	CO2	C2H6	C2H4	C2H2
1	0.0000	1.611E-01	1.902E-01	5.579E-01	3.309E-02	0.000E+00	1.985E-02	6.617E-03	0.000E+00	0.000E+00	0.000E+00
2	0.2400	0.000E+00	0.000E+00	5.000E-01	2.000E-01	0.000E+00	1.200E-01	4.000E-02	0.000E+00	0.000E+00	0.000E+00
3	0.4800	0.000E+00	0.000E+00	5.000E-01	2.000E-01	0.000E+00	1.200E-01	4.000E-02	0.000E+00	0.000E+00	0.000E+00
4	0.7200	0.000E+00	0.000E+00	5.000E-01	2.000E-01	0.000E+00	1.200E-01	4.000E-02	0.000E+00	0.000E+00	0.000E+00
5	0.9600	0.000E+00	0.000E+00	5.000E-01	2.000E-01	0.000E+00	1.200E-01	4.000E-02	0.000E+00	0.000E+00	0.000E+00
6	1.2000	0.000E+00	0.000E+00	5.000E-01	2.000E-01	0.000E+00	1.200E-01	4.000E-02	0.000E+00	0.000E+00	0.000E+00

	X	CH2CO	CH3CHO	C*C*C	CH3O2	CH3O	CH3OH	CH2OH	C4H2	CH2	CH3
1	0.0000	0.000E+00	0.000E+00	0.000E+00	0.000E+00	0.000E+00	0.000E+00	0.000E+00	0.000E+00	4.304E-05	4.304E-03
2	0.2400	0.000E+00	0.000E+00	0.000E+00	0.000E+00	0.000E+00	0.000E+00	0.000E+00	0.000E+00	1.113E-07	1.113E-05
3	0.4800	0.000E+00	0.000E+00	0.000E+00	0.000E+00	0.000E+00	0.000E+00	0.000E+00	0.000E+00	4.572E-21	4.572E-19
4	0.7200	0.000E+00	0.000E+00	0.000E+00	0.000E+00	0.000E+00	0.000E+00	0.000E+00	0.000E+00	2.982E-45	2.982E-43
5	0.9600	0.000E+00	0.000E+00	0.000E+00	0.000E+00	0.000E+00	0.000E+00	0.000E+00	0.000E+00	3.089E-80	3.089E-78
6	1.2000	0.000E+00	0.000E+00	0.000E+00	0.000E+00	0.000E+00	0.000E+00	0.000E+00	0.000E+00	5.081-126	5.081-124

	X	HCO	HCN	NCO	C2H5	C2H3	C2H	HCCO	C3H3	C*CC	H
1	0.0000	0.000E+00	4.304E-05	4.304E-10	1.291E-04	2.152E-04	0.000E+00	0.000E+00	0.000E+00	0.000E+00	2.152E-03

2	0.2400	0.000E+00	1.113E-07	1.113E-12	3.339E-07	5.565E-07	0.000E+00	0.000E+00	0.000E+00	0.000E+00	5.565E-06
3	0.4800	0.000E+00	4.572E-21	4.572E-26	1.372E-20	2.286E-20	0.000E+00	0.000E+00	0.000E+00	0.000E+00	2.286E-19
4	0.7200	0.000E+00	2.982E-45	2.982E-50	8.946E-45	1.491E-44	0.000E+00	0.000E+00	0.000E+00	0.000E+00	1.491E-43
5	0.9600	0.000E+00	3.089E-80	3.089E-85	9.267E-80	1.545E-79	0.000E+00	0.000E+00	0.000E+00	0.000E+00	1.545E-78
6	1.2000	0.000E+00	5.081-126	5.081-131	1.524-125	2.541-125	0.000E+00	0.000E+00	0.000E+00	0.000E+00	2.541-124

	X	O	HO2	NO2	HNO	NH2	N	N2O	NNH	C4H2O	NH2O
1	0.0000	4.304E-05	4.304E-05	0.000E+00	2.152E-07	4.304E-07	2.152E-06	4.304E-09	4.304E-09	0.000E+00	0.000E+00
2	0.2400	1.113E-07	1.113E-07	0.000E+00	5.565E-10	1.113E-09	5.565E-09	1.113E-11	1.113E-11	0.000E+00	0.000E+00
3	0.4800	4.572E-21	4.572E-21	0.000E+00	2.286E-23	4.572E-23	2.286E-22	4.572E-25	4.572E-25	0.000E+00	0.000E+00
4	0.7200	2.982E-45	2.982E-45	0.000E+00	1.491E-47	2.982E-47	1.491E-46	2.982E-49	2.982E-49	0.000E+00	0.000E+00
5	0.9600	3.089E-80	3.089E-80	0.000E+00	1.545E-82	3.089E-82	1.545E-81	3.089E-84	3.089E-84	0.000E+00	0.000E+00
6	1.2000	5.081-126	5.081-126	0.000E+00	2.541-128	5.081-128	2.541-127	5.081-130	5.081-130	0.000E+00	0.000E+00

	X	HONO	C2H5O	HNNOH	H2O2	NH2NO	CH3CO	CH2S	C	CH2N
1	0.0000	0.000E+00	0.000E+00	0.000E+00	0.000E+00	0.000E+00	0.000E+00	0.000E+00	0.000E+00	0.000E+00
2	0.2400	0.000E+00	0.000E+00	0.000E+00	0.000E+00	0.000E+00	0.000E+00	0.000E+00	0.000E+00	0.000E+00
3	0.4800	0.000E+00	0.000E+00	0.000E+00	0.000E+00	0.000E+00	0.000E+00	0.000E+00	0.000E+00	0.000E+00
4	0.7200	0.000E+00	0.000E+00	0.000E+00	0.000E+00	0.000E+00	0.000E+00	0.000E+00	0.000E+00	0.000E+00
5	0.9600	0.000E+00	0.000E+00	0.000E+00	0.000E+00	0.000E+00	0.000E+00	0.000E+00	0.000E+00	0.000E+00
6	1.2000	0.000E+00	0.000E+00	0.000E+00	0.000E+00	0.000E+00	0.000E+00	0.000E+00	0.000E+00	0.000E+00

TWOPNT: LOG OF THE BOUNDARY VALUE PROBLEM SOLVER.

ACTIVITY	LOG10 MAX NORM RESIDUAL	LOG10 MAX CONDITION NUMBER	POINTS	STEPS JACOBIANS	CPU TIME H:MM:SS.F	REMARK
START			6			
NEWTON		15.30		0 1	3.5	FAILURE
TIMSTP	1.92	11.74		150 5	56.6	
NEWTON	-3.30	14.77		10 3	11.1	
REFINE	2.18		11		.0	NEW MESH
NEWTON	-4.34	13.51		25 4	33.0	
REFINE	2.84		14		.0	NEW MESH
NEWTON	-1.68	13.67		15 3	31.6	
REFINE	3.79		19		.0	NEW MESH
NEWTON	-6.40	13.46		36 3	47.8	
REFINE	3.25		26		.0	NEW MESH
NEWTON	-5.25	13.65		29 4	1:28.2	
REFINE	2.74		35		.0	NEW MESH
NEWTON	-1.36	13.06		11 1	30.2	
REFINE	2.35		44		.0	NEW MESH
NEWTON	-1.06	13.75		4 1	36.0	
REFINE	1.72		48		.0	NEW MESH
NEWTON	-1.52	13.70		2 1	38.7	
REFINE	-1.39		49		.0	NEW MESH
NEWTON	-2.79	13.68		1 1	39.2	
REFINE			49		.0	

TWOPNT: FINAL SOLUTION:

	X	T	V	RHO	CH	NO	OH	NH	CN	H2	NH3
1	0.0000	3.500E+02	8.979E+00	8.909E-04	-2.864E-18	1.240E-06	9.376E-09	3.199E-15	8.618E-17	3.213E-02	5.935E-04
2	0.0075	4.612E+02	1.192E+01	6.714E-04	-1.706E-22	1.496E-06	1.063E-08	3.615E-15	1.040E-16	3.786E-02	5.749E-04
3	0.0150	5.724E+02	1.489E+01	5.374E-04	-7.823E-24	2.169E-06	9.585E-09	7.937E-14	8.037E-16	4.333E-02	5.576E-04
4	0.0225	6.837E+02	1.789E+01	4.472E-04	4.779E-22	3.308E-06	1.684E-08	1.436E-12	6.239E-15	4.861E-02	5.410E-04

	x										
5	0.0300	7.949E+02	2.093E+01	3.823E-04	6.052E-20	5.094E-06	9.371E-08	1.626E-11	9.939E-14	5.373E-02	5.248E-04
6	0.0319	8.227E+02	2.169E+01	3.688E-04	3.347E-19	5.698E-06	1.459E-07	3.486E-11	1.929E-13	5.499E-02	5.208E-04
7	0.0337	8.505E+02	2.246E+01	3.562E-04	1.663E-18	6.374E-06	2.124E-07	6.505E-11	3.443E-13	5.624E-02	5.169E-04
8	0.0356	8.783E+02	2.322E+01	3.445E-04	6.653E-18	7.130E-06	2.935E-07	1.150E-10	5.760E-13	5.748E-02	5.129E-04
9	0.0375	9.061E+02	2.399E+01	3.334E-04	2.438E-17	7.974E-06	3.911E-07	1.969E-10	9.214E-13	5.872E-02	5.090E-04
10	0.0412	9.617E+02	2.554E+01	3.133E-04	2.572E-16	9.949E-06	6.548E-07	5.108E-10	2.169E-12	6.117E-02	5.011E-04
11	0.0450	1.017E+03	2.709E+01	2.953E-04	2.709E-15	1.236E-05	1.114E-06	1.267E-09	5.122E-12	6.359E-02	4.933E-04
12	0.0469	1.045E+03	2.787E+01	2.871E-04	9.215E-15	1.373E-05	1.480E-06	1.991E-09	8.046E-12	6.479E-02	4.894E-04
13	0.0487	1.073E+03	2.865E+01	2.792E-04	2.959E-14	1.520E-05	1.960E-06	3.036E-09	1.259E-11	6.598E-02	4.855E-04
14	0.0506	1.101E+03	2.943E+01	2.718E-04	8.941E-14	1.676E-05	2.564E-06	4.510E-09	1.948E-11	6.716E-02	4.816E-04
15	0.0525	1.129E+03	3.022E+01	2.648E-04	2.512E-13	1.837E-05	3.285E-06	6.525E-09	2.961E-11	6.834E-02	4.777E-04
16	0.0544	1.156E+03	3.100E+01	2.581E-04	6.504E-13	2.000E-05	4.100E-06	9.195E-09	4.394E-11	6.950E-02	4.737E-04
17	0.0562	1.184E+03	3.179E+01	2.517E-04	1.553E-12	2.163E-05	4.971E-06	1.262E-08	6.350E-11	7.066E-02	4.698E-04
18	0.0600	1.240E+03	3.337E+01	2.398E-04	6.932E-12	2.472E-05	6.748E-06	2.197E-08	1.230E-10	7.293E-02	4.620E-04
19	0.0637	1.295E+03	3.495E+01	2.289E-04	2.413E-11	2.744E-05	8.571E-06	3.523E-08	2.203E-10	7.516E-02	4.541E-04
20	0.0675	1.351E+03	3.654E+01	2.189E-04	7.187E-11	2.976E-05	1.071E-05	5.326E-08	3.770E-10	7.735E-02	4.462E-04
21	0.0750	1.462E+03	3.974E+01	2.013E-04	4.738E-10	3.349E-05	1.731E-05	1.081E-07	1.019E-09	8.161E-02	4.303E-04
22	0.0787	1.518E+03	4.134E+01	1.935E-04	1.147E-09	3.515E-05	2.273E-05	1.512E-07	1.648E-09	8.369E-02	4.223E-04
23	0.0825	1.573E+03	4.296E+01	1.862E-04	2.620E-09	3.674E-05	3.007E-05	2.071E-07	2.616E-09	8.574E-02	4.143E-04
24	0.0862	1.629E+03	4.457E+01	1.795E-04	5.603E-09	3.828E-05	3.969E-05	2.768E-07	4.056E-09	8.775E-02	4.063E-04
25	0.0900	1.685E+03	4.620E+01	1.732E-04	1.107E-08	3.979E-05	5.172E-05	3.591E-07	6.105E-09	8.973E-02	3.983E-04
26	0.0937	1.740E+03	4.782E+01	1.673E-04	1.995E-08	4.126E-05	6.604E-05	4.505E-07	8.877E-09	9.167E-02	3.905E-04
27	0.0975	1.796E+03	4.945E+01	1.618E-04	3.246E-08	4.266E-05	8.205E-05	5.462E-07	1.240E-08	9.357E-02	3.829E-04
28	0.1012	1.833E+03	5.055E+01	1.583E-04	4.666E-08	4.397E-05	9.610E-05	6.448E-07	1.593E-08	9.504E-02	3.757E-04
29	0.1050	1.833E+03	5.059E+01	1.581E-04	5.950E-08	4.520E-05	1.039E-04	7.465E-07	1.820E-08	9.567E-02	3.690E-04
30	0.1125	1.834E+03	5.065E+01	1.579E-04	8.135E-08	4.727E-05	1.145E-04	9.269E-07	2.228E-08	9.680E-02	3.566E-04
31	0.1200	1.834E+03	5.071E+01	1.578E-04	9.596E-08	4.878E-05	1.205E-04	1.056E-06	2.575E-08	9.775E-02	3.456E-04
32	0.1275	1.835E+03	5.075E+01	1.576E-04	1.015E-07	4.973E-05	1.227E-04	1.130E-06	2.844E-08	9.855E-02	3.359E-04
33	0.1350	1.835E+03	5.079E+01	1.575E-04	9.887E-08	5.018E-05	1.217E-04	1.152E-06	3.026E-08	9.924E-02	3.277E-04
34	0.1500	1.836E+03	5.085E+01	1.573E-04	7.821E-08	4.984E-05	1.128E-04	1.070E-06	3.122E-08	1.004E-01	3.157E-04
35	0.1650	1.834E+03	5.083E+01	1.574E-04	5.406E-08	4.859E-05	9.942E-05	9.107E-07	2.961E-08	1.013E-01	3.079E-04
36	0.1800	1.833E+03	5.080E+01	1.575E-04	3.517E-08	4.694E-05	8.575E-05	7.379E-07	2.687E-08	1.021E-01	3.031E-04
37	0.1950	1.831E+03	5.077E+01	1.576E-04	2.244E-08	4.519E-05	7.341E-05	5.829E-07	2.383E-08	1.027E-01	3.002E-04
38	0.2100	1.829E+03	5.072E+01	1.577E-04	1.435E-08	4.351E-05	6.280E-05	4.561E-07	2.090E-08	1.033E-01	2.984E-04
39	0.2400	1.825E+03	5.060E+01	1.581E-04	6.376E-09	4.051E-05	4.708E-05	2.848E-07	1.615E-08	1.042E-01	2.968E-04
40	0.2700	1.823E+03	5.056E+01	1.582E-04	3.148E-09	3.803E-05	3.685E-05	1.850E-07	1.289E-08	1.050E-01	2.960E-04
41	0.3000	1.823E+03	5.057E+01	1.582E-04	1.722E-09	3.596E-05	2.999E-05	1.265E-07	1.065E-08	1.058E-01	2.955E-04
42	0.3600	1.816E+03	5.040E+01	1.587E-04	7.116E-10	3.274E-05	2.184E-05	7.211E-08	7.887E-09	1.068E-01	2.950E-04
43	0.4800	1.803E+03	5.006E+01	1.598E-04	2.851E-10	2.821E-05	1.546E-05	4.013E-08	5.691E-09	1.083E-01	2.943E-04
44	0.6000	1.792E+03	4.976E+01	1.608E-04	1.778E-10	2.472E-05	1.275E-05	2.963E-08	4.759E-09	1.095E-01	2.936E-04
45	0.7200	1.792E+03	4.978E+01	1.607E-04	1.542E-10	2.184E-05	1.207E-05	2.676E-08	4.570E-09	1.105E-01	2.929E-04
46	0.8400	1.792E+03	4.980E+01	1.607E-04	1.484E-10	1.943E-05	1.186E-05	2.600E-08	4.544E-09	1.114E-01	2.923E-04
47	0.9600	1.792E+03	4.980E+01	1.606E-04	1.472E-10	1.751E-05	1.179E-05	2.583E-08	4.563E-09	1.120E-01	2.919E-04
48	1.0800	1.792E+03	4.981E+01	1.606E-04	1.471E-10	1.626E-05	1.177E-05	2.582E-08	4.584E-09	1.124E-01	2.916E-04
49	1.2000	1.792E+03	4.981E+01	1.606E-04	1.471E-10	1.626E-05	1.177E-05	2.582E-08	4.584E-09	1.124E-01	2.916E-04

	x	CH_4	O_2	N_2	H_2O	CH_2O	CO	CO_2	C_2H_6	C_2H_4	C_2H_2
1	0.0000	1.420E-01	1.757E-01	5.507E-01	6.848E-02	1.574E-08	2.204E-02	6.108E-03	4.522E-04	2.676E-04	1.233E-03
2	0.0075	1.328E-01	1.645E-01	5.464E-01	8.058E-02	1.989E-08	2.657E-02	7.727E-03	5.801E-04	3.372E-04	1.544E-03
3	0.0150	1.238E-01	1.535E-01	5.426E-01	9.203E-02	1.748E-07	3.114E-02	9.418E-03	7.155E-04	4.093E-04	1.866E-03
4	0.0225	1.150E-01	1.423E-01	5.392E-01	1.031E-01	4.946E-07	3.581E-02	1.119E-02	8.594E-04	4.846E-04	2.202E-03
5	0.0300	1.061E-01	1.311E-01	5.359E-01	1.140E-01	1.078E-06	4.061E-02	1.307E-02	1.013E-03	5.633E-04	2.554E-03
6	0.0319	1.039E-01	1.282E-01	5.351E-01	1.166E-01	1.302E-06	4.182E-02	1.355E-02	1.052E-03	5.833E-04	2.645E-03
7	0.0337	1.017E-01	1.254E-01	5.344E-01	1.193E-01	1.564E-06	4.305E-02	1.404E-02	1.093E-03	6.035E-04	2.738E-03
8	0.0356	9.946E-02	1.225E-01	5.336E-01	1.220E-01	1.854E-06	4.429E-02	1.454E-02	1.134E-03	6.238E-04	2.832E-03
9	0.0375	9.723E-02	1.196E-01	5.329E-01	1.247E-01	2.155E-06	4.554E-02	1.505E-02	1.176E-03	6.442E-04	2.928E-03
10	0.0412	9.275E-02	1.138E-01	5.315E-01	1.300E-01	2.718E-06	4.806E-02	1.608E-02	1.261E-03	6.846E-04	3.125E-03
11	0.0450	8.824E-02	1.080E-01	5.301E-01	1.353E-01	3.009E-06	5.060E-02	1.714E-02	1.347E-03	7.240E-04	3.335E-03
12	0.0469	8.597E-02	1.051E-01	5.294E-01	1.380E-01	2.994E-06	5.187E-02	1.769E-02	1.390E-03	7.427E-04	3.448E-03
13	0.0487	8.370E-02	1.022E-01	5.287E-01	1.406E-01	2.893E-06	5.314E-02	1.824E-02	1.433E-03	7.605E-04	3.570E-03
14	0.0506	8.142E-02	9.923E-02	5.281E-01	1.433E-01	2.711E-06	5.440E-02	1.879E-02	1.475E-03	7.773E-04	3.702E-03
15	0.0525	7.913E-02	9.631E-02	5.274E-01	1.459E-01	2.462E-06	5.564E-02	1.936E-02	1.516E-03	7.928E-04	3.847E-03
16	0.0544	7.684E-02	9.340E-02	5.268E-01	1.485E-01	2.172E-06	5.687E-02	1.993E-02	1.556E-03	8.067E-04	4.010E-03
17	0.0562	7.454E-02	9.051E-02	5.261E-01	1.511E-01	1.869E-06	5.806E-02	2.050E-02	1.593E-03	8.189E-04	4.192E-03
18	0.0600	6.995E-02	8.479E-02	5.249E-01	1.563E-01	1.315E-06	6.038E-02	2.168E-02	1.656E-03	8.378E-04	4.618E-03
19	0.0637	6.538E-02	7.914E-02	5.237E-01	1.614E-01	9.088E-07	6.257E-02	2.287E-02	1.697E-03	8.499E-04	5.122E-03

	x										
20	0.0675	6.086E-02	7.357E-02	5.225E-01	1.664E-01	6.442E-07	6.466E-02	2.409E-02	1.704E-03	8.577E-04	5.690E-03
21	0.0750	5.199E-02	6.266E-02	5.203E-01	1.762E-01	3.769E-07	6.857E-02	2.655E-02	1.587E-03	8.715E-04	6.970E-03
22	0.0787	4.770E-02	5.737E-02	5.192E-01	1.808E-01	3.122E-07	7.042E-02	2.778E-02	1.450E-03	8.908E-04	7.650E-03
23	0.0825	4.354E-02	5.224E-02	5.181E-01	1.853E-01	2.715E-07	7.220E-02	2.899E-02	1.266E-03	9.220E-04	8.349E-03
24	0.0862	3.952E-02	4.729E-02	5.171E-01	1.896E-01	2.441E-07	7.390E-02	3.018E-02	1.051E-03	9.657E-04	9.058E-03
25	0.0900	3.569E-02	4.258E-02	5.161E-01	1.936E-01	2.233E-07	7.551E-02	3.132E-02	8.259E-04	1.018E-03	9.766E-03
26	0.0937	3.208E-02	3.816E-02	5.151E-01	1.973E-01	2.056E-07	7.703E-02	3.240E-02	6.148E-04	1.070E-03	1.046E-02
27	0.0975	2.873E-02	3.408E-02	5.141E-01	2.007E-01	1.891E-07	7.843E-02	3.341E-02	4.390E-04	1.109E-03	1.112E-02
28	0.1012	2.571E-02	3.036E-02	5.134E-01	2.039E-01	1.711E-07	7.976E-02	3.435E-02	3.136E-04	1.117E-03	1.174E-02
29	0.1050	2.303E-02	2.700E-02	5.132E-01	2.068E-01	1.504E-07	8.105E-02	3.525E-02	2.358E-04	1.088E-03	1.231E-02
30	0.1125	1.853E-02	2.123E-02	5.129E-01	2.118E-01	1.159E-07	8.335E-02	3.684E-02	1.541E-04	9.499E-04	1.327E-02
31	0.1200	1.509E-02	1.659E-02	5.126E-01	2.156E-01	9.013E-08	8.526E-02	3.817E-02	1.082E-04	7.833E-04	1.396E-02
32	0.1275	1.250E-02	1.294E-02	5.124E-01	2.186E-01	7.126E-08	8.682E-02	3.925E-02	7.867E-05	6.276E-04	1.444E-02
33	0.1350	1.057E-02	1.011E-02	5.122E-01	2.208E-01	5.741E-08	8.808E-02	4.014E-02	5.835E-05	4.981E-04	1.474E-02
34	0.1500	8.170E-03	6.372E-03	5.120E-01	2.234E-01	3.986E-08	8.986E-02	4.144E-02	3.493E-05	3.226E-04	1.498E-02
35	0.1650	6.796E-03	4.136E-03	5.118E-01	2.247E-01	2.954E-08	9.101E-02	4.236E-02	2.286E-05	2.204E-04	1.500E-02
36	0.1800	5.973E-03	2.769E-03	5.117E-01	2.252E-01	2.319E-08	9.178E-02	4.304E-02	1.604E-05	1.604E-04	1.493E-02
37	0.1950	5.454E-03	1.909E-03	5.116E-01	2.254E-01	1.912E-08	9.231E-02	4.357E-02	1.190E-05	1.237E-04	1.483E-02
38	0.2100	5.111E-03	1.346E-03	5.116E-01	2.253E-01	1.639E-08	9.269E-02	4.398E-02	9.213E-06	1.000E-04	1.472E-02
39	0.2400	4.737E-03	7.572E-04	5.115E-01	2.249E-01	1.335E-08	9.317E-02	4.457E-02	6.217E-06	7.457E-05	1.450E-02
40	0.2700	4.524E-03	4.518E-04	5.114E-01	2.244E-01	1.173E-08	9.349E-02	4.500E-02	4.420E-06	6.084E-05	1.431E-02
41	0.3000	4.386E-03	2.781E-04	5.112E-01	2.239E-01	1.078E-08	9.372E-02	4.532E-02	3.268E-06	5.259E-05	1.413E-02
42	0.3600	4.232E-03	1.234E-04	5.111E-01	2.229E-01	9.852E-09	9.406E-02	4.579E-02	2.187E-06	4.496E-05	1.383E-02
43	0.4800	4.082E-03	3.477E-05	5.109E-01	2.213E-01	9.214E-09	9.454E-02	4.640E-02	1.478E-06	4.080E-05	1.336E-02
44	0.6000	3.982E-03	9.302E-06	5.107E-01	2.201E-01	8.922E-09	9.495E-02	4.685E-02	1.225E-06	3.998E-05	1.295E-02
45	0.7200	3.892E-03	2.279E-06	5.105E-01	2.189E-01	8.820E-09	9.537E-02	4.718E-02	1.081E-06	3.863E-05	1.258E-02
46	0.8400	3.813E-03	5.220E-07	5.103E-01	2.180E-01	8.812E-09	9.579E-02	4.742E-02	1.013E-06	3.758E-05	1.225E-02
47	0.9600	3.749E-03	1.160E-07	5.102E-01	2.172E-01	8.836E-09	9.618E-02	4.761E-02	9.728E-07	3.675E-05	1.196E-02
48	1.0800	3.707E-03	2.891E-08	5.102E-01	2.168E-01	8.856E-09	9.646E-02	4.773E-02	9.503E-07	3.618E-05	1.176E-02
49	1.2000	3.707E-03	2.891E-08	5.102E-01	2.168E-01	8.856E-09	9.646E-02	4.773E-02	9.503E-07	3.618E-05	1.176E-02

	x	CH2CO	CH3CHO	C*C*C	CH3O2	CH3O	CH3OH	CH2OH	C4H2	CH2	CH3
1	0.0000	2.241E-05	7.850E-06	5.213E-06	1.595E-05	9.576E-05	1.181E-04	1.407E-07	1.046E-06	-6.320E-17	3.917E-10
2	0.0075	2.927E-05	1.027E-05	6.967E-06	2.058E-05	1.214E-04	1.498E-04	1.780E-07	1.474E-06	3.393E-19	4.658E-10
3	0.0150	3.655E-05	1.285E-05	8.899E-06	2.521E-05	1.479E-04	1.825E-04	2.165E-07	1.971E-06	3.312E-17	4.838E-09
4	0.0225	4.431E-05	1.562E-05	1.103E-05	2.941E-05	1.754E-04	2.165E-04	2.563E-07	2.542E-06	3.163E-15	2.664E-07
5	0.0300	5.256E-05	1.858E-05	1.336E-05	2.697E-05	2.041E-04	2.520E-04	2.982E-07	3.193E-06	3.266E-13	5.052E-06
6	0.0319	5.469E-05	1.935E-05	1.398E-05	2.375E-05	2.110E-04	2.612E-04	3.094E-07	3.371E-06	9.901E-13	8.461E-06
7	0.0337	5.684E-05	2.014E-05	1.461E-05	1.972E-05	2.176E-04	2.704E-04	3.212E-07	3.556E-06	2.501E-12	1.275E-05
8	0.0356	5.902E-05	2.094E-05	1.526E-05	1.548E-05	2.237E-04	2.797E-04	3.335E-07	3.749E-06	5.579E-12	1.776E-05
9	0.0375	6.121E-05	2.176E-05	1.593E-05	1.166E-05	2.291E-04	2.892E-04	3.467E-07	3.950E-06	1.150E-11	2.337E-05
10	0.0412	6.562E-05	2.344E-05	1.731E-05	6.313E-06	2.373E-04	3.085E-04	3.767E-07	4.380E-06	4.183E-11	3.681E-05
11	0.0450	7.004E-05	2.520E-05	1.875E-05	3.712E-06	2.407E-04	3.281E-04	4.154E-07	4.852E-06	1.519E-10	5.724E-05
12	0.0469	7.224E-05	2.610E-05	1.950E-05	2.989E-06	2.400E-04	3.381E-04	4.405E-07	5.108E-06	2.996E-10	7.245E-05
13	0.0487	7.443E-05	2.703E-05	2.026E-05	2.481E-06	2.375E-04	3.482E-04	4.704E-07	5.380E-06	5.812E-10	9.192E-05
14	0.0506	7.659E-05	2.797E-05	2.104E-05	2.104E-06	2.329E-04	3.583E-04	5.063E-07	5.671E-06	1.105E-09	1.166E-04
15	0.0525	7.873E-05	2.894E-05	2.184E-05	1.812E-06	2.257E-04	3.684E-04	5.490E-07	5.983E-06	2.044E-09	1.473E-04
16	0.0544	8.085E-05	2.992E-05	2.266E-05	1.577E-06	2.160E-04	3.786E-04	5.994E-07	6.321E-06	3.653E-09	1.847E-04
17	0.0562	8.294E-05	3.090E-05	2.349E-05	1.381E-06	2.036E-04	3.887E-04	6.578E-07	6.688E-06	6.299E-09	2.294E-04
18	0.0600	8.706E-05	3.284E-05	2.521E-05	1.066E-06	1.716E-04	4.086E-04	7.992E-07	7.521E-06	1.661E-08	3.411E-04
19	0.0637	9.122E-05	3.452E-05	2.700E-05	8.217E-07	1.348E-04	4.276E-04	9.736E-07	8.514E-06	3.871E-08	4.822E-04
20	0.0675	9.557E-05	3.564E-05	2.887E-05	6.321E-07	9.973E-05	4.453E-04	1.187E-06	9.695E-06	8.312E-08	6.518E-04
21	0.0750	1.053E-04	3.525E-05	3.283E-05	3.735E-07	4.850E-05	4.747E-04	1.768E-06	1.269E-05	3.193E-07	1.073E-03
22	0.0787	1.110E-04	3.321E-05	3.492E-05	2.871E-07	3.339E-05	4.843E-04	2.183E-06	1.457E-05	5.975E-07	1.320E-03
23	0.0825	1.174E-04	2.999E-05	3.709E-05	2.196E-07	2.360E-05	4.896E-04	2.683E-06	1.675E-05	1.069E-06	1.580E-03
24	0.0862	1.243E-04	2.586E-05	3.932E-05	1.662E-07	1.734E-05	4.897E-04	3.247E-06	1.924E-05	1.817E-06	1.833E-03
25	0.0900	1.315E-04	2.126E-05	4.161E-05	1.238E-07	1.324E-05	4.840E-04	3.825E-06	2.202E-05	2.910E-06	2.058E-03
26	0.0937	1.386E-04	1.668E-05	4.392E-05	9.047E-08	1.042E-05	4.727E-04	4.347E-06	2.506E-05	4.361E-06	2.231E-03
27	0.0975	1.448E-04	1.258E-05	4.622E-05	6.486E-08	8.396E-06	4.570E-04	4.746E-06	2.822E-05	6.073E-06	2.336E-03
28	0.1012	1.498E-04	9.253E-06	4.849E-05	4.950E-08	7.014E-06	4.402E-04	5.040E-06	3.134E-05	7.682E-06	2.367E-03
29	0.1050	1.532E-04	6.733E-06	5.074E-05	4.338E-08	6.105E-06	4.255E-04	5.285E-06	3.428E-05	8.808E-06	2.338E-03
30	0.1125	1.547E-04	3.609E-06	5.483E-05	3.168E-08	4.626E-06	3.980E-04	5.345E-06	3.944E-05	1.032E-05	2.177E-03
31	0.1200	1.508E-04	1.961E-06	5.815E-05	2.227E-08	3.384E-06	3.693E-04	5.020E-06	4.349E-05	1.101E-05	1.961E-03
32	0.1275	1.435E-04	1.092E-06	6.065E-05	1.534E-08	2.410E-06	3.386E-04	4.492E-06	4.642E-05	1.098E-05	1.735E-03
33	0.1350	1.345E-04	6.185E-07	6.242E-05	1.047E-08	1.688E-06	3.067E-04	3.893E-06	4.840E-05	1.041E-05	1.519E-03
34	0.1500	1.154E-04	2.356E-07	6.424E-05	5.032E-09	8.387E-07	2.424E-04	2.771E-06	5.008E-05	8.431E-06	1.163E-03

35	0.1650	9.924E-05	9.925E-08	6.497E-05	2.542E-09	4.282E-07	1.860E-04	1.919E-06	5.021E-05	6.341E-06	8.990E-04
36	0.1800	8.655E-05	4.618E-08	6.521E-05	1.350E-09	2.276E-07	1.400E-04	1.329E-06	4.968E-05	4.637E-06	7.083E-04
37	0.1950	7.685E-05	2.339E-08	6.523E-05	7.533E-10	1.263E-07	1.044E-04	9.318E-07	4.892E-05	3.375E-06	5.698E-04
38	0.2100	6.944E-05	1.258E-08	6.517E-05	4.399E-10	7.297E-08	7.771E-05	6.659E-07	4.808E-05	2.472E-06	4.673E-04
39	0.2400	5.994E-05	4.777E-09	6.495E-05	1.817E-10	2.942E-08	4.503E-05	3.714E-07	4.645E-05	1.419E-06	3.359E-04
40	0.2700	5.373E-05	2.064E-09	6.471E-05	8.308E-11	1.315E-08	2.670E-05	2.254E-07	4.511E-05	8.785E-07	2.556E-04
41	0.3000	4.934E-05	9.888E-10	6.449E-05	4.074E-11	6.313E-09	1.631E-05	1.476E-07	4.399E-05	5.837E-07	2.036E-04
42	0.3600	4.426E-05	3.608E-10	6.414E-05	1.343E-11	1.996E-09	8.150E-06	8.007E-08	4.193E-05	3.198E-07	1.469E-04
43	0.4800	3.924E-05	1.421E-10	6.361E-05	2.860E-12	4.026E-10	4.296E-06	4.237E-08	3.857E-05	1.703E-07	1.045E-04
44	0.6000	3.579E-05	9.759E-11	6.317E-05	6.699E-13	9.122E-11	3.245E-06	3.021E-08	3.584E-05	1.222E-07	8.691E-05
45	0.7200	3.314E-05	8.596E-11	6.273E-05	1.526E-13	2.073E-11	2.799E-06	2.660E-08	3.384E-05	1.096E-07	8.077E-05
46	0.8400	3.142E-05	8.179E-11	6.231E-05	3.375E-14	4.617E-12	2.627E-06	2.525E-08	3.213E-05	1.057E-07	7.803E-05
47	0.9600	3.029E-05	7.973E-11	6.193E-05	7.354E-15	1.033E-12	2.549E-06	2.461E-08	3.069E-05	1.042E-07	7.649E-05
48	1.0800	2.962E-05	7.865E-11	6.166E-05	1.812E-15	2.793E-13	2.513E-06	2.429E-08	2.971E-05	1.036E-07	7.563E-05
49	1.2000	2.962E-05	7.865E-11	6.166E-05	1.812E-15	2.793E-13	2.513E-06	2.429E-08	2.971E-05	1.036E-07	7.563E-05

	x	HCO	HCN	NCO	C2H5	C2H3	C2H	HCCO	C3H3	CHCC	H
1	0.0000	1.046E-10	2.997E-05	2.140E-08	7.438E-09	8.309E-12	5.399E-16	2.050E-17	7.086E-15	5.672E-08	1.158E-11
2	0.0075	1.320E-10	3.797E-05	2.706E-08	9.526E-09	1.042E-11	6.746E-16	2.390E-17	9.460E-15	7.580E-08	1.315E-11
3	0.0150	2.920E-10	4.618E-05	3.450E-08	2.370E-08	2.882E-11	8.662E-15	2.100E-15	1.300E-14	9.684E-08	2.175E-11
4	0.0225	1.571E-09	5.468E-05	4.387E-08	1.168E-07	1.938E-10	9.036E-14	9.668E-14	3.308E-14	1.200E-07	3.162E-10
5	0.0300	1.904E-08	6.352E-05	5.562E-08	6.258E-07	3.458E-09	1.793E-12	2.880E-12	2.582E-13	1.455E-07	7.935E-09
6	0.0319	3.538E-08	6.579E-05	5.906E-08	1.026E-06	7.107E-09	3.637E-12	8.154E-12	4.406E-13	1.522E-07	1.679E-08
7	0.0337	6.093E-08	6.808E-05	6.271E-08	1.595E-06	1.343E-08	6.776E-12	2.012E-11	7.061E-13	1.592E-07	3.230E-08
8	0.0356	1.003E-07	7.040E-05	6.660E-08	2.401E-06	2.425E-08	1.179E-11	4.743E-11	1.082E-12	1.662E-07	5.930E-08
9	0.0375	1.608E-07	7.275E-05	7.074E-08	3.534E-06	4.284E-08	1.953E-11	1.098E-10	1.616E-12	1.735E-07	1.064E-07
10	0.0412	3.706E-07	7.752E-05	7.984E-08	7.096E-06	1.224E-07	4.861E-11	4.943E-10	3.521E-12	1.884E-07	3.154E-07
11	0.0450	7.856E-07	8.239E-05	9.020E-08	1.347E-05	3.399E-07	1.181E-10	2.091E-09	8.465E-12	2.037E-07	9.330E-07
12	0.0469	1.108E-06	8.486E-05	9.596E-08	1.826E-05	5.597E-07	1.852E-10	4.300E-09	1.412E-11	2.114E-07	1.618E-06
13	0.0487	1.474E-06	8.736E-05	1.022E-07	2.430E-05	8.697E-07	2.876E-10	8.365E-09	2.413E-11	2.192E-07	2.699E-06
14	0.0506	1.840E-06	8.989E-05	1.088E-07	3.175E-05	1.267E-06	4.387E-10	1.554E-08	4.202E-11	2.269E-07	4.321E-06
15	0.0525	2.148E-06	9.244E-05	1.160E-07	4.074E-05	1.718E-06	6.530E-10	2.760E-08	7.380E-11	2.345E-07	6.613E-06
16	0.0544	2.339E-06	9.501E-05	1.238E-07	5.129E-05	2.162E-06	9.438E-10	4.683E-08	1.296E-10	2.419E-07	9.656E-06
17	0.0562	2.390E-06	9.761E-05	1.322E-07	6.335E-05	2.529E-06	1.322E-09	7.615E-08	2.270E-10	2.489E-07	1.346E-05
18	0.0600	2.143E-06	1.029E-04	1.509E-07	9.152E-05	2.882E-06	2.380E-09	1.771E-07	6.517E-10	2.612E-07	2.318E-05
19	0.0637	1.703E-06	1.082E-04	1.722E-07	1.229E-04	2.759E-06	3.974E-09	3.609E-07	1.784E-09	2.682E-07	3.518E-05
20	0.0675	1.315E-06	1.136E-04	1.955E-07	1.545E-04	2.423E-06	6.444E-09	6.695E-07	4.761E-09	2.653E-07	4.957E-05
21	0.0750	8.635E-07	1.246E-04	2.456E-07	2.077E-04	1.753E-06	1.677E-08	1.078E-06	2.754E-08	2.126E-07	8.834E-05
22	0.0787	7.649E-07	1.301E-04	2.695E-07	2.209E-04	1.524E-06	2.727E-08	2.966E-06	6.312E-08	1.623E-07	1.164E-04
23	0.0825	7.126E-07	1.356E-04	2.915E-07	2.229E-04	1.346E-06	4.400E-08	4.473E-06	1.334E-07	1.092E-07	1.517E-04
24	0.0862	6.842E-07	1.411E-04	3.104E-07	2.133E-04	1.201E-06	6.982E-08	6.433E-06	2.637E-07	6.843E-08	1.947E-04
25	0.0900	6.625E-07	1.466E-04	3.253E-07	1.938E-04	1.075E-06	1.079E-07	8.791E-06	4.908E-07	4.391E-08	2.452E-04
26	0.0937	6.356E-07	1.520E-04	3.350E-07	1.680E-04	9.594E-07	1.614E-07	1.138E-05	8.553E-07	3.014E-08	3.011E-04
27	0.0975	5.973E-07	1.574E-04	3.380E-07	1.406E-04	8.461E-07	2.318E-07	1.392E-05	1.378E-06	2.168E-08	3.592E-04
28	0.1012	5.629E-07	1.628E-04	3.315E-07	1.156E-04	8.154E-07	3.010E-07	1.582E-05	2.021E-06	1.942E-08	4.141E-04
29	0.1050	5.472E-07	1.683E-04	3.151E-07	9.475E-05	9.426E-07	3.379E-07	1.671E-05	2.724E-06	2.596E-08	4.613E-04
30	0.1125	4.865E-07	1.795E-04	2.703E-07	6.653E-05	1.159E-06	3.951E-07	1.696E-05	4.355E-06	4.271E-08	5.391E-04
31	0.1200	4.141E-07	1.902E-04	2.271E-07	4.812E-05	1.320E-06	4.332E-07	1.602E-05	6.226E-06	6.312E-08	5.963E-04
32	0.1275	3.442E-07	2.002E-04	1.894E-07	3.538E-05	1.423E-06	4.530E-07	1.444E-05	8.185E-06	8.466E-08	6.328E-04
33	0.1350	2.826E-07	2.092E-04	1.575E-07	2.634E-05	1.471E-06	4.571E-07	1.262E-05	1.007E-05	1.043E-07	6.499E-04
34	0.1500	1.889E-07	2.242E-04	1.105E-07	1.566E-05	1.430E-06	4.297E-07	9.260E-06	1.304E-05	1.280E-07	6.343E-04
35	0.1650	1.278E-07	2.353E-04	7.818E-08	1.001E-05	1.317E-06	3.786E-07	6.679E-06	1.497E-05	1.366E-07	5.824E-04
36	0.1800	8.885E-08	2.433E-04	5.623E-08	6.817E-06	1.171E-06	3.249E-07	4.874E-06	1.612E-05	1.329E-07	5.178E-04
37	0.1950	6.398E-08	2.491E-04	4.122E-08	4.885E-06	1.026E-06	2.762E-07	3.633E-06	1.677E-05	1.233E-07	4.537E-04
38	0.2100	4.782E-08	2.534E-04	3.074E-08	3.640E-06	8.994E-07	2.343E-07	2.771E-06	1.713E-05	1.129E-07	3.959E-04
39	0.2400	3.018E-08	2.588E-04	1.885E-08	2.264E-06	7.053E-07	1.725E-07	1.790E-06	1.720E-05	9.326E-08	3.061E-04
40	0.2700	2.106E-08	2.624E-04	1.234E-08	1.504E-06	5.598E-07	1.334E-07	1.257E-06	1.750E-05	7.726E-08	2.441E-04
41	0.3000	1.583E-08	2.649E-04	8.476E-09	1.052E-06	4.551E-07	1.076E-07	9.415E-07	1.831E-05	6.652E-08	2.010E-04
42	0.3600	1.092E-08	2.684E-04	4.718E-09	6.280E-07	3.491E-07	7.640E-08	6.268E-07	2.110E-05	6.274E-08	1.510E-04
43	0.4800	7.742E-09	2.730E-04	2.348E-09	3.619E-07	2.737E-07	5.158E-08	4.098E-07	3.091E-05	8.147E-08	1.125E-04
44	0.6000	6.550E-09	2.764E-04	1.566E-09	2.690E-07	2.458E-07	4.081E-08	3.203E-07	4.495E-05	1.184E-07	9.676E-05
45	0.7200	6.154E-09	2.793E-04	1.372E-09	2.326E-07	2.291E-07	3.777E-08	2.847E-07	5.933E-05	1.498E-07	9.286E-05
46	0.8400	6.061E-09	2.817E-04	1.326E-09	2.164E-07	2.216E-07	3.632E-08	2.671E-07	7.078E-05	1.775E-07	9.226E-05
47	0.9600	6.059E-09	2.836E-04	1.321E-09	2.072E-07	2.170E-07	3.542E-08	2.571E-07	7.872E-05	1.978E-07	9.250E-05
48	1.0800	6.073E-09	2.850E-04	1.324E-09	2.022E-07	2.140E-07	3.487E-08	2.515E-07	8.333E-05	2.100E-07	9.279E-05
49	1.2000	6.073E-09	2.850E-04	1.324E-09	2.022E-07	2.140E-07	3.487E-08	2.515E-07	8.333E-05	2.100E-07	9.279E-05

x	O	HO2	NO2	HNO	NH2	N	N2O	NNH	C4H2O	NH2O
1	0.0000	7.763E-12	1.690E-05	8.783E-06	4.448E-11	7.827E-10	3.060E-16	1.260E-07	3.058E-15	3.561E-07	1.183E-07
2	0.0075	8.782E-12	2.035E-05	1.089E-05	5.361E-11	8.827E-10	3.509E-16	1.596E-07	3.692E-15	5.083E-07	1.500E-07
3	0.0150	4.598E-11	2.888E-05	1.259E-05	1.185E-10	2.261E-09	7.863E-16	1.932E-07	2.580E-14	6.864E-07	1.816E-07
4	0.0225	2.927E-10	4.322E-05	1.385E-05	3.233E-10	6.206E-09	3.323E-15	2.270E-07	1.554E-13	8.927E-07	2.126E-07
5	0.0300	2.061E-09	6.541E-05	1.450E-05	8.817E-10	1.703E-08	2.090E-14	2.608E-07	7.958E-13	1.130E-06	2.410E-07
6	0.0319	4.163E-09	7.276E-05	1.450E-05	1.136E-09	2.247E-08	4.614E-14	2.692E-07	1.226E-12	1.194E-06	2.468E-07
7	0.0337	7.593E-09	8.090E-05	1.444E-05	1.450E-09	2.926E-08	9.065E-14	2.775E-07	1.839E-12	1.262E-06	2.518E-07
8	0.0356	1.340E-08	8.984E-05	1.430E-05	1.839E-09	3.774E-08	1.744E-13	2.857E-07	2.712E-12	1.332E-06	2.557E-07
9	0.0375	2.329E-08	9.953E-05	1.407E-05	2.319E-09	4.836E-08	3.355E-13	2.939E-07	3.952E-12	1.405E-06	2.584E-07
10	0.0412	6.358E-08	1.207E-04	1.331E-05	3.608E-09	7.776E-08	1.105E-12	3.099E-07	7.978E-12	1.560E-06	2.586E-07
11	0.0450	1.708E-07	1.416E-04	1.208E-05	5.514E-09	1.252E-07	3.798E-12	3.253E-07	1.557E-11	1.728E-06	2.484E-07
12	0.0469	2.804E-07	1.497E-04	1.128E-05	6.789E-09	1.594E-07	7.413E-12	3.327E-07	2.151E-11	1.819E-06	2.381E-07
13	0.0487	4.424E-07	1.553E-04	1.036E-05	8.320E-09	2.017E-07	1.375E-11	3.399E-07	2.919E-11	1.913E-06	2.241E-07
14	0.0506	6.718E-07	1.573E-04	9.344E-06	1.016E-08	2.530E-07	2.460E-11	3.467E-07	3.881E-11	2.014E-06	2.069E-07
15	0.0525	9.798E-07	1.550E-04	8.264E-06	1.238E-08	3.135E-07	4.239E-11	3.533E-07	5.041E-11	2.120E-06	1.870E-07
16	0.0544	1.370E-06	1.486E-04	7.160E-06	1.507E-08	3.829E-07	7.016E-11	3.595E-07	6.385E-11	2.233E-06	1.654E-07
17	0.0562	1.836E-06	1.384E-04	6.076E-06	1.838E-08	4.604E-07	1.114E-10	3.653E-07	7.880E-11	2.354E-06	1.435E-07
18	0.0600	2.950E-06	1.105E-04	4.089E-06	2.728E-08	6.359E-07	2.456E-10	3.755E-07	1.116E-10	2.622E-06	1.017E-07
19	0.0637	4.173E-06	8.210E-05	2.552E-06	4.082E-08	8.322E-07	4.757E-10	3.837E-07	1.451E-10	2.931E-06	6.874E-08
20	0.0675	5.425E-06	5.901E-05	1.487E-06	6.084E-08	1.051E-06	8.435E-10	3.894E-07	1.785E-10	3.287E-06	4.549E-08
21	0.0750	7.988E-06	3.167E-05	4.805E-07	1.252E-07	1.588E-06	2.225E-09	3.929E-07	2.514E-10	4.156E-06	2.194E-08
22	0.0787	9.440E-06	2.393E-05	2.535E-07	1.709E-07	1.943E-06	3.603E-09	3.903E-07	3.008E-10	4.685E-06	1.611E-08
23	0.0825	1.096E-05	1.869E-05	1.346E-07	2.224E-07	2.364E-06	5.709E-09	3.848E-07	3.616E-10	5.284E-06	1.267E-08
24	0.0862	1.249E-05	1.502E-05	7.406E-08	2.735E-07	2.846E-06	8.849E-09	3.766E-07	4.349E-10	5.955E-06	1.061E-08
25	0.0900	1.389E-05	1.236E-05	4.343E-08	3.164E-07	3.375E-06	1.334E-08	3.659E-07	5.194E-10	6.696E-06	9.305E-09
26	0.0937	1.504E-05	1.037E-05	2.755E-08	3.447E-07	3.923E-06	1.943E-08	3.533E-07	6.121E-10	7.495E-06	8.372E-09
27	0.0975	1.577E-05	8.866E-06	1.897E-08	3.573E-07	4.449E-06	2.726E-08	3.394E-07	7.078E-10	8.327E-06	7.590E-09
28	0.1012	1.599E-05	7.803E-06	1.420E-08	3.640E-07	4.902E-06	3.703E-08	3.251E-07	8.034E-10	9.168E-06	6.955E-09
29	0.1050	1.573E-05	7.106E-06	1.147E-08	3.764E-07	5.251E-06	4.889E-08	3.111E-07	8.951E-10	9.999E-06	6.563E-09
30	0.1125	1.436E-05	5.992E-06	8.482E-09	3.893E-07	5.699E-06	7.721E-08	2.832E-07	1.045E-09	1.152E-05	5.830E-09
31	0.1200	1.245E-05	4.988E-06	6.561E-09	3.746E-07	5.915E-06	1.084E-07	2.564E-07	1.149E-09	1.276E-05	5.077E-09
32	0.1275	1.040E-05	4.093E-06	5.173E-09	3.401E-07	5.953E-06	1.386E-07	2.317E-07	1.209E-09	1.369E-05	4.351E-09
33	0.1350	8.452E-06	3.325E-06	4.133E-09	2.960E-07	5.857E-06	1.641E-07	2.092E-07	1.230E-09	1.433E-05	3.687E-09
34	0.1500	5.361E-06	2.195E-06	2.787E-09	2.060E-07	5.381E-06	1.892E-07	1.716E-07	1.177E-09	1.492E-05	2.611E-09
35	0.1650	3.302E-06	1.461E-06	1.977E-09	1.375E-07	4.757E-06	1.845E-07	1.420E-07	1.063E-09	1.502E-05	1.848E-09
36	0.1800	2.031E-06	9.873E-07	1.459E-09	9.077E-08	4.130E-06	1.617E-07	1.187E-07	9.321E-10	1.489E-05	1.325E-09
37	0.1950	1.268E-06	6.803E-07	1.111E-09	6.071E-08	3.563E-06	1.326E-07	1.001E-07	8.075E-10	1.468E-05	9.676E-10
38	0.2100	8.068E-07	4.774E-07	8.658E-10	4.177E-08	3.074E-06	1.048E-07	8.512E-08	6.979E-10	1.444E-05	7.220E-10
39	0.2400	3.724E-07	2.635E-07	5.823E-10	2.281E-08	2.343E-06	6.326E-08	6.364E-08	5.316E-10	1.397E-05	4.401E-10
40	0.2700	1.892E-07	1.528E-07	4.041E-10	1.401E-08	1.849E-06	3.844E-08	4.853E-08	4.188E-10	1.357E-05	2.884E-10
41	0.3000	1.039E-07	9.108E-08	2.831E-10	9.516E-09	1.510E-06	2.422E-08	3.762E-08	3.415E-10	1.323E-05	2.007E-10
42	0.3600	4.173E-08	3.879E-08	1.545E-10	5.960E-09	1.118E-06	1.206E-08	2.453E-08	2.526E-10	1.262E-05	1.193E-10
43	0.4800	1.447E-08	1.058E-08	5.835E-11	3.906E-09	8.145E-07	5.771E-09	1.348E-08	1.838E-10	1.161E-05	6.971E-11
44	0.6000	7.857E-09	2.813E-09	2.430E-11	3.139E-09	6.880E-07	3.959E-09	8.650E-09	1.550E-10	1.079E-05	5.287E-11
45	0.7200	6.341E-09	6.866E-10	1.371E-11	2.671E-09	6.525E-07	3.476E-09	6.294E-09	1.467E-10	1.018E-05	4.744E-11
46	0.8400	5.978E-09	1.590E-10	1.032E-11	2.384E-09	6.422E-07	3.365E-09	5.065E-09	1.440E-10	9.666E-06	4.551E-11
47	0.9600	5.911E-09	3.693E-11	8.852E-12	2.178E-09	6.394E-07	3.356E-09	4.359E-09	1.431E-10	9.233E-06	4.467E-11
48	1.0800	5.911E-09	1.065E-11	8.108E-12	2.048E-09	6.388E-07	3.367E-09	3.971E-09	1.427E-10	8.934E-06	4.428E-11
49	1.2000	5.911E-09	1.065E-11	8.108E-12	2.048E-09	6.388E-07	3.367E-09	3.971E-09	1.427E-10	8.934E-06	4.428E-11

x	HONO	C2H5O	HNNOH	H2O2	NH2NO	CH3CO	CH2S	C	CH2N
1	0.0000	1.851E-07	1.029E-06	5.210E-11	7.038E-05	2.197E-10	3.795E-10	2.856E-21	7.642E-17	4.471E-11
2	0.0075	2.264E-07	1.383E-06	6.093E-11	8.482E-05	2.880E-10	4.960E-10	3.581E-21	1.026E-20	5.350E-11
3	0.0150	2.623E-07	1.772E-06	6.824E-11	9.694E-05	3.508E-10	7.906E-11	1.574E-19	2.644E-24	6.207E-11
4	0.0225	2.831E-07	2.197E-06	7.319E-11	1.065E-04	4.056E-10	5.743E-11	4.068E-17	2.344E-25	7.078E-11
5	0.0300	2.707E-07	2.661E-06	7.398E-11	1.125E-04	4.456E-10	2.551E-10	8.963E-15	5.073E-22	8.109E-11
6	0.0319	2.579E-07	2.783E-06	7.303E-11	1.131E-04	4.509E-10	3.220E-10	2.742E-14	1.624E-24	8.508E-11
7	0.0337	2.406E-07	2.909E-06	7.155E-11	1.133E-04	4.540E-10	3.738E-10	7.023E-14	3.516E-24	8.982E-11
8	0.0356	2.186E-07	3.037E-06	6.949E-11	1.130E-04	4.544E-10	4.082E-10	1.561E-13	2.651E-23	9.561E-11
9	0.0375	1.920E-07	3.169E-06	6.681E-11	1.121E-04	4.516E-10	4.285E-10		1.976E-22	1.028E-10
10	0.0412	1.271E-07	3.441E-06	5.961E-11	1.085E-04	4.356E-10	4.491E-10	1.089E-12	6.342E-21	1.227E-10
11	0.0450	6.257E-08	3.725E-06	5.041E-11	1.020E-04	4.033E-10	4.893E-10	3.827E-12	1.917E-19	1.553E-10
12	0.0469	3.891E-08	3.873E-06	4.546E-11	9.734E-05	3.808E-10	5.271E-10	7.520E-12	1.192E-18	1.788E-10
13	0.0487	2.239E-08	4.024E-06	4.043E-11	9.183E-05	3.543E-10	5.748E-10	1.485E-11	6.518E-18	2.074E-10

```
14  0.0506  1.245E-08  4.180E-06  3.549E-11  8.546E-05  3.243E-10  6.322E-10  2.918E-11  3.212E-17  2.410E-10
15  0.0525  7.182E-09  4.340E-06  3.076E-11  7.833E-05  2.916E-10  6.979E-10  5.634E-11  1.406E-16  2.797E-10
16  0.0544  4.514E-09  4.505E-06  2.637E-11  7.059E-05  2.573E-10  7.702E-10  1.057E-10  5.429E-16  3.231E-10
17  0.0562  3.065E-09  4.677E-06  2.239E-11  6.246E-05  2.226E-10  8.467E-10  1.916E-10  1.887E-15  3.714E-10
18  0.0600  1.615E-09  5.037E-06  1.578E-11  4.575E-05  1.560E-10  1.003E-09  5.603E-10  1.485E-14  4.840E-10
19  0.0637  9.148E-10  5.422E-06  1.093E-11  3.046E-05  1.020E-10  1.151E-09  1.428E-09  8.306E-14  6.294E-10
20  0.0675  5.542E-10  5.826E-06  7.566E-12  1.812E-05  6.382E-11  1.286E-09  3.288E-09  3.817E-13  8.295E-10
21  0.0750  2.498E-10  6.655E-06  3.942E-12  4.369E-06  2.690E-11  1.513E-09  1.409E-08  4.942E-12  1.477E-09
22  0.0787  1.858E-10  7.017E-06  2.988E-12  1.613E-06  1.849E-11  1.606E-09  2.733E-08  1.710E-11  2.052E-09
23  0.0825  1.451E-10  7.321E-06  2.348E-12  4.924E-07  1.343E-11  1.677E-09  5.050E-08  5.451E-11  2.838E-09
24  0.0862  1.173E-10  7.550E-06  1.892E-12  1.273E-07  1.012E-11  1.715E-09  8.840E-08  1.598E-10  3.852E-09
25  0.0900  9.680E-11  7.695E-06  1.549E-12  3.197E-08  7.798E-12  1.711E-09  1.455E-07  4.224E-10  5.058E-09
26  0.0937  8.068E-11  7.754E-06  1.277E-12  1.112E-08  6.083E-12  1.661E-09  2.236E-07  9.903E-10  6.350E-09
27  0.0975  6.718E-11  7.736E-06  1.060E-12  6.506E-09  4.789E-12  1.568E-09  3.196E-07  2.026E-09  7.606E-09
28  0.1012  6.165E-11  7.656E-06  9.688E-13  5.175E-09  4.226E-12  1.496E-09  4.089E-07  3.566E-09  9.197E-09
29  0.1050  6.838E-11  7.537E-06  1.044E-12  4.804E-09  4.571E-12  1.498E-09  4.592E-07  5.498E-09  1.179E-08
30  0.1125  7.855E-11  7.222E-06  1.181E-12  4.340E-09  5.171E-12  1.428E-09  5.179E-07  1.044E-08  1.712E-08
31  0.1200  8.506E-11  6.903E-06  1.262E-12  3.860E-09  5.523E-12  1.312E-09  5.331E-07  1.621E-08  2.151E-08
32  0.1275  8.800E-11  6.618E-06  1.292E-12  3.370E-09  5.651E-12  1.179E-09  5.143E-07  2.155E-08  2.424E-08
33  0.1350  8.781E-11  6.379E-06  1.280E-12  2.898E-09  5.595E-12  1.046E-09  4.734E-07  2.533E-08  2.510E-08
34  0.1500  8.030E-11  6.036E-06  1.163E-12  2.087E-09  5.077E-12  8.149E-10  3.655E-07  2.583E-08  2.214E-08
35  0.1650  6.975E-11  5.818E-06  1.011E-12  1.482E-09  4.420E-12  6.397E-10  2.640E-07  2.064E-08  1.687E-08
36  0.1800  5.875E-11  5.678E-06  8.555E-13  1.049E-09  3.745E-12  5.097E-10  1.870E-07  1.432E-08  1.179E-08
37  0.1950  4.895E-11  5.587E-06  7.169E-13  7.464E-10  3.142E-12  4.135E-10  1.326E-07  9.223E-09  7.908E-09
38  0.2100  4.093E-11  5.526E-06  6.029E-13  5.384E-10  2.647E-12  3.419E-10  9.508E-08  5.746E-09  5.242E-09
39  0.2400  2.959E-11  5.459E-06  4.401E-13  3.056E-10  1.941E-12  2.494E-10  5.283E-08  2.286E-09  2.418E-09
40  0.2700  2.199E-11  5.422E-06  3.291E-13  1.831E-10  1.453E-12  1.911E-10  3.207E-08  9.782E-10  1.206E-09
41  0.3000  1.692E-11  5.399E-06  2.542E-13  1.152E-10  1.122E-12  1.526E-10  2.105E-08  4.619E-10  6.675E-10
42  0.3600  1.178E-11  5.376E-06  1.782E-13  5.733E-11  7.915E-13  1.120E-10  1.127E-08  1.535E-10  3.098E-10
43  0.4800  7.927E-12  5.356E-06  1.211E-13  2.546E-11  5.442E-13  8.222E-11  5.808E-09  4.914E-11  1.636E-10
44  0.6000  6.234E-12  5.343E-06  9.604E-14  1.594E-11  4.357E-13  7.026E-11  4.057E-09  2.753E-11  1.272E-10
45  0.7200  5.212E-12  5.332E-06  8.046E-14  1.317E-11  3.650E-13  6.559E-11  3.608E-09  2.280E-11  1.165E-10
46  0.8400  4.556E-12  5.321E-06  7.045E-14  1.240E-11  3.196E-13  6.364E-11  3.455E-09  2.168E-11  1.140E-10
47  0.9600  4.083E-12  5.312E-06  6.321E-14  1.219E-11  2.868E-13  6.264E-11  3.392E-09  2.146E-11  1.137E-10
48  1.0800  3.785E-12  5.305E-06  5.865E-14  1.213E-11  2.661E-13  6.212E-11  3.363E-09  2.146E-11  1.138E-10
49  1.2000  3.785E-12  5.305E-06  5.865E-14  1.213E-11  2.661E-13  6.212E-11  3.363E-09  2.146E-11  1.138E-10
```

TWOPNT: TOTAL CPU TIME.

6:59.8 MINUTES : SECONDS . FRACTION

TWOPNT: PERCENT OF TOTAL CPU TIME.

GRID POINTS	GRID TOTAL	ACTIVITY			EVENT		
		TIMESTEP	NEWTON	REFINE	FUNCTION	JACOBIAN	SOLVE
6	17.0	13.5	3.5	0.0	9.6	7.0	0.3
11	7.9	0.0	7.9	0.0	0.8	7.1	0.0
14	7.6	0.0	7.5	0.0	0.5	7.0	0.0
19	11.5	0.0	11.4	0.0	1.4	9.9	0.1
26	21.1	0.0	21.0	0.0	2.3	18.7	0.1
35	7.3	0.0	7.2	0.0	0.8	6.4	0.0
44	8.7	0.0	8.6	0.0	0.5	8.2	0.0
48	9.4	0.0	9.2	0.0	0.4	9.0	0.0
49	9.5	0.0	9.3	0.0	0.3	9.2	0.0
TOTAL		13.5	85.6	0.0	16.8	82.5	0.6

TWOPNT: AVERAGE CPU TIME.

GRID POINTS	AVERAGE SECONDS			NUMBER OF EVENTS		
	FUNCTION	JACOBIAN	SOLVE	FUNCTION	JACOBIAN	SOLVE
6	0.034	3.283	0.001	1200	9	1053

11	0.072	7.403	0.003	47	4	48
14	0.094	9.824	0.003	24	3	24
19	0.132	13.908	0.005	46	3	46
26	0.185	19.630	0.007	52	4	53
35	0.254	27.001	0.009	14	1	12
44	0.322	34.354	0.012	7	1	5
48	0.352	37.646	0.013	5	1	3
49	0.360	38.456	0.013	4	1	2

TWOPNT: SUCCESS. BOUNDARY VALUE PROBLEM SOLVED.

Reference

1. Bartok W., Crawford A. R. and Piegari G. J., " Systematic field Study of NO_x emission control methods for Utility Boilers ", Esso Research and Engineering Co. Report No. GRU 4GNOS. 71 to the Office of Air Programs, Research Triangle Park, North Carolina (1971).

2. Bachmaier, F., Eberius K. H. and Just Th.," the formation of nitric oxide and the detection of HCN in Premixed hydrocarbon-air flames at 1 atmosphere," Combustion Science and Technology, 7, 77, 1973.

3. Bartok W., Crawford A. R. and A. Skopp, " Control of NO_x Emissions from Stationary Sources ", Chem Engg Prog., 67, 64 (1971).

4. Benson S. W., " Thermochemical Kinetics", 2nd Ed., Wiley, NY., 1976.

5. Blauwens J., Smets B., and Peeters, J.," Mechanism of Prompt Nitrogen Oxide Formation of Hydrocarbon Flames", Sixteenth symposium (International) on Combustion, The Combustion Institute, The Combustion Institute, Pittsburgh, Pa, 1977, 1055.

6. Burcat A. "Combustion Chemistry", W.C. Gardiner, Jr., Ed., Springer-Verlag, New York 1984 p 173.

7. Berman, M. R., Fleming, J. W., Harvey, A. B., and Lin, M. C., " Temperature dependence of CH radical

reactions with oxygen, nitric oxide, carbon monox ide, and carbon dioxide", in Nineteenth Symposium (International) on Combustion, The Combustion Institute, Pittsburg, Pa., 1982, 73.

8. Berman M. C. and Lin M. C.," Kinetics and Mecha nisms of the reactions of CH with CH_4, C_2H_6, and $n-C_4H_{10}$ ", Chemical Physics., 82, 435, 1983.

9. Berman M. R. and Lin M. C., " Kinetics and Mecha- nism of the CH + N_2. Temperature and Pressure dependence Studies and Transition State Theory Analysis.", J. Phys. Chem. 87, 3933, 1983.

10. Berman M. R. and Lin M. C., " Kinetics and mecha nisms of the reaction of CH and CD with H_2, and D_2 ", J. Chem. Phys. 81, 5743, 1984.

11. Bowman C. T., "Kinetics of Pollutants Formation and Destruction in Combustion", Tenth Symposium (International) on Combustion, The Combustion Institute, Pittsburgh, 503, 1965.

12. Bowman C. T., Dean A. J., and Hanson R. K., " High temperature shock tube study of reaction of CH and C- atoms with N_2", Twenty third Symposium (Inter- national) on Combustion, Orleans, France.

13. Bozzelli J. W. and Dean A. M., " Chemical Activa tion analysis of the Reaction of C_2H_5 with O_2.", Jou. Phy. Chem. 3313, 90, 1990.

14 Bozzelli J. W. and Dean A. M., " Energized Complex

Quantum Rice-Ramsperger-Kassel Analysis on reac
tions of NH_2, with HO_2, O_2, and O atoms", Jou.
Phys. Chem., 1058, 23, 1989.

15. Brooks B., R. and Schaefer H. F., " Reactions of
carbynes. Potential energy surfaces for the dou-
blet and quartet methylidyne (CH) reactions with
molecular hydrogen.", J. Chem. Phys., 67, 5146,
1977.

17. Bosnali M., W. and Perner D., Z., " Reaction of
pulse radiolytically generated methylidyne radical
with methane and other substances", Naturforscher,
26a, 1768, 1971.

18. Braun W., Mcnesby, J. R., and Bass, A., M.,
" Flash photolysis of methane in the vacuum ul-
traviolet. II. Absolute rate constant for reac-
tions of CH with methane, hydrogen, and nitrogen
", J. Chem. Phys., 46, 2071, 1967.

19. Butler J., E., Fleming J., W., Harvey A., B., Lin
M., C., " Kinetics of CH radical with selected
molecule at room temperature ", Chem. Phys., 56,
335, 1981.

20. Chapman S. and Cowling T. G.,(1970), " The Mathe
matical Theory of Non Uniform Gases ", Third Edi-
tion, Cambridge University Press, Cambridge.

21. Coffee T. P. and Heimerl J. M. (1981), " A Trans

port Algorithym for Premixed Laminar Steady State Flames", Combust and Flame, 43, p. 273.

22. Cobos C. J. Hippler, H., Luther K. and Ravishanka ra A. R., J. Phys. Chem. 89, 4332 (1985)

23. Curtiss C. F. and Hirschfelder J. O., " Transport Properties of Multicomponent Gas mixtures.," Jou. Chem. Phys., 17, 550, 1949.

24. Darwin D. C., Young A. T., Johnston H. S. and Moore B.," Rate constants for CH_2 removal by O_2, NO, and C_2H_2 fron Infrared Diode Laser flash Kinetic Spectroscopy.", American Chemical Society, 93, 1076, 1989.

25. Dean A. M., Chou M. S., Stern D., Int. J. Chem. Kinetics (1984).

26. Dean A. M., Chou M. S., "Absolute Concentration Measurements of NO, NH, CN, CH, and OH in Rich CH_4 Flames", Personal Communication.

27. Dean A. M., " Prediction of Temperature and pres sure effect upon radical addition and recombina- tion reactions. ", J. of Phys. Chem. 89, 4600, 1985.

28. Dean A. M. and Westmoreland P. R., " Bimolecular QRRK Analysis of Methyl Reactions ", Int. Jou. of Chem. Kinetics, 19, 207, 1987.

29. de Soete, G. G., " An overall mechanism for NO formation from ammonia and ammines added to pre-

mixed flames ", Combustion Institute European
Symposium, Academic Press, 439, 1973.

30. de Soete, G. G., "Overall reaction rates of NO and
    N_2 formation from fuel nitrogen " , Fifteenth
    Symposium International on Combustion, The Com-
    bustion Institute, Pittsburg, 1093 1975.

31. Fenimore C. P., "Destruction of Methane in Water
    gas by reaction of CH_3 with OH radical," Twelve
    Symposium (International) on Combsution, The
    Combustion Institute, Pittsburgh, 373, 1969.

32. Fenimore C. P. " Formation of Nitric Oxide in
    Premixed flames" ,13th Symposium (International)
    on Combustion , The Combustion Institute Pitts
    burgh, PA, 373, 1971.

33. Fenimore C. P., " Formation of Nitric oxide from
    fuel nitrogen in Ethylene flames", Combustion and
    Flame, 19, 289, 1972.

34. Fenimore C. P., " Reaction of fuel -nitrogen in
    rich flame gases," Combustion and Flame, 26, 249,
    1976.

35. Fenimore C. P., " Studies of fuel nitrogen species
    in rich flame gases", Seventeenth Symposium
    (International) on Combustion, The Combustion
    Institute, Pittsburgh, 661, 1979.

36. Forst W' " Theory of Unimolecular reactions. ",

Academic Press: New York, p 184, 1973.

37. Gutman, D., Slagle I. R., J. Am. Chem. Soc. 106 4356, 1986.

38. Hatakeyama S., Bandow H., Okuda M. and Akimoto H., J. Phys. Chem., 84, 3394, 1980.

39. Haynes, B. S., " The formation and behaviour of nitrogen species in fuel rich hydrcarbon flames", Ph. D. Thesis, University of New Soth Wales 1975.

40. Haynes B. S., " Reactions of Ammonia and Nitric Oxide in the burnt gases of fuel rich hydrocarbon air flames", Combustion and flame, 28, 113 1977.

41. Haynes B. S., "The Oxidation of Hydrogen Cyanide in fuel rich flames", Combustion and Flames, 28, 113 1977.

42. Haynes B. S., "kinetics of nitric oxide formation in combustion", Alternative hydrocarbon fuels: Combustion and Chemical Kinetics. Progress in Astronautics and Aeronautics, 62, American Insti tute of Astronautics and Aeronautics, 359 1978.

43. Hilaire C., Puechberty D. and Cottereau M. J., Poster PS35, presented at the Twentieth Symposium (International) on Combustion, Ann Arbor, Michigan, August 1984.

44. Hinshelwood C.N., Proc. Roy. Soc. (A). 113 230 1927.

45 Hirschfelder, J. O., Curtiss C. F.,and Bird R. B.,

" Molecular theory of Gases and Liquuids", Wiley, New York, 1954.

46. Hirschfelder J. O., Curtiss C. F. and Campbell D. E., " The Theory of Flames and Detonations," Nine teenth Symposium (International) on Combustion, The Combustion Institute, Pittsburgh, PA, 1953.

47. Kassel L. S., J. Phys. Chem., 32, 225, 1928.

48. Kassel L. S., J. Phys. Chem., 32, 1065, 1928.

49. Kee R. J., Miller J. A. and Jefferson T. H., " A general-purpose Problem Independent, Transportable, Fortran chemical Kinetics Code Package." Sandia Lab., ReportSand 80-8003, Livermore, CA, 1980.

50. Kee R. J., Grcar J. F., Smooke M. D. and Miller J. A., " A Fortran program for Modeling Steady Laminar One Dimensional Premixed flames." Sandia report SAND85-8240, Livermore, CA, 1987.

51. Kee R. J., Warnatz R., and Miller J. A., " A Fortran Computer Code Package for the Evaluation of Gas-Phase Viscosities, Conductivities, and Diffusion Coeficients,"Sandia laboratories Report SAND83-8209 1983.

52. Kerr J. A. and Moss S. J., " CRC Handbook of Bimolecular and Termolecular Gas Reactions ", Volume I and II, Florida, CRC Press, 1981.

53. Kistiakowsky G. B. and Michael J. V., " Mechanism of chemi-ionization in hydrocarbon oxidations ", J. Chem. Phys., 40, 1447, 1964

54. Laufer A. H. and Bass A. M., " Rate constants of the combination of Methyl radicals with Nitric oxide and oxygen.", Int. Jou. of Chem. Kinetics VII 639 1975.

55. Levy J. M. " Modeling of Fuel-Nitrogen Chemistry in Combustion: The Influence of Hydrocarbons", presented at Fifth E.P.A. Fundamental Combustion Research Workshop, Newport Beach, California 1980.

56. Lichtin D. A., Berman M. R., and Lin M. C.,"Immi dogen (NH)$(A^3\pi --->X^3\Sigma^-)$chemiluminescence from the methylidyne (CH) $(X^2\pi)$ + nitric oxide reaction ", Chem. Phys. Lett., 108, 18, 1984.

57. Marcus R. A., J. Chem. Phy., 20, 359, 1952.

58. Marcus R. A., and Rice O. K., J. Phys. and Colloid Chem., 55 894 1951.

59. Mathur, S., Tondon, P. K., and Saxena S. C., (1967) " Thermal Conductivity of Binary Ternary and Quaternary Mixtures of Rare Gases", Mol. Phys., 12, p. 569.

60. Matsui Y. and T. Nomaguchi, Combustion Flame, 32, 205 (1978).

61 Melius C., " BAC-MP4 Heats of Formation and Free", 1989, A personal communication.

62. Messing, I., Sadowski, C. M., and Filseth, S. V.,
" Absolute rate constant for the reaction of
methylidyne radical with molecular oxygen ", Chem.
Phys. Lett., 66, 95, 1979.

63. Miller J. A. and Bowman C. T., " Mechanism and
Modeling of Nitrogen Chemistry in Combustion ",
Journal of Progress in Combustion and
Flame, 1989.

64 Miyauchi T., Mori Y. and Imamura A " 16th Symposi
um (International) on Combustion", The Combustion
Institute, Pittsburgh, PA, 1977, p 1073.

65. Page M., " Fragmentation Versus Isomerization: A
theoretical Study o the Methoxy Radical"; Chemical
and Physical Processes in Combustion, 9-1   all
Technical Meeting of Eastern Section of Combus-
tion Institute 1989.

66. Perry, R. A. and Melius C. F., " The rate and
mechanism of the reaction of HCN with O atoms
over the temperature range 540-900 K ", 20th Sympo
sium (International) on Combustion. The Combustion
Institute 1073, 1984.

67. Piling J., Robertson J. A. and Rogers G. J., " The
flash photolysis of Azomethane. Minor Products
from the photolysis of methyl radicals and a rate
constant for CH_3 + NO ", Jou. of Chem. kinetics,

VIII, 883 (1976).

68. Reid R. C., Prausnitz J. M and Sherwood T. K., " The Properties of Gases and Liquids ", Mcgraw Hill Company, 3rd Edition 1979.

69. Ritter E. Ph.D Thesis NJIT. 1989.

70. Robinson P. J., and Holbrook K. A., " Unimolecular Reaction Theory ", Wiley -Interscience, London 1975.

71 Sanders, W. A., Lin, C. Y. and Lin, M.C., Com bustion Science Techno. 51, 103 1987.

71. Sarofim A. F., comments, Eighteenth Symposium (International) on combustion, The Combustion Institute, Pittsburgh, 143 1981.

72. Sarofim A. F. and Flagan R. C., " NO_x Control for Stationary combustion Sources ", Progress in Energy and Combustion Sciences, 2 1 1976.

73. Sarofim A. F. and Pohl J. H., " Kinetics of Nitric oxide formation in Premixed Laminar flames", Four teenth Symposium (International) on combustion, the Combustion Institute, Pittsburgh, 739, 1973.

74. Schatz G. C., Fitzcharles, M. S. and Harding, L. B., " State-to-state chemistry fast Hydrogen Atoms." Faraday Discuss. Chem. Soc. 84, 359, 1987.

75. Semmes D. H., Ravishankara A. R., Gump-Perkins C. A. and Wine P. H., Int. Jou. Chem. Kinetics, 17, 303 1985.

76. Strobel D. F., " Chemistry and evolution of Ti
    tan's atmosphere ", Plant, Space Sci., 30. 839,
    1982.

77. Taylor B. R., "Ph.D Thesis", M.I.T. 1984.

78. Troe, J., J. Chem. Phys, 4745 and 4758 1977.

79. Wagal S. S., Carrington T., Filseth S. V. and
    Sadowski C. M., Absolute rate constants of CH with
    NO, N_2O, NO_2, and N_2 at room temperature, Chem.
    Phys., 69, 61, 1982.

80. Wagner H. Gg. and Wolff, " An investigation of the
    reaction betwen CH_3 radicals and NO at High Tem
    peratures", Ber. Bunsenges. Phys. Chem. 92, 678,
    1988.

81. Warnatz J, "Mechanism of High Temperature Combus
    tion of Propane and Butane", Comb. Sci. and Tech.
    34, 177, 1983.

82. Westmoreland P. R.," Ph.D Thesis", M.I.T., 1986

83. Washida N. and Bayes K. D., Int. J. Chem. Kinet.,
    8, 777 1976.

84. Zabarnick, S., Fleming, J. W. and Lin., M. C.,
    " Kinetic study of reaction CH + H_2 <-----> CH_2 +
    H in the temperature range 372 to 675 K, J. Chem.
    Phys. 85, 1984.

85. Zeldovich Y. B., Acta physicochimica U.S.S.R., 21,
    577 1946.